

UNCLASSIFIED

AD NUMBER
AD093327
CLASSIFICATION CHANGES
TO: <b>unclassified</b>
FROM: <b>secret</b>
LIMITATION CHANGES
TO: <b>Approved for public release, distribution unlimited</b>
FROM: <b>British Embassy, 3100 Massachusetts Ave, NW, Washington, DC 20008.</b>
AUTHORITY
<b>20091022 - dstl ltr AVIA 6/17315.</b>

THIS PAGE IS UNCLASSIFIED

# SECRET

# AD 93327

## Armed Services Technical Information Agency

Reproduced by

**DOCUMENT SERVICE CENTER**

**KNOTT BUILDING, DAYTON, 2, OHIO**

This document is the property of the United States Government. It is furnished for the duration of the contract and shall be returned when no longer required, or upon recall by ASTIA to the following address: Armed Services Technical Information Agency, Document Service Center, Knott Building, Dayton 2, Ohio.

**NOTICE: WHEN GOVERNMENT OR OTHER DRAWINGS, SPECIFICATIONS OR OTHER DATA ARE USED FOR ANY PURPOSE OTHER THAN IN CONNECTION WITH A DEFINITELY RELATED GOVERNMENT PROCUREMENT OPERATION, THE U. S. GOVERNMENT THEREBY INCURS NO RESPONSIBILITY, NOR ANY OBLIGATION WHATSOEVER; AND THE FACT THAT THE GOVERNMENT MAY HAVE FORMULATED, FURNISHED, OR IN ANY WAY SUPPLIED THE SAID DRAWINGS, SPECIFICATIONS, OR OTHER DATA IS NOT TO BE REGARDED BY IMPLICATION OR OTHERWISE AS IN ANY MANNER LICENSING THE HOLDER OR ANY OTHER PERSON OR CORPORATION, OR CONVEYING ANY RIGHTS OR PERMISSION TO MANUFACTURE, USE OR SELL ANY PATENTED INVENTION THAT MAY IN ANY WAY BE RELATED THERETO.**

# SECRET

**NOTICE: THIS DOCUMENT CONTAINS INFORMATION AFFECTING THE  
NATIONAL DEFENSE OF THE UNITED STATES WITHIN THE MEANING  
OF THE ESPIONAGE LAWS, TITLE 18, U.S.C., SECTIONS 793 and 794.  
THE TRANSMISSION OR THE REVELATION OF ITS CONTENTS IN  
ANY MANNER TO AN UNAUTHORIZED PERSON IS PROHIBITED BY LAW.**

100-93327-1

ASTIA FILE COPY

TECH. NOTE  
G.W.402

# FC

SECRET

TECH. NOTE  
G.W.402

## ROYAL AIRCRAFT ESTABLISHMENT

FARNBOROUGH, HANTS

TECHNICAL NOTE No: G.W.402

JSRP	Control No.
560196	
Date	8-MAY 1956

### VISUAL COMMAND GUIDANCE SYSTEMS FOR G.W. DEFENCE AGAINST LOW-FLYING AIRCRAFT

by

M. SQUIRES,

G. BROWN, (Short Bros. & Harland Ltd.)

and D.W.ALLEN

#### CONDITIONS OF RELEASE

1. THIS INFORMATION IS DISCLOSED ONLY FOR OFFICIAL USE BY THE RECIPIENT GOVERNMENT AND SUCH OF ITS CONTRACTORS, UNDER SEAL OF SECRECY, AS MAY BE ENGAGED ON A DEFENCE PROJECT. DISCLOSURE TO ANY OTHER GOVERNMENT OR RELEASE TO THE PRESS OR IN ANY OTHER WAY WOULD BE A BREACH OF THESE CONDITIONS.
2. THE INFORMATION SHOULD BE SAFEGUARDED UNDER RULES DESIGNED TO GIVE THE SAME STANDARD OF SECURITY AS THAT MAINTAINED BY HIS MAJESTY'S GOVERNMENT IN THE UNITED KINGDOM.

MINISTRY OF SUPPLY

THIS DOCUMENT IS THE PROPERTY OF H.M. GOVERNMENT AND ATTENTION IS CALLED TO THE PENALTIES ATTACHING TO ANY INFRINGEMENT OF THE OFFICIAL SECRETS ACT, 1911-1939

It is intended for the use of the recipient only, and for communication to such officers under him as may require to be acquainted with its contents in the course of their duties. The officers exercising this power of communication are responsible that such information is imparted with due caution and reserve. Any person other than the authorised holder, upon obtaining possession of this document, by finding or otherwise, should forward it, together with his name and address, in a closed envelope to:-

THE SECRETARY, MINISTRY OF SUPPLY, LONDON, W.C.2

Letter postage need not be prepaid, other postage will be refunded. All persons are hereby warned that the unauthorised retention or destruction of this document is an offence against the Official Secrets Act.

SECRET

THE RECIPIENT IS WARNED THAT INFORMATION CONTAINED IN THIS DOCUMENT MAY BE SUBJECT TO PRIVATELY OWNED RIGHTS.

MAY 20 1956

56AA

79923-SD-4-6

SECRET

U.D.C. No. 623.451-519 : 623.55 : 621.396.933.4

Technical Note No. G.W.402

March, 1956

ROYAL AIRCRAFT ESTABLISHMENT, FARNBOROUGH

Visual Command Guidance Systems for G.W. Defence  
against Low-flying Aircraft

by

M. Squires  
G. Brown (Short Bros. & Harland Ltd.)  
D.W. Allen

---

SUMMARY

The use of visual command guidance to control the flight of a missile from sea-level so as to intercept approaching, low-flying aircraft is examined. It is found that a human operator can perform this task by means of a thumb-operated joystick if (i) a suitable relation between joystick deflection and output signal is chosen, and (ii) an anatomically correct form of target tracking mechanism is provided so as to minimize effort and concentration.

An effective two-man system, which has the advantage that the aimer's task is virtually the relatively simple one of hitting a fixed target, has also been found. Only preliminary studies have been undertaken, using experimental apparatus. Miss distances of up to 15 feet are to be expected at the present stage of development, although skilled experimenters can halve this figure under laboratory conditions.

---

SECRET

56A1

12323-50-4-6

LIST OF CONTENTS

	<u>Page</u>
List of Principal Symbols Used	5
<u>Part I</u> The Guidance Problem and its Treatment	
1     Introduction	6
2     The Tactical Situation	7
3     The Missile	8
3.1   Forward Speed	8
3.2   Lateral Acceleration	8
3.3   Transient Response	9
4     The Guidance Loop	9
4.1   The Aimer's Task	9
4.2   The Input to the Guidance Loop	10
4.3   Dynamic Stability	11
4.4   A Form of Guidance Loop	11
5     Some Preliminary Comparisons	11
5.1   An Existing Technique	11
5.2   Application to "Green Light"	12
6     Extensions of Anti-tank Guidance Parameters	13
7     A Non-linear Joystick Deflection-output Relation	14
8     A Two-man Guidance System	16
8.1   General	16
8.2   Experimental Checks of Two-man Guidance	17
8.3   Some Drawbacks of the Two-man Guidance System	19
8.4   Use of Angular Accelerometers	19
9     Comparative Tests of Competing Techniques	19
<u>Part II</u> Description of the Simulators	
1     Introduction	21
2     Laboratory Simulator	21
2.1   General	21
2.2   Display Unit	21
2.2.1   Function	21
2.2.2   Display	21
2.2.3   G.G.S. Mirror Driving Stage	22
2.2.4   Range Unit Amplifier	22
2.2.5   Missile Speed Programme	23
2.2.6   Initial Conditions at Instant of Launch	23
2.3   Missile Unit	23
2.3.1   Function	23
2.3.2   Missile Aerodynamic Analogue	24
2.3.3   Variation of Aerodynamic Stiffness with Missile Speed	24
2.3.4   Computing Lateral Displacement	25
2.3.5   Wing Stops	25
2.4   Control Unit	25
2.4.1   Function	25
2.4.2   Aimer's Demand Channel	25
2.4.3   Tracker's Demand Channel	26
2.5   Target Simulator	27
2.5.1   Function	27
2.5.2   Target Analogue	27
2.5.3   Description of Target Simulator	27
2.5.4   Computation of Impact Range	28

# SECRET

Technical Note No. G.W.402

## LIST OF CONTENTS (Contd.)

	<u>Page</u>
3 The Field Simulator	28
3.1 General	28
3.2 The Aiming Stand	29
3.3 Missile Simulation	29
3.4 Launcher Angle Storage	29
3.5 Target Aiming Point	30
3.6 Communications	30
Conclusions	30
References	31
Advance Distribution	32
Detachable Abstract Cards	

## LIST OF APPENDICES

	<u>Appendix</u>
The Lateral Acceleration of a Missile which is maintained on the Aimer-Target Line of Sight	A
Simulator Techniques for Applying Two-operator Guidance	B
1 Networks for Maintaining Sight-line Coincidence by means of Binocular Tracking of the Target	
2 To determine the Parameters of a Simulator Shaping Unit for converting Sight-line rates into Missile Acceleration	
Lateral-Acceleration - Total Requirement	C
The Validity of "Demand Storage"	D
1 General	
2 Linear Operation	
3 Operation of Limits	
4 Phase-advanced Acceleration Control with Demand Storage	
5 Control of Limiting Amplitude	
6 Minimum Velocity Response Time	
A Relation between Guidance Parameters and Missile Speed	E

## LIST OF ILLUSTRATIONS

	<u>Fig.</u>
Attack on constant velocity target	1
Estimated velocity-time relation for G.L.T.V. in Level Flight	2
Lateral acceleration transient responses of G.L.T.V. and its analogue	3
Lateral displacement responses of G.L.T.V. and its analogue	4
Simplified block schematic of guidance loop	5
Combinations of crossing distance $d$ and target speeds $v_T$ for which the missile lateral acceleration at impact is 12.5 ft/sec. Also experimental relation with phase-advanced joystick output	6
Schematic arrangement for maintaining missile on aimer-target sight-line	7
Results of dummy attacks on a "Meteor" aircraft using the Field Simulator	8
Miss-distance with linear joystick law. Control stiffness 12.5 ft/sec <sup>2</sup>	
" " " " " " " " $T_F = 4$	9-9a
" " " " " " " " $T_F = 2$	10-10a
" " " " " " " " $T_F = 4$	11-11a
" " " " " " " " $T_F = 1$	12-12a

## LIST OF ILLUSTRATIONS (Contd.)

	<u>Fig.</u>
Miss-distances with linear joystick law. Control stiffness 50 ft/sec <sup>2</sup> T <sub>F</sub> = 2	13-13a
" " " " " " " " 50 ft/sec <sup>2</sup> T <sub>F</sub> = 4	14-14a
" " " " " " " " 100 ft/sec <sup>2</sup> T <sub>F</sub> = 0.5	15-15a
" " " " " " " " 100 ft/sec <sup>2</sup> T <sub>F</sub> = 1	16-16a
" " " " " " " " 100 ft/sec <sup>2</sup> T <sub>F</sub> = 2	17-17a
" " " " " " " " 200 ft/sec <sup>2</sup> T <sub>F</sub> = 0.5	18-18a
" " " " " " " " 200 ft/sec <sup>2</sup> T <sub>F</sub> = 1	19-19a
" " " " " " " " 400 ft/sec <sup>2</sup> T <sub>F</sub> = 0.5	20-20a
" " " " " " " " 600 ft/sec <sup>2</sup> T <sub>F</sub> = 0.5	21-21a
Arrangement for giving non-linear joystick law	22
Miss-distances with non-linear joystick law. Max. demand 100 ft/sec <sup>2</sup> T <sub>F</sub> = 4	23-23a
" " " " " " " " 150 ft/sec <sup>2</sup> T <sub>F</sub> = 2	24-24a
" " " " " " " " 300 ft/sec <sup>2</sup> T <sub>F</sub> = 1	25-25a
Curve of joystick displacement J as a function of normalized output V/v	26
Air look-out sight designed by A.P.R.U. for tracking	27
Block diagram of Laboratory Simulator	28
The Laboratory Simulator	29
Display unit (one plane only)	30
Gyro-gunsight mirror linearity	31
Frequency-responses of gyro-gunsight mirror	32
Missile unit (one plane only)	33
Control unit (one plane only)	34
"Demand storage" circuit	35
Control unit responses (lateral velocity demands only)	36
Missile lateral velocity response to a stepwise joystick deflection	37
Frequency-response of tracking generator noise filter	38
Target geometry	39
Basic target simulator construction	40
Schematic diagram of Laboratory Target Simulator	41
Method of determining impact range	42
Missile range errors in computing impact range	43
Trainable aiming stand (field simulator)	44
Construction of field simulator aiming stand	45
Optical arrangements of the field simulator	46
Idealized effect of joystick displacement	47
Launcher angle storage unit	48

List of Principal Symbols Used

$d$	crossing distance (feet) - the length of the perpendicular on to the (straight) flight path of the target from the guided weapon aiming point
$\delta$	angular displacement of missile wing (radians)
$J$	joystick deflection ( $J_{\max} = 1$ )
$r_i$	impact range (feet) from aimer measured parallel to target flight path
$r_M$	missile " " " " " " " " " "
$r_T$	target " " " " " " " " " "
$r_{T_0}$	initial or acquisition range of target (feet) from aimer measured parallel to target flight path
$\theta_T$	aimer-target sight line direction with respect to (straight) target flight path
$\theta_M$	aimer-missile sight line direction with respect to (straight) target flight path
$\phi_M$	missile flight path direction with respect to (straight) target flight path
$T_P$	preparation time, between target acquisition and missile firing
$T_B$	missile boost period
$T_G$	time available to aimer for gathering and aiming missile
$T_F$	phase advance time-constant inserted in manual guidance loop between joystick output, and missile control surface actuator input
$T'$	time constant of exponential lag associated with $T_F$ in some circuit arrangements
$v_M$	missile forward speed along its flight path
$v_T$	target " " " " " "
$v_A$	change in missile's lateral velocity ( $= \dot{y}$ )
$y$	lateral displacement of missile from initial flight path

Part IThe Guidance Problem and its Treatment1 Introduction

1.1 The programme of work described in this Note was designed to assess the accuracy with which a guided missile launched from a fixed point at sea-level against an approaching low-flying aircraft in daylight, could be guided to its target by means of a visual command link with manual guidance. This technique has commended itself on the ground of relative simplicity and because its usefulness is not impaired by low sight-line elevations.

1.2 Concurrently, Messrs. Short Bros. and Harland Ltd. have been developing the "Green Light" test vehicle (G.L.T.V.) to R.A.E. requirements for the experimental study of the same problem in the field. A close collaboration has been maintained with the firm, which has taken the form, among others, of keeping in touch with its current views as to the parameters and expected behaviour of the test vehicle, and of embodying these, wherever relevant, in our own studies. We have however concentrated our attention in the main on the wider problems of guidance and general practicability rather than on the detailed development of G.L.T.V.

1.3 This Note is essentially an interim report. It reflects the state of affairs at a point where, owing to pressure of other work, the investigation is to be transferred to the hands of Messrs. Short Bros. and Harland Ltd. It goes as far as to show that the task of engaging an oncoming aircraft with some prospect of success is within the capacity of a human operator and to suggest how he can be enabled to fulfil the task. Matters of detailed development of apparatus, and precise evaluations of accuracy have however necessarily been left unfinished.

1.4 The form of the Note is largely fixed by these considerations. Thus a good deal of experimental data which might have been omitted from a final account, has been included so as to be available for subsequent comparisons or checking. Also the experimental apparatus has been described in more detail than might otherwise be justified.

1.5 For similar reasons, no attempt has been made to establish statistical properties. This would have consumed time which, it was felt, was more profitably devoted to the general appraisal of the problem at this stage. We have therefore confined ourselves to intuitive comparisons based on comparatively limited data, but we have on the other hand considered all the possibilities that have suggested themselves for meeting the specified tactical situations.

1.6 One aspect of the problem which we have largely ignored is that of gathering the missile on to its course after launching. The absence of information regarding boost dispersions etc. would have made it difficult to do otherwise, but in any case it seemed desirable to tackle the main guidance problem first. In all our experiments therefore we have so arranged matters that when the missile first comes under the aimer's control, it is very close to the required trajectory, and very little gathering has been required.

1.7 We have adopted throughout an "open-loop" control system; that is, one in which no aspect of the missile's response (e.g. its lateral acceleration, heading angle etc.) has been measured internally, and the result subtracted from the applied external demand in order to give some desired response - in other words, there is no autopilot. The only input to the missile control surface actuators has been the aimer's demand in the form of a voltage, shaped by intermediate circuits where necessary to produce the required response. It is easier with such an open-loop system to confine oneself to the guidance problem, without being concerned with the stability of a secondary feedback loop, and it is felt that at this stage any other approach would be unduly specific as to detailed missile design.

1.8 The Note is divided into two parts. Part I is concerned with the problem to be solved and with the presentation of results. Part II is given over to descriptions of experimental apparatus.

## 2 The Tactical Situation

2.1 Targets are to be engaged whose forward speeds may be as great as 900 ft/sec, flying in the general direction of the guided weapon aiming point. For present purposes the target is assumed to fly at constant speed along a straight line whose perpendicular distance  $d$  from the aiming point (Fig.1) lies between zero and 900 ft. This distance is referred to in what follows as the "crossing distance". As far as possible, the target is to be intercepted at a range greater than about 4500 feet. The general situation in the plane containing the target flight path and the aiming point is shown in Fig.1. For simplicity of presentation the missile is depicted in the same plane.  $\theta_T$  and  $\theta_M$  are the angles made by the aimer-target and aimer-missile sight-lines respectively, with a line through the aiming point, parallel with the target flight path, which is taken as a datum. The flight path of the missile is defined by the angle  $\phi_M$  with respect to the same datum. The forward speeds of the target and missile are  $v_T$ ,  $v_M$  respectively.

2.2 The range at which the target is first sighted (or acquired) will depend on a variety of factors. On the basis of available data (Ref.4), a conservative estimate, namely 15,000 ft is adopted here as standard. Some field experiments conducted at Farnborough however, using a very fast aircraft of small frontal area as the target ("Hunter") suggest that the acquisition range may sometimes be less if the design and use of the locating gear is not carefully thought out.

2.3 After the target has been sighted, an interval of up to five seconds may elapse (preparation and aiming) before the missile is fired (Refs.3,10). Thereafter the task of the aimer is to bring the missile on to the aimer-target sight-line as quickly as possible and to hold it there until impact. The missile trajectory is therefore characteristic of beam-riding. Experience indicates that the aimer should be given not less than five seconds in which to perform his task.

2.4 If it is assumed that the relevant angles are small enough for the missile velocity component parallel to the target flight path (Fig.1) to be sensibly equal to its forward speed  $v_M$ , then the range of impact  $r_i$  is given by

$$r_i = \frac{v_M}{v_M + v_T} \{r_{T_0} - v_T(T_P + \frac{1}{2}T_B)\} \text{ feet} \quad (1.2)$$

where  $r_{T_0}$  is the acquisition range (taken as 15,000 ft here),  $T_P$  is the preparation time, for which a maximum figure of 5 seconds has been quoted, and  $T_B$  is the boost time.

2.5 If it is assumed that no missile guidance is possible during boost, the time available for gathering and guiding the missile is

$$T_G = \frac{r_{T_0} - v_T T_P - r_i}{v_T} - T_B = \frac{r_{T_0} - v_T(T_P + T_B) - \frac{1}{2}v_M T_B}{v_M + v_T} \text{ seconds} \quad (2.2)$$

and this, from para. 2.3, should be not less than five seconds.

2.6 From Appendix C, the maximum lateral acceleration is required of the missile at impact, and this is given approximately by

$$v_M \phi_M = \frac{2v_T d}{r_i^2} (v_M + v_T) \text{ ft/sec}^2 \quad (3.2)$$

### 3 The Missile

#### 3.1 Forward Speed

3.1.1 In Ref.10 the maximum time of preparation is given as  $T_p = 5$  secs. This is the interval which may elapse between visual acquisition of the target and launching the missile. In the same place a boost time of 3-4 secs preferably in the neighbourhood of 3 seconds is called for. There have been subsequent suggestions that the boost time may be yet shorter, but in our work we have standardized on  $T_B = 3$  seconds.

3.1.2 In these circumstances the missile speed, if constant after boost, would have to be about 870 ft/sec if the minimum impact range were not to fall below 4500 ft. If no missile control were possible during boost the time  $T_G$  available for guidance would be  $3\frac{2}{3}$  secs which is well below the desired minimum of 5 secs. On the other hand, to give a minimum guidance time of 5 secs the missile speed would need to be about 500 ft/sec. In this case the minimum impact range would fall to about 3300 ft. There is therefore a contradiction between the requirements.

3.1.3 Present estimates of test vehicle performance indicate a forward speed at the end of boost of about 705 ft/sec. At the same time there is some possibility of effective control at least during the last second of boost. There are then rather more than 5 seconds of control time available against the fastest target, but the impact range, assuming constant missile forward speed after boost, is only 4000 ft. We have taken this missile performance as a basis for our work on the ground that it represents roughly what is practically achievable at this time.

3.1.4 In addition, the test vehicle is assumed to contain a sustainer motor which gives it a forward acceleration in level flight subsequent to boost of about  $7.5 \text{ ft/sec}^2$ . We have incorporated this figure in our experimental programme. It is perhaps worth pointing out however that when attacking fast targets at high crossing distances, the missile may climb at about  $30^\circ$  to the horizontal; also induced drag may be significant at the high lateral accelerations called for in the later phases of such engagements. The forward speed of the missile and more especially its component parallel to the datum, which governs the impact range, may be materially affected. We do not consider therefore that we have any strong justification for having taken account in our work, of the level-flight forward acceleration subsequent to boost, of G.L.T.V.

#### 3.2 Lateral Acceleration

3.2.1 For control surfaces, the projected test vehicle has moving wings, whose maximum deflections are  $\pm 0.2$  radian. We have assumed that all of this is available for lateral control and in our experimental work we have taken it that there is full control of the wings from launch. However the lateral acceleration per unit wing deflection has been assumed proportional to the square of forward speed so that in fact, control is only effective during the latter part of boost and subsequently.

3.2.2 The steady-state lateral acceleration available on the assumption that, for a given forward speed, it is linearly proportional to wing

deflection, has been taken as  $\pm 8 \times 10^{-5} v_M^2 \text{ g ft/sec}^2/\text{radian}$  of wing deflection. Just subsequent to boost therefore, lateral accelerations of up to  $1.6 \times 10^{-5} \times 705^2 \text{ g} \approx 8 \text{ g}$  are possible. Assuming the level-flight velocity-time programme for G.L.T.V. (para. 3.1.4, Fig.2) this acceleration rises to about 10g at the end of powered flight.

3.2.3 From equation (3.2) the maximum lateral acceleration required to maintain sight-line coincidence at an impact range of 4000 ft is about 5g.

3.2.4 When quoting lateral accelerations per unit (full) joystick (or control handle) deflection, which will be referred to in what follows as "control stiffnesses" and suitably qualified where necessary, it is evidently essential to relate the figures quoted to some forward speed. For this purpose we have taken the speed at the end of boost, namely 705 ft/sec.

### 3.3 Transient Response

3.3.1 Previous experience indicates that in an investigation as general as this, nothing is gained by taking account of the missile's weathercock properties. We therefore omit any discussion of these, confining ourselves to the observation that the missile is dynamically stable, and to giving a plot of the linearized G.L.T.V. response in lateral acceleration to a step of wing deflection (Fig.3).

3.3.2 For the same reason we have replaced the missile in our experimental work by a simplified analogue in which, in addition to assuming perfect roll stabilization and no interaction between the two control planes, we arrange that (a) the initial and steady-state lateral accelerations per unit wing deflection are as for G.L.T.V.; (b) the total change in lateral velocity at any time in the steady state subsequent to a step of wing deflection is as for G.L.T.V. and (c) the wing deflection is similarly restricted to  $\pm 0.2$  radian.

3.3.3 Consequently the lateral displacement of the missile analogue from its initial flight path at any time in the steady state subsequent to a step of full wing deflection is about 16 feet less than for G.L.T.V. (Fig.4). The resulting simplified relationship between wing deflection  $\delta$  and lateral acceleration  $\ddot{y}$  can then be represented by

$$\frac{\ddot{y}}{\delta} = 8 \times 10^{-5} v_M^2 \text{ g } \left( \frac{1+0.04p}{1+0.136p} \right) \text{ ft/sec}^2/\text{radian} \quad (1.3)$$

The corresponding time relation is given in Fig.34.

## 4 The Guidance Loop

### 4.1 The Aimer's Task

4.1.1 When the missile, having been fired, first appears in the field of view of the aimer's binoculars (or monocular) which already contains the target, his first objective is to "gather" it; that is, to bring it into apparent coincidence with the target as quickly as possible. This implies a reasonably rapid response on the part of the missile, to the aimer's commands.

4.1.2 Having been gathered, the missile must be kept as nearly as possible on the aimer-target line-of-sight until impact. The aimer must therefore eliminate as far as possible any steady-state lags of the missile behind the target sight-line; he must also ensure that any corrections he makes result in well damped recoveries.

4.1.3 It is shown in Appendix A that for a constant speed missile the lateral acceleration required to maintain sight-line coincidence is given by

$$v_M \dot{\phi}_M = 2v_M \dot{\theta}_T + r_M \ddot{\theta}_T \quad (1.4)$$

where  $r_M$  is the instantaneous missile range.

4.1.4  $\theta_T$  is given by

$$\theta_T = \frac{\pi}{2} - \tan^{-1} \left( \frac{r_{T0} - v_T t}{d} \right) = \tan^{-1} \frac{d}{r_T} \quad (2.4)$$

where the time  $t$  is reckoned from the instant at which the target range is  $r_{T0}$ , and  $\theta_T$  is measured from a line through the aiming point, parallel to the target flight path. Hence

$$\dot{\theta}_T = \frac{v_T d}{d^2 + (r_{T0} - v_T t)^2} = \frac{v_T d}{r_T^2 + d^2} \quad (3.4)$$

and

$$\ddot{\theta}_T = \frac{2 v_T^2 d (r_{T0} - v_T t)}{[d^2 + (r_{T0} - v_T t)^2]^2} = \frac{2d v_T^2 r_T}{(r_T^2 + d^2)^2} \quad (4.4)$$

4.1.5 From (1.4), (3.4) and (4.4) if  $\frac{d^2}{r_T^2} \ll 1$  as is invariably true in our context

$$v_M \dot{\phi}_M = \frac{2 v_M v_T d \left( r_T + \frac{v_T}{v_M} r_M \right)}{r_T^3} \quad (5.4)$$

Since in a given engagement,  $v_M$ ,  $v_T$ ,  $d$  and  $\left( r_T + \frac{v_T}{v_M} r_M \right)$  are constant, the missile's lateral acceleration must increase as the inverse cube of the target range, to a final value which may be as high as 5g (para. 3.2.3)

## 4.2 The Input to the Guidance Loop

4.2.1 The input to the guidance system is the angle  $\theta_T$  (Fig.5). From equation (3.4)  $\theta_T$  is increasing throughout any engagement of interest here. Also all higher derivatives of  $\theta_T$  can be expressed as polynomials in  $\theta_T$ . It is therefore reasonable to suppose that none, however high its order, remains zero throughout the trajectory.

4.2.2 No linear system therefore, however high its order, will entirely prevent the missile from lagging behind the target sight-line. It does not of course follow that the resulting errors are serious; there is however a clear suggestion that a high order servo loop is called for.

### 4.3 Dynamic Stability

4.3.1 The choice of means for maintaining dynamic stability in a guidance loop containing a human operator is largely a matter of experience. More particularly it is found that the order of the system, that is the number of successive error integrations performed in the loop (apart from any performed by the operator himself) is severely restricted. At the most, in our experiments, two integrations have proved permissible and even here, if the loop gain is to be sufficiently great for our purposes, the joystick output signal must be heavily phase-advanced.

4.3.2 Systems of lower order are unacceptable for reasons which need not be discussed here since from para. 4.2 the order should be as high as possible.

### 4.4 A Form of Guidance Loop

4.4.1 At its simplest, the guidance loop may be represented by Fig.5. The aimer acts as an error detector, noting differences between target and missile sight-line orientations, and acting to reduce them.

4.4.2 For this purpose we have provided him with a thumb-operated joystick (Ref.8) to be moved in the direction in which a change of missile motion is required. The output signal from the joystick is shown in Fig.5 as being applied directly to the missile's control surfaces. The missile is treated as a particle whose lateral acceleration is therefore proportional to joystick deflection.

4.4.3 Since the aimer sees the angular displacement of the missile, the latter in effect introduces two integrations into the loop, while the effective loop gain varies inversely with range\*. No additional integrations are, from para. 4.3, permissible.

4.4.4 Numerically, the only property which can be ascribed to the guidance loop in its final form without experiment is that it should be possible (para. 4.1) to generate an increasing lateral acceleration throughout the trajectory; the end value being  $\ddot{y}_{\max}$  where  $|\ddot{y}|_{\max} \leq 5g$ . In addition we may assert from para. 4.3 that the output signals of the joystick will very probably need to be phase-advanced before being applied to the control surface actuators.

4.4.5 For further data we have recourse to simulator experiments. The simulators used for this purpose are described in Part II of this Note.

## 5 Some Preliminary Comparisons

### 5.1 An Existing Technique

5.1.1 In exploring guidance systems for Project "Malkara" (Ref.2), an anti-tank missile, the arrangement eventually adopted was qualitatively similar to that which has been described above. That is, the missile's lateral acceleration was made proportional to joystick deflection in the steady state. The output signal of the joystick was however heavily phase advanced (para. 4.3).

---

\* This implies that the modulus of the human operator's transfer function remains constant. It is a matter of observation that the operator can vary this parameter over a wide range, and he uses this faculty, it would seem, as a means of reducing transient oscillations. In addition it seems likely that he increases it with time, thereby offsetting in some measure, the reduction in loop gain arising from range-dependence.

5.1.2 In the "Malkara" Project the target was always either stationary or moving comparatively slowly across the field of view. The need for sustained lateral accelerations was therefore a secondary consideration.

5.1.3 A primary consideration on the other hand was dynamic stability. The problem therefore provided an occasion for finding combinations of parameters which led to rapid and well-damped recoveries to more or less fixed aimer-target sight-lines.

5.1.4 It was found that, assuming a linear relation between joystick output and deflection, full deflection should not demand more than about 0.4g. The phase-advance time constant  $T_F$  should be of the order of 4 seconds. Greater control stiffnesses were indeed practicable, but they added noticeably to the difficulty of the aimer's task and were in any case unnecessary.

## 5.2 Application to "Green Light"

5.2.1 If the parameters given in para. 5.1.4 are compared with the minimum requirement of 5g quoted in para. 3.2.3 for "Green Light", it would seem unlikely that the anti-tank system could be simply extended to cover the new problem. It therefore seemed desirable as a first step to find out how far short of the "Green Light" specification a system would fall if "Malkara" parameters were used.

5.2.2 Neglecting lateral accelerations due to joystick rate of deflection (arising from the phase-advance) there is a unique relation between steady-state lateral acceleration and joystick deflection at a given missile speed. A rough estimate can therefore be quickly made, from a knowledge of the maximum lateral acceleration required in each type of trajectory, of what can be achieved with a control stiffness of, say, 12.5 ft/sec<sup>2</sup>. This is the figure arrived at in the course of our "Malkara" simulator experiments. The left-hand full line in Fig.6 shows, from theoretical considerations, the limiting combinations of target speed and crossing distance that can be dealt with when unit (full) joystick deflection demands a lateral acceleration of 12.5 ft/sec<sup>2</sup>. In the same figure, the hatched line indicates what was achieved experimentally on the laboratory simulator (Part II para.2) where the joystick signal was phase-advanced with a time constant  $T_F = 4$  secs.

5.2.3 In comparing the theoretical with the experimental results it is necessary to bear in mind the additional lateral acceleration available in the latter case due to phase-advance. Again, in the simulator work, the effective lateral acceleration per unit joystick deflection was made proportional to the square of the forward speed (para. 3.2.1) and the available lateral accelerations quoted refer only to a specific forward speed of 705 ft/sec in the case of the anti-aircraft missile; also the missile speed varies as indicated in Fig.7. The effective mean control stiffness during any particular engagement was therefore rather greater than the quoted figure would suggest.

5.2.4 Concurrently, experiments were carried out using the field simulator (Part II para.3) and the parameters stated in para. 5.1.4 above. The object of these was partly to confirm the laboratory experiments, but mainly to gain familiarity with field conditions when engaging oncoming aircraft. Similar assumptions underlie the work on both simulators except that in the case of the field simulator it was arranged that there was no guidance during the 3 second boost, and the missile speed subsequent to boost was constant at 705 ft/sec. Up to the present it has only been possible to experiment with small or zero crossing distances, so that the results are

chiefly of interest here as a comparison of low sight-line rate conditions when the target is an oncoming aircraft, with previous experience against tanks.

5.2.5 The target was a "Meteor" aircraft flying at about 300 knots, the crossing distances varying between 0 and 300 feet. The target was usually acquired at ranges greater than 15,000 ft; the choice of the instant for firing was left to the aimer's judgement.

5.2.6 The aimer viewed the target through X10 binoculars on a trainable mounting, but the direction of approach of the target was known within close limits. Acquisition usually took place at from 3 to 5 miles. No missile dispersion was assumed and the missile appeared in the field of view about 3 seconds after firing.

5.2.7 The results of one series of tests are shown diagrammatically in Fig.8. Apart from one run in which the missile was deliberately fired late, the greatest miss distance from some part of the aircraft structure was 27 inches and the greatest distance from the centre of the target was 10 feet. Assuming a missile wing and fin span of about 30 inches, 8 of the 11 simulated attacks are direct hits. In the case of the miss due to late firing, the lateral acceleration required to maintain sight-line coincidence was beyond the demand capacity of the guidance system; range coincidence occurred at 3690 feet.

5.2.8 In applying a set of guidance parameters arrived at with one missile configuration to another for purposes of comparison, matters should be so arranged that the operator's task is as nearly as possible unchanged; for the operator's reactions are the principal limiting factor in the choice of guidance parameters. But the aimer, when he has demanded a change in missile motion, observes the result as a change in missile sight-line orientation. That result and the operator's consequent reaction are therefore a function of range and hence, after any given interval of time from launch, of forward speed. From the reasoning of Appendix E the control stiffness should be changed in linear proportion to forward speed when transferring from one missile configuration to another. This change would present little difficulty if both missiles could be assumed to have constant forward speeds subsequent to boost. In the case of the missile analogue used in our laboratory simulator work on "Green Light" however, not only was the forward speed not constant (para. 3.1.4) but the lateral acceleration response to wing deflections was made proportional to the square of forward speed. In these circumstances it is difficult to conceive of a set of guidance parameters which would allow of a strict comparison with "Malkara", where a constant speed was assumed, without giving rise to a degree of complication disproportionate with the significance of the results. We have therefore contented ourselves with the relatively crude comparative tests described above.

5.2.9 It is clear that the conclusions arrived at by means of the comparative tests referred to become meaningless if they are overstrained. They suffice however to show that considerable changes must be envisaged if the "Green Light" specification is to be met.

## 6 Extensions of Anti-tank Guidance Parameters

6.1 One possibility of meeting the "Green Light" specification lay in increasing the control stiffness and varying the phase-advance time-constant of the anti-tank arrangement discussed above; that is in purely quantitative extensions.

6.2 From para. 3.2.3 it is clearly necessary to be able to demand lateral accelerations rising to some  $160 \text{ ft/sec}^2$ . It does not follow however, where

the joystick output is phase-advanced, that this must be provided by static deflection alone, for some lateral acceleration is obtained by virtue of the rate of movement of the joystick.

6.3 A range of control stiffnesses between  $12.5 \text{ ft/sec}^2$  and  $600 \text{ ft/sec}^2$  for full joystick deflection (for definition see para. 3.2.4) has been tried on the laboratory simulator. Phase advance time-constants  $T_F$  have varied between 0.5 sec and 4 secs. A selection of the results is displayed in Figs. 9-21a inclusive. These diagrams cover a range of target speeds between  $200 \text{ ft/sec}$  and  $900 \text{ ft/sec}$ ; crossing distances range from zero to 900 ft.

6.4 A feature of Figs. 9-21a is the comparatively small scatter of miss-distances indicated, despite the high control stiffnesses. This is indicative of a fair degree of dynamic stability, a circumstance which was borne out by direct observation of the aimer's performance. On the other hand there is little doubt that a good deal of practice and concentration is necessary as compared with the anti-tank task. It was also observable that when the target sight-line rates were relatively high, for example when the target speed was high and the crossing distance large, the tendency to oscillation in the system was less for a given control stiffness, if this was high, than when the target sight-line was stationary or nearly so.

6.5 Figs. 9-21a do not clearly indicate the choice of guidance parameters within particularly narrow limits. It is evident however that there is a transition somewhere between a control stiffness of  $100 \text{ ft/sec}^2$  and  $200 \text{ ft/sec}^2$ . Below this it is impossible to maintain sight-line coincidence for top-speed targets at maximum crossing distance other than by a degree of anticipation on the part of the aimer. Above this transition region, it is technically possible to track in all cases, although in these just referred to there is a distinct tendency for lags to develop. In these experiments the azimuth bearing of the target analogue remained constant so that it flew as though to pass over the aimer's head. These lags therefore appear in Figs. 9-21a as a tendency for the missile to pass below the centre of the target.

6.6 The main practical conclusion drawn from these results is that some arrangement is desirable which ensures that for comparatively low sight-line rates the control stiffness is low and vice versa. Also there is a need to reduce, if possible, the lags which occur at the higher sight-line rates.

## 7 A Non-linear Joystick Deflection-output Relation

7.1 It has been established in para. 6 above that there is a case for arranging that the guidance loop gain should increase with sight-line angular rate.

7.2 If as in the present case the joystick demands lateral acceleration (or, more strictly, wing deflection) then when the angular rate of the sight-line is small, the position of the joystick tends more or less rapidly to neutral; for in these circumstances, once sight coincidence has been achieved the demand for lateral acceleration is low.

7.3 On the other hand if the sight-line rate increases, so also must the lateral acceleration of the missile. The joystick deflection must therefore increase. It follows that if we can arrange that the loop gain is low when the joystick deflection is small, and that it increases suitably with deflection, some approximation to the desired compromise will have been achieved.

7.4 In our experiments the joystick has been arranged to displace the sliders of two rotary potentiometers (Ref.8) about two mutually perpendicular axes. Each potentiometer is linked electrically with the missile control surface: that which is varied by an up-down motion of the joystick lever giving control in the pitch plane while the other gives control in yaw. Simultaneous manoeuvre can therefore be demanded in two mutually perpendicular planes of which one is vertical if the missile is roll stabilized so that the pitch control surfaces turn about a horizontal axis; the planes intersect on the missile's longitudinal axis. One such potentiometer is shown diagrammatically in Fig.22. Let its total resistance be  $2R$  and let it be spanned by a constant D.C. voltage  $2v$  whose mid point is earthed. The slider of the potentiometer is connected to earth via a fixed resistance  $R'$ . Suppose the slider to be displaced from its electrical mid position so that the potentiometer resistances to either side of it are  $R(1-J)$  and  $R(1+J)$  respectively.  $J$  is here the joystick deflection, unit value of which corresponds to full deflection. Thus  $-1 \leq J \leq 1$ . Then the output voltage  $V_o$  of the joystick is given by

$$\frac{V_o}{2v} = \frac{J}{2 + \frac{R}{R'}(1-J^2)} \quad (1.7)$$

Equation (1.7) determines the steady state wing-deflection and hence lateral acceleration demand at a given missile speed, for all possible  $J$ . The introduction of  $R'$  gives a smaller  $|V_o|$  for a given  $|J|$  than would otherwise be present unless  $|J| = 1$ . The factor  $\frac{R}{R'}$  may be used as a convenient indication of the degree of non-linearity in the relation connecting  $V_o$  with  $J$ . No special virtue is claimed for the particular form of relationship obtained in this way other than that it is obtained by the addition to a linear control of only one cheap and uncritical component.

7.5 The control stiffness insofar as it affects dynamic stability is substantially the incremental stiffness

$$\frac{dV_o}{dJ} = \frac{2v \left[ 2 + \frac{R}{R'}(1+J^2) \right]}{\left[ 2 + \frac{R}{R'}(1-J^2) \right]^2} \quad (2.7)$$

The introduction of  $R'$  can therefore be made to give a relatively low incremental control stiffness when  $|J|$  is small, which increases as  $|J|$  increases. This is in general conformity with the requirements expressed in para. 6.6. In the linear case ( $R' \rightarrow \infty$ ) the incremental stiffness of course is given by  $v$ , and is independent of  $J$ . The introduction of  $R'$  therefore reduces the incremental stiffness in the ratio given by the R.H.S. of equation (2.7) divided by  $v$ .

7.6 The considerations of para. 6 have suggested that full joystick deflection should demand about  $150 \text{ ft/sec}^2$  of lateral acceleration. If  $V_o$  is the output voltage from the joystick and the corresponding steady-state lateral acceleration  $\ddot{y} = K V_o$ , this means that in equation (1.7) when  $J = 1$  so that  $V_o = v$  we require

$$Kv = 150 \text{ ft/sec}^2 \quad (3.7)$$

7.7 If now for example we put  $R/R' = 4$  then in (1.7) the incremental stiffness

$$\frac{d\ddot{y}}{dJ} = K \frac{dV_0}{dJ} = \frac{300 \left[ 2 + \frac{R}{R'} (1+J^2) \right]}{\left[ 2 + \frac{R}{R'} (1-J^2) \right]^2} = \frac{300 [2 + 4(1+J^2)]}{[2 + 4(1-J^2)]^2} \dots\dots\dots (4.7)$$

so that for  $J = 0$

$$\frac{d\ddot{y}}{dJ} = 50 \text{ ft/sec}^2 \text{ per unit deflection} \quad (5.7)$$

7.8 There is however no suggestion that  $R/R' = 4$  is necessarily the best value: it must be regarded as no more than a starting point for investigation of non-linear joystick deflection-output laws which time has not permitted us to undertake. For example it may be that larger values of  $R/R'$  will give more uniform rates of joystick movement than that chosen.

However, owing to the presence of phase-advance there is no unique relation between joystick deflection and required lateral acceleration, except perhaps when for a significant fraction of the engagement, the lateral acceleration requirement has been negligible i.e. slow target and/or small value of  $\dot{d}$ . The maximum incremental stiffness occurs when  $|J| = 1$  and

this from (2.7) is  $v \left( 1 + \frac{R}{R'} \right)$ ; that is  $1 + \frac{R}{R'}$  times the value obtaining in the absence of  $R'$ .

7.9 Our admittedly sparse results are shown in Figs. 23-25a. The value  $R/R' = 4$  was retained throughout. The maximum demandable lateral acceleration has been varied from 100 ft/sec<sup>2</sup> to 300 ft/sec<sup>2</sup> and the phase-advance time-constant  $T_F$  from 1 to 4 secs. We interpret these results as broadly confirming that a non-linear joystick law based on our earlier reasoning is helpful in achieving a compromise between low and high target sight-line rate conditions. Also a maximum steady-state lateral acceleration demand of about 150 ft/sec<sup>2</sup> seems appropriate.

7.10 Fig.26 illustrates the relation between joystick deflection  $J$  and lateral acceleration demand when  $R/R' = 4$ . The following table gives the maximum and minimum incremental control stiffnesses corresponding to the three cases illustrated by Figs. 19-21a, together with the maximum demandable lateral acceleration, i.e. joystick held steady at  $J = 1$ .

Max. demandable lateral acceleration	Incremental Control Stiffness	
	$J = 0$	$J = 1$
100 ft/sec <sup>2</sup>	33.3 ft/sec <sup>2</sup>	500 ft/sec <sup>2</sup>
150 ft/sec <sup>2</sup>	50 ft/sec <sup>2</sup>	750 ft/sec <sup>2</sup>
300 ft/sec <sup>2</sup>	100 ft/sec <sup>2</sup>	1500 ft/sec <sup>2</sup>

## 8 A Two-man Guidance System

### 8.1 General

8.1.1 It has appeared from paras. 4.2, 4.3, 5.1, 5.2 that there are theoretical and practical difficulties in the design of a guidance loop in

which a man can aim at other than fixed or slowly crossing targets. These difficulties may be summarized as (a) a contradiction between the need for a high-order system to counteract lags, and for a low order system to ensure dynamic stability; (b) a contradiction between the need for relatively low capacity to demand lateral acceleration, in the interest of dynamic stability, and the large lateral accelerations required to ensure sight-line coincidence. We have therefore examined the possibility of reducing the aimer's task virtually to that of hitting a fixed target, by relieving him of some parts of the overall task. The following proposal to that end involves the use of an additional operator.

8.1.2 One man whom we designate A, has in his control a pair of trainable binoculars mounted on a stand. The binoculars possess cross-wires or something similar, and A endeavours to bring the intersection of these cross-wires as quickly as possible on to the target. Thereafter, as the target approaches, he continually moves the binoculars, trying to keep the target on the cross-wires throughout.

8.1.3 Connected to the binoculars, either by a mechanical or a servo linkage, is a second set through which the missile aimer, whom we call B, views the target. B has no control over the movement of his binoculars, and if A is successful, the target appears to B at a fixed point in his field of view, although of course any background such as cloud will appear to move.

8.1.4 If now, once B has gathered the missile on to the target sight-line, it could be arranged that without further action on B's part, the missile was automatically maintained on the target sight-line, then it could be said that B's task was virtually that of engaging a fixed target. The gathering operation also would be similar to that which occurs against a fixed target if by the same automatic means, the effect of target motion was cancelled out in this phase.

8.1.5 A good approximation to this state of affairs is possible if suitable voltage generators and pick-offs are attached to the binoculars. These must provide signals which are such functions of binocular, i.e. target sight-line rotations, that when applied to the missile control surfaces they produce the desired effect. It is shown in Appendix B that by generating voltages proportional to target sight-line rate, and suitably shaping these, a good approximation to the required acceleration demand is obtained.

## 8.2 Experimental Checks of Two-man Guidance

8.2.1 The primary objects of these checks were to confirm the relations established in Appendix B between binocular motion and missile lateral acceleration, and to ascertain how nearly the expected simplification of the aimer's task could be realised. The ultimate criterion was of course accuracy in attack. This latter aspect however was more fully considered within the framework of a later series of tests. In this, the two man guidance was one of several systems operated by service personnel, which were compared both from the standpoints of learning rate and accuracy. The outcome of this series is discussed elsewhere (para. 9 and Ref.6).

8.2.2 Preliminary tests showed clearly the importance of eliminating backlash in the binocular drive, of smoothing the generator output and of incorporating a flywheel to reduce the chance of excessive spurious acceleration demands on the missile due to spasmodic angular acceleration of the binoculars. Where, as in all these tests, the binoculars are mechanically driven by a crank handle through a gear train, the choice of gear ratio proves to be important though not unduly critical. The same is true of the crank radius.

8.2.3 A cranking rate of about 200 times the binocular angular rate gave conveniently smooth operation without excessive effort. The crank handle radius was 2 inches. To ensure reasonable freedom from excessive angular acceleration, a flywheel was driven at some 4.5 times the cranking speed. The moment of inertia of this flywheel was about 45 oz-in<sup>2</sup>. There was a small additional inertia due to the voltage generator and the gears, but this was largely swamped by friction. The maximum angular rate and angular acceleration required of the binoculars for correct target tracking are respectively

$$\dot{\theta}_T \approx 0.05 \text{ rad/sec} \quad \text{and} \quad \ddot{\theta}_T \approx 0.025 \text{ rad/sec}^2.$$

These figures lead to a maximum cranking speed of about 100 r.p.m. and a maximum force exerted on the handle of some 0.5 lb. The starting force is about 0.5 lb making a maximum total force of the order of 1 lb.

8.2.4 It is interesting to compare this crank diameter, cranking speed and inertia loading with some quoted in Ref.11. In para.44 loc.cit. it is suggested for example, that for compensatory tracking with no mechanical load, the optimum cranking diameter is in the range 3"-9" with a "useful general size of 4 $\frac{1}{2}$ " diameter". The optimum speed of turning is stated in para.41 loc.cit. to be related to the task and size of control. "High winding speeds, but not the maximum achievable have been found most effective in compensatory tracking tasks". "For smaller diameter cranks - of the order of 4" in diameter - speed of turning can be of the order of 200 r.p.m. .... With loads up to 5 Kg-cm the max. speed is only slightly reduced". Again, in para.47 loc.cit.: "Where there is friction it has been shown (Helson<sup>20</sup>) that inertia in the crank may have a beneficial effect .... (inertia) may be increased with beneficial effects up to a value where the force on the hand-wheel handle required to provide maximum acceleration is at least 10 lb."

8.2.5 Having overcome the mechanical problems it was possible to show that within the ranges of  $\dot{\theta}_T$  and  $\ddot{\theta}_T$  implicit in the specification, the missile could be made to remain at the intersection of the binocular cross-wires except perhaps at the greatest values. Here there was a tendency for the missile to lag behind. It is difficult to determine how far this is due to the natural limitations of the tracker and how far to the imperfection of the apparatus. However the errors were well within the capacity of the aimer B to correct even though the parameters of his apparatus were chosen for fixed target conditions.

8.2.6 For reasons discussed in Appendix D it is necessary to arrange that the acceleration demand limits embodied in aimer B's apparatus are controlled by the magnitude of the acceleration demand arising from binocular motion. The immediate object is to ensure that at any instant the sum of the two demands should not exceed the missile's capacity. No detailed thought has been given to circuits for this purpose. It was thought sufficient at this stage to devise a simple but adequate expedient. It is worth noticing that the lateral acceleration demand from the binoculars at any instant only requires the aimer's limits to be restricted in one polarity. It proved desirable however, to apply the restriction to both sides. If this is not done the aimer is aware of an asymmetry of response to his joystick in that lateral velocity is more slowly built up in the direction of rotation of the sight-line than in any other. This is disturbing to his performance. However in the tests described in this Note, no attempt was made to keep the limits symmetrical. It therefore remains to carry out further tests in which this provision is made.

### 8.3 Some Drawbacks of the Two-man Guidance System

8.3.1 The binocular-operated guidance signal is subject to error. For example, the binoculars will almost certainly not keep accurate track of the target: one good reason for this is that it is impracticable to include a sufficient number of integrations in the tracking loop to eliminate lags without losing dynamic stability. On the other hand, such experiments as have been made show that a skilled tracker contrives to keep these lags quite small even with directly driven binoculars. Also the aimer, using his joystick, tends to correct errors arising in this way.

8.3.2 If the apparatus is mounted on a rolling and pitching platform, such as the deck of a ship, the tracker will have to move his binoculars to offset this. This corrective action will produce spurious demands for missile manoeuvre, so that a stabilized platform is necessary or else an additional corrective signal from a gyro-stabilized source.

8.3.3 The fact that two skilled men rather than one are needed is an additional drawback since, in addition to increasing manpower needs, this halves the freedom of choice in selecting personnel. Finally it is obvious that relatively complicated apparatus will be needed, with its attendant maintenance problems, probably in adverse conditions.

### 8.4 Use of Angular Accelerometers

8.4.1 As an alternative to using a generator producing a voltage proportional to  $\dot{\theta}_T$  and deriving from it another proportional to  $\ddot{\theta}_T$ , it is possible, in theory at least, to use an angular accelerometer. This would produce a voltage proportional to  $\ddot{\theta}_T$  which could be time-integrated to give  $\dot{\theta}_T$ . For well-known technical reasons the integrating process is preferable to differentiation. However, no suitable accelerometers have come to hand.

## 9 Comparative Tests of Competing Techniques

9.1 Ten Naval ratings from H.M.S. "Excellent", were chosen for a series of tests designed to investigate learning patterns for control tasks of the type discussed in this Note. These tests were designed and controlled by the Applied Psychology Research Unit of the Medical Research Council, using the apparatus built and installed here for the "Green Light" studies. The results are fully treated in Ref.6. We concern ourselves here only with those bearing on the relative merits of the various techniques dealt with by this Note.

9.2 The experimental conditions were as in the work described in this Note except that the range of target properties was restricted. To represent the worst conditions, a target having a speed of 900 ft/sec and a crossing distance of 900 ft was simulated. Intermediate conditions were represented by a target speed of 700 ft/sec and a crossing distance of 600 ft. Finally a 700 ft/sec target at zero crossing distance was used to observe performance with zero sight-line rotation.

9.3 All the subjects were trained, using crossing targets only, on a monocular having X10 magnification. This was rigidly coupled to a similar instrument used by a trained tracker. The sole function of the latter was to keep the target within the aimer's field of view at all times, not necessarily at the centre, except in system (b) quoted in para. 9.4 below.

9.4 The following systems were compared:

- (a) A two-man system in which the tracker's sole task was to keep the target in the aimer's field of view. No aiding signal was derived from the monocular rotation.

(b) A two-man system as described in para.8. Here the tracker attempted to keep the target accurately at the intersection of cross-wires in his field of view.

(c) A one-man system in which the aimer used X5 binoculars mounted on a specially designed sight (Fig.27). This is arranged so that the axes of rotation of the binoculars coincide as nearly as possible with those of the aimer's head, and all weights are counterbalanced in it. The joystick was added for our purposes, being mounted so as to move with the aimer's right hand as he moved the binoculars.

(d) A one-man system using open sights.

(e) A one-man system using a fixed X10 monocular.

9.5 The best results were obtained with system (b), with system (c) a close second; these were followed in order of merit by (d), (e) and (a) well behind. System (b) gives the impression of being easier to operate from the aimer's point of view than (c), but the differences between the degrees of success obtained are not great enough to support this impression. In the particular monoculars used, the cone of view in degrees is given by

$\frac{60}{\text{magnification}}$ . Using these, an X10 magnification seemed desirable having regard to the so-called space threshold of the human operator. This is the phenomenon whereby the operator is insensitive to angular displacements or errors below a more or less definite limit. The magnification must be such as to render this angle insignificant. On the other hand such high magnification leads to difficulty in locating the target and in keeping the missile in the field of view. Difficulty would probably arise especially at the beginning of an engagement owing to launching dispersions, and also at the end if the changes in sight-line direction are large. In the most adverse conditions, this angular change may well be  $10^\circ$  or more. The sight referred to under (c) in para. 9.4 is a standard Naval pattern Air Look-out Sight. It is understood that this is comparable in performance with existing forms of gyro-stabilized sights.

9.6 None of the systems tested appears to give a high chance of a direct hit for the greater sight-line rates. In these circumstances miss distances of the order of 15 ft occurred. It is clear that the implications in terms of further system development and/or proximity fuses call for some thought. In this connection it is worth recalling that the non-linear joystick might repay closer study. Also the two-man system of para.8, while not significantly better in performance at this stage than the Air Look-out Sight, is probably the one, of those considered, most capable of further development, and this may possibly outweigh the disadvantages of additional manpower requirement and relative complexity.

## Part II

### Description of the Simulators

#### 1 Introduction

The following paragraphs describe, in principle, the two simulators used to study the control of a ship to air visual command link guided missile. The two simulators are designated Laboratory and Field Simulators respectively and their use in the control system investigation for this type of missile is dealt with in Part I of this Note.

#### 2 Laboratory Simulator

##### 2.1 General

2.1.1 The Laboratory Simulator has been constructed to present the operator with a display in which the relative angular positions of target and missile are identical to those which would be encountered in the practical case, subject to the assumptions made in producing the analogue; namely that roll stabilization is perfect and that the missile aerodynamics can be sufficiently represented by simple networks. Also no account is taken of gravity and the horizontal missile range at any instant is assumed equal to the length of the sight-line.

2.1.2 All the D.C. amplifiers used in the simulator are of a high gain, drift corrected type except for those in the control unit, which have a gain of approximately 200 and no drift correction.

2.1.3 In general the errors in setting up individual computing units within the simulator do not lie outside the limits of  $\pm 1\%$  of the desired values.

2.1.4 For the purpose of the following description the simulator will be sub-divided into four separate units:-

- (i) Display Unit
- (ii) Missile Unit
- (iii) Control Unit
- (iv) Target Simulator.

2.1.5 A block diagram of the simulator is given in Fig.28 showing the control loop closed by the human operators. Fig.29 shows a photograph of the complete simulator.

#### 2.2 Display Unit

2.2.1 Function. The function of this unit is to compute the angular position of the missile from a knowledge of its lateral displacement and range at any instant. Fig.30 shows a block diagram of the unit. In Fig.29 the Display Unit computing equipment is contained in the right hand cabinet.

2.2.2 Display. Illustrated in Fig.30 is the general arrangement of the display. A beam of light reflected from a gyro-gunsight mirror is focussed on to a screen 184 inches distant, where it forms a small spot of light representing the missile flare. Currents through the deflection coils of the G.G.S. mirror will cause this spot to move. The computing equipment of the Display Unit is then required to produce the deflection current. Fig.31 shows a graph of "missile" angular displacement (beam deflection) against deflection current.

2.2.3 G.G.S. Mirror Driving Stage. This stage consists of a high gain, drift corrected D.C. amplifier with a cathode follower output to match the low impedance of the G.G.S. mirror deflection coils, the latter being re-wound to give a resistance of  $450 \Omega$ . The overall steady state gain of the driving stage is unity and the scale of the input is  $K_2 = 2$  volts/degree, taking into account the optical gain of two between incident and reflected angles of the light generating the "missile flare". Included in the input circuit is a phase advancing network  $C$ ,  $R$  and  $R_1$  which improves the G.G.S. mirror frequency response so that it is substantially level up to 3 c/s (see Fig.32), i.e. slightly greater than the missile weathercock frequency of 2.83 c/s. Component values of the phase advancing network were determined empirically.

2.2.4 Range Unit Amplifier. The computation of missile angular position from lateral displacement and range information is carried out by this unit. Consideration of the geometry of the sight line between operator and missile when the latter is displaced by a distance  $y$  from a datum, at range  $r_M$ , gives the angle subtended at the operator's eye to be

$$\theta = \frac{y}{r_M} \quad \text{for small values of } \theta.$$

Re-writing the above equation we have

$$\frac{\theta}{y} = \frac{1}{r_M} \quad (1)$$

Referring to Fig.30 and using the symbols noted, the gain of the Range Unit Amplifier can be derived as follows, assuming the open loop gain to be  $-\infty$  and that  $R_3/R_4 \gg 1$ . (In practice the open loop gain is  $> 10^5$  and  $R_3/R_4 = 10$ .) Equating currents through  $R_2$  and  $R_3$ , we have

$$\frac{y K_1}{R_2} = - \frac{\alpha \theta K_2}{R_3}$$

where  $\alpha$  is the position of the wiper of  $R_4$  expressed as a fraction of its total movement, and  $K_1$  and  $K_2$  are the scale factors for  $y$  and  $\theta$  respectively. Thus the amplifier gain is

$$\frac{\theta K_2}{y K_1} = - \frac{R_3}{R_2} \cdot \frac{1}{\alpha} \quad (2)$$

Comparing equations (1) and (2), it is seen that if  $\alpha$  is proportional to  $r_M$ , the output of the Range Unit Amplifier is proportional to  $\theta$ . The proportionality is achieved in practice by driving the wiper of  $R_4$  by a velodyne (Range Unit Velodyne in Fig.30) whose speed is scaled to the missile velocity.

In equation (2)  $R_3/R_2$  sets the maximum missile range (i.e. when  $\alpha = 1$ ) and in this case it is equivalent to 19,500 ft.

The minimum range which can be simulated depends on the open loop gain of the D.C. amplifier. When the open loop gain is  $-M$ , and  $M$  is positive, it can be shown that

$$\frac{\theta K_2}{y K_1} = - \frac{R_3}{R_2} \left[ \frac{1}{\alpha + \frac{1}{M} \left( \frac{R_3}{R_2} + 1 \right)} \right] \quad (3)$$

But the relations on which the simulation is based imply that

$$\frac{1}{M} \left( \frac{R_3}{R_2} + 1 \right) \ll \alpha ;$$

thus, if an accuracy is stipulated and  $M$  is known, the least permissible  $\alpha$  is determined. There is, however, a practical lower limit for  $\alpha$  governed by increase in amplifier output drift and noise as the closed loop gain increases. This is insignificant after about  $\frac{1}{2}$  second from launching. Since the analogue is based on the assumptions that changes in sight-line angle are small and that the normal distance between the operator's eye and the light beam is negligible, it would in any case be contradictory to take account of very small ranges which invalidate these assumptions.

In the present study there is moreover no advantage in a simulation from the instant of launch because aerodynamic control during the very early stages of boost will be negligible.

A minimum value of  $\alpha$  was chosen equivalent to a range of about 30 feet which corresponds to the distance travelled by the missile in 0.5 seconds of flight. This gives from (3) a minimum  $\alpha$  of  $\frac{30}{19500} = 6.5 \times 10^{-3}$  and hence a maximum  $R_3/\alpha R_2$  from (3) of 45.2.

**2.2.5 Missile Speed Programme.** Fig.2 shows a graph of the estimated speed/time characteristic for G.L.T.V. and a table of expected weight and thrust figures, which were taken as data for the simulated missile speed programme. Referring to Fig.30 it can be seen that a Thrust Programme is obtained from a potentiometer between H.T. and earth, the voltageappings being scaled to the boost and sustainer accelerations. The scale factor chosen was 3.2 volts/'g' ( $K_3$  on Fig.30) and the missile accelerations were taken to be 6.8'g' and 1.1'g', assuming mean weights for the boost and sustainer phases. The programme of acceleration is obtained by indexing a uni-selector by means of a suitable time delay circuit to give a boost period of 3 seconds and sustainer period of 14.5 seconds. The selected acceleration is subsequently integrated to supply a "velocity" input to the Range Unit Velodyne. Included in the input of the Thrust/Velocity integrator is a subtracting term, proportional to minus the square of the missile velocity, which simulates profile drag. This voltage is derived from a multiplier in the Missile Unit and its amplitude was adjusted empirically until the desired Speed/Time characteristic was obtained from the velodyne.

**2.2.6 Initial Conditions at Instant of Launch.** The distance between the aimer and launcher, and the initial angular dispersion of the missile at launch are represented by the addition of constant input voltages to the Range Unit Amplifier and Driving Stage. The voltage sources are potentiometers denoted as "Set Lateral Displacement" and "Set Angular Dispersion" on Fig.30. The potentiometers are calibrated in feet for Lateral Displacement and in degrees for Angular Dispersion.

**2.2.7** Also available in the Display Unit are voltages proportional to missile speed and range for use elsewhere in the simulator. The derivation of these quantities is indicated on Fig.30.

## 2.3 Missile Unit

**2.3.1 Function.** The function of the Missile Unit is to compute lateral displacement from a knowledge of the missile aerodynamic properties and the demanded wing angles. In other words, the unit is an analogue of the missile subject to some approximations yet to be discussed. Fig.32 gives a detailed block diagram of the simulation; in Fig.29 the missile unit occupies the centre cabinet.

2.3.2 Missile Aerodynamic Analogue. On the strength of previous experience, the missile weathercock properties are disregarded for simulation purposes. It is however assumed to have the following properties: (i) it is subject to profile drag, (ii) a large part of its lateral acceleration depends on developing incidence, which is assumed subject to an exponential growth, (iii) lateral acceleration per unit wing deflection is proportional to  $v_M^2$ , and (iv) there is a fixed maximum wing deflection. Condition (i) is satisfied within the Display Unit (see para. 2.2.5), and (iii) and (iv) are dealt with in paras. 2.3.3 and 2.3.5 respectively. Here we are concerned with (ii).

Referring to Fig.33, the summing amplifier  $\Sigma_1$  is used to compute the lateral acceleration of the missile from an input proportional to wing angle  $\delta$ . (No actuator is simulated, therefore  $\delta_D = \delta$ .) The transfer function of  $\Sigma_1$  is

$$\frac{V_o}{\delta K_6} = \frac{R_F(2R_2+R_1)}{2R_2} \left( \frac{1 + p \tau_2}{1 + p \tau_1} \right) \quad (4)$$

in terms of the symbols noted on Fig.33. The voltage  $V_o$  corresponds to the lateral acceleration developed when  $v_M = 1000$  ft/sec (see para. 2.3.3).

Substituting component values in (4) and expressing as a function of time for a unit step of  $\delta K_6$ , we have

$$\frac{V_o}{\delta K_6} = 2.61 \left[ 1 - 0.705 e^{-7.36t} \right] \quad (5)$$

Fig.34 shows the above curve (plotted to a steady state value of 1243 ft/sec<sup>2</sup>) compared with the lateral acceleration response of G.L.T.V. This is the estimated steady state lateral acceleration per unit step wing deflection at a forward speed of 705 ft/sec.

The difference between simulator and G.L.T.V. lateral motion is more easily seen in Fig.4, in which the lateral displacement response of G.L.T.V. - without an actuator and weathercock damping - is compared with its analogue. For  $\delta_{max}$  of 0.2 rad. the difference in displacement when the steady state is reached ( $t > 0.8$  sec) is approximately 16 feet. However, in this general study of the ship to air command link missile, it was considered that an approximate representation of lateral response would suffice, given that the lateral acceleration due to incidence had a time constant sufficiently great to be pessimistic for this type of missile. Then, to some extent allowance is made for unknown parameters such as wing actuator and guidance lags.

2.3.3 Variation of Aerodynamic Stiffness with Missile Speed. For the purpose of investigating control during the boost phase, a method was required of varying the lateral acceleration response with missile speed, to give a more accurate simulation of its performance.

As shown on Fig.3

$$\frac{\ddot{y}}{\delta} = 1243 \text{ ft/sec}^2/\text{rad.}$$

in the steady state when  $v_M = 705$  ft/sec. Making the assumption that  $\ddot{y}/\delta$  varies as the square of the forward velocity we can write

$$\frac{\ddot{y}}{\delta} = 26.1 \times 10^{-4} \cdot v_M^2 \text{ ft/sec}^2/\text{rad.} \quad (6)$$

where  $v_M$  is the missile velocity.

The method used to give this stiffness law is shown in Fig.33 where the output of  $\Sigma_1$  is applied to the multiplying potentiometer of an electro-mechanical multiplier. The second input for this unit is derived from a similar multiplier which squares a voltage proportional to  $v_M$  - the latter obtained from the Display Unit. The transfer function of  $\Sigma_1$  is arranged to be the simulation of the missile for a forward speed of 1000 ft/sec and similarly the maximum input to the multiplier is also equivalent to this speed. The resultant scale factors are noted on the block diagram.

2.3.4 Computing Lateral Displacement. The missile lateral acceleration analogue voltage,  $\dot{y} K_7$ , is integrated twice to produce a voltage  $y K_1$  to feed into the Display Unit.

2.3.5 Wing Stops. The maximum values of  $\delta$  are given as  $\pm 0.2$  radians. In the analogue the wing stops are represented in  $\Sigma_1$  by diodes which limit the lateral acceleration to the value produced by the maximum wing deflection. From equation (7), substituting  $\delta = 0.2$  and  $v_M = 1000$  ft/sec we have  $\dot{y} = 522$  ft/sec<sup>2</sup> which is represented by limiting at 52.2 volts (scale factor  $K_7 = 0.1$  volt/ft/sec<sup>2</sup>). The diodes are connected to the cathode follower grid within  $\Sigma_1$  to obtain a sharp limiting characteristic (Ref.7).

## 2.4 Control Unit

2.4.1 Function. The function of the control unit is to translate joystick deflections into wing angle demands and where relevant to perform a like operation on movements of the tracking monocular.

Fig.34 shows a block diagram of the control unit and for the purpose of this description it will be sub-divided as follows:

- (i) Aimer's Demand Channel
- (ii) Tracker's Demand Channel

where the "aimer" is the man operating the joystick whose monocular is controlled for him by the "tracker" (see para.8, Part I).

2.4.2 Aimer's Demand Channel. The aimer is equipped with a thumb-operated joystick (Ref.8) by means of which he can demand, in pitch or yaw, a wing angle  $\delta_1$  proportional to joystick deflection together with an angle which, assuming linear operation, is

$$\delta_2 = \frac{K_1 p J}{1 + p T'}$$

where  $\delta$  is the wing deflection,  $J$  the joystick deflection and  $K_1, T'$  are constants. Since the lateral acceleration is proportional to wing deflection at a given missile speed, this second channel may be regarded as producing a change in lateral velocity proportional to joystick deflection, subject to an exponential time lag of time constant  $T'$ . It will be convenient in this para. to refer to this as a lateral velocity-demanding channel while the direct application of the joystick voltage to the wing actuator is defined as a lateral acceleration-demanding channel. If the wing angle in the latter case is  $\delta_1$  we have for the combination

$$\delta = \delta_1 + \delta_2 = K_2 J + \frac{K_1 p J}{1 + p T'} = \frac{K_2 J (1 + p T_F)}{1 + p T'}$$

where  $K_2, T_F$  are constants. The arrangement may therefore also be regarded as a phase-advanced acceleration demand - the form in which it has been discussed previously.

The lateral velocity demand is achieved by means of the closed loop  $\Sigma_1$ ,  $R_1$  and  $I_1$  shown in Fig.34, whose output is such that the time-integral of wing-deflection demanded is proportional to joystick deflection, but with an exponential lag.

Included in reversing amplifier  $R_1$  are limiting diodes. The effect of these is to limit the demand for wing deflection to  $\pm 0.2$  radian while ensuring that the time-integral of wing deflection remains proportional to joystick deflection, whatever the movement of the joystick. This is intended to mitigate any loss of the effects of phase advancing the joystick output which might arise if the demand for wing angle were excessive. Its operation and validity are more fully discussed in Appendix D. Fig.35 shows the relevant part of Fig.34. The limiting voltages in  $R_1$  are asymmetrically controlled about the steady state values by the total acceleration demand, i.e. the output of  $\Sigma_4$ . This is necessary to ensure that wing angle demands to maintain the missile on a rotating sight-line do not exceed the maximum wing angle available (see para. 8.2.5 Part I). From Fig.34 it will be seen that  $\Sigma_2$  and  $\Sigma_3$  compute the limiting voltages. The diodes  $L_1$  and  $L_2$  associated with  $\Sigma_2$  and  $\Sigma_3$  prevent polarity reversal of the limiting voltages which would otherwise occur when the tracker's monocular rate was high. Fig.36 shows recordings of demanded wing angle  $\delta_D$  for various amplitudes of stepwise joystick deflection. It will be seen that when the demand increases beyond the level at which the limits act, the demanded wing angle  $\delta_D$  is maintained at its maximum for an increasing length of time. This ensures that the desired time-integral of wing-angle and hence change in lateral velocity is achieved, even though this takes longer than is the case in the linear regime. A typical lateral velocity response to a stepwise joystick movement is shown in Fig.37.

The lateral acceleration component of the aimer's control is obtained through  $R_2$ ,  $\Sigma_4$  in Fig.34 and finally added to the velocity wing angle demand at  $\Sigma_5$ . The output of  $R_2$  supplies a potentiometer which is calibrated in terms of the acceleration/velocity stiffness ratio, denoted by  $a = 1/T_F$ , for values from zero to two.

To vary the aimer's control stiffness the joystick supply voltage was made variable and connected to a suitable meter which was calibrated in lateral velocity stiffness. The maximum lateral velocity demand available was 450 ft/sec. A further requirement for the purpose of control system investigation was to provide a non-linear output from the joystick (Ref.2). As shown in Fig.34 this is accomplished by loading the output with a resistor denoted as  $R'$ . Fig.26 shows a curve of the joystick output against deflection for  $R' = 11 \text{ K}\Omega$ , the value used in the simulator work, when the joystick potentiometer resistance was 45 K approx.

**2.4.3 Tracker's Demand Channel.** The principle and design of the Tracker's Demand Channel are dealt with in para.8 Part I and Appendix B of this Note; the following paragraphs will only note the practical difficulties encountered in setting the circuit in operation.

To simplify the mechanical construction required to rotate the monoculars, only tracking in the up/down plane was considered. The arrangement used was a simple anti-backlash gear-box and attached to the appropriate shafts were the monoculars, a D.C. generator and a handle. The gear ratio between generator and monocular shaft was approximately 3600:1 and between handle and monocular shaft approximately 200:1. No attempt was made to optimise the latter gear ratio with respect to the operator. From Fig.34 it will be seen that the Tracker's Demand Channel consists of generator  $G$  and computing elements  $R_3$ ,  $D_1$  and  $\Sigma_6$ , the output of the latter being added at the input of  $\Sigma_4$  to the joystick acceleration demand.

Generator G (in fact, an integrating motor) had a three segment commutator which immediately gave rise to noise difficulties when the output was differentiated by  $D_1$ . This led to the inclusion, in the generator output, of a low pass filter to reduce the noise level to tolerable proportions. Details of the filter are shown on Fig.38.

Further noise was introduced into the system by natural tremor on the part of the tracker. To counter this, the inertia load on the tracker's handwheel was greatly increased by adding a flywheel (para 8.2.3, Part I) rotating at about 4.5 times the cranking speed.

A more elaborate Binocular Tracking Stand has been constructed which will permit a more realistic and wider approach to this type of two-man control system than was possible with the laboratory built equipment described in the text. The new tracking stand is now in the hands of the G.L.T.V. contractors.

## 2.5 Target Simulator

2.5.1 Function. To facilitate the study of possible control systems for the ship to air command link missile an idealised target is required whose apparent motion can be accurately controlled. This type of target then lends itself to analytical treatment (Ref.9). The analogue used was set up to simulate a target flying towards the aimer at a given height and speed so that it would pass directly overhead. Referring to Fig.29 the Target Simulator is on the right hand side of the aiming stand and its associated control panel is situated in the centre of the left hand cabinet.

2.5.2 Target Analogue. Fig.39 shows the flight path geometry of the type of target considered, which has velocity  $v_T$  ft/sec, crossing distance  $d$  feet and is visually acquired at range  $r_{T_0}$ . Then the aimer's sight-line angle expressed as a function of time is

$$\theta_T = \tan^{-1} \frac{d}{r_{T_0} - v_T t} \quad (7)$$

Equation (7) suggests a method of simulating the target in which the sight line angle is computed by the method of similar triangles. Fig.40 shows the basic construction of the analogue where

$$\theta_T = \tan^{-1} \frac{d}{r_{T_0} - v_T t} = \tan^{-1} \frac{d'}{r'_0 - v'_T t}$$

The scale chosen for  $d'$ ,  $r'_0$  and  $v'_T$  was  $0.001" = 4$  ft, which resulted in a compact unit where  $r'_{0\max} = 5$  inches ( $\equiv 20,000$  ft),  $d'_{\max} = 0.25$  inches ( $\equiv 1000$  ft) and  $v'_{\max} = 0.25$  inches/sec ( $\equiv 1000$  ft/sec). Due to this scaling precision manufacturing techniques were essential.

2.5.3 Description of Target Simulator. Fig.41 shows a schematic diagram of the simulator. The leadscrew is driven by a velodyne through a 10:1 reduction gear and the sight-line arm is spring loaded to maintain contact with the pin attached to the leadscrew nut: movement of the nut imparts the required rotational motion to the sight-line arm.

To effect the target display a beam of light is directed on to the mirror attached to the pivot shaft of the sight-line arm. The resultant reflection appears on the display screen as a spot of light  $1\frac{1}{2}$  inches in

diameter with superimposed crossed lines. The axis of rotation of the mirror coincides with the incident light beam so that the angle between the incident light and the normal to mirror surface at the point of reflection is constant at all times; thereby ensuring that the angular movement of the sight-line arm is reproduced by the light beam to the screen.

The analogue of crossing distance  $d'$  (Fig.40) is set by a micrometer adjustment which moves the datum level with respect to the centre line of the leadscrew. Target speed is controlled by RV2 (Fig.41) and a suitable voltmeter connected to the control potential is calibrated in feet per second. Target range information is obtained from RV1 whose wiper is mechanically coupled to the leadscrew nut; a meter is connected to the wiper and calibrated in target range.

2.5.4 Computation of Impact Range. Fig.42 shows a circuit of the method adopted to compute the impact range of target and missile. A voltage proportional to target range is obtained from RV1 and to missile range from RV3 in the Display Unit (Fig.30), so that if the voltage scales are equal impact occurs when the potential between wipers of RV1 and RV3 is zero. In practice the scale of RV3 was adjusted to equal that of RV1 by trimming resistors, and equality of outputs was detected by a sensitive polarised relay, REL.1 as shown in Fig.42. It is appreciated that this method of computing impact range is subject to errors due to the finite release current of REL.1, but it has the obvious advantage of simplicity and in practice the errors were sufficiently small to be neglected (see Fig.43). Initially the release current was adjusted to be  $4\mu A$  but this led to unreliability of operation; consequently it was increased to  $10\mu A$  where satisfactory performance was achieved.

The release of REL.1 at impact range is used to operate further relays which stop both target and missile simulators thereby allowing a measurement of the miss distance to be made. The target simulator was stopped by removing both H.T. and 24 volt supplies and the fairly high friction load on the velodyne was used as a brake. The missile simulator was stopped by shorting the inputs of  $\int_2$  (Fig.33) and the Range Unit Velodyne (Fig.33) to earth and the former holding the "missile" in its position at impact range. The finite time required to bring the Range Unit Velodyne to rest resulted in a small movement of the "missile" after the impact instant which was subsequently reduced by addition of phase advance to the velodyne input. However, any future applications of this system would benefit by using an electromagnetic clutch between the velodyne and range potentiometers.

### 3 The Field Simulator

#### 3.1 General

3.1.1 The field simulator, which is installed in a trailer, is similar to the laboratory simulator described in para.2, Part II in respect of missile and guidance simulation. That is, the circuits connecting the joystick output to a gyro gunsight mirror which controls the display of angular motion of the aimer-missile sight-line, is similar. The methods of missile display and target presentation are quite different.

3.1.2 In place of the artificial target used in the laboratory, real targets are viewed through binoculars. This fact gives the field simulator the advantage of enabling field experience to be gained and of providing a realistic check on the laboratory work. The missile display is described under the heading of the aiming stand (para.3.2 below).

### 3.2 The Aiming Stand

3.2.1 The aiming stand (Fig.44) provides for two operators, each having a pair of binoculars. These are constrained always to view in parallel directions and the assembly, being counterbalanced, is readily brought to bear on the target, within a small cone whose angle is approximately 20 degrees.

3.2.2 As in the laboratory simulator, the missile is presented to the observer as a spot of light representing a tail flare. It is necessary to arrange that as the viewing direction is changed, the apparent position of the missile in space is unaltered, as would of course be the case in reality. It is also necessary to avoid the application of precessing torques to the gunsight mirror other than through the action of its deflection coils.

3.2.3 The requirements of para. 3.2.2 are met by a freely pivoted arrangement of parallel bars which is illustrated diagrammatically for the horizontal plane, in Fig.45. ABCDEF is this arrangement, there being free pivots at the lettered points. Training the binoculars in azimuth consists in their rotation, together with the two stools on which the observers sit about the main pivot P. When this occurs, the member FC also rotates, carrying with it a camera (d), the prisms (e) (f), the two binoculars and the joystick. The member AE however is unable to rotate so that the member BD only undergoes translational movement.

3.2.4 A collimator and light source, together with the gyro gunsight (a) and a glass plate (b) are rigidly attached to BD and therefore these too cannot rotate. The glass plate (b) reflects into the aimer's left eye, the light reflected by the gunsight mirror (a) received from the collimator, and it is this that represents the missile. If therefore the mirror is not precessed, the apparent aimer-missile sight-line does not change its direction with respect to earth when the binoculars are moved. Nor is the mirror subjected to any precession torques by this movement - only translational motion is demanded of it.

3.2.5 The prism (f) which transmits light from the collimator to the aimer's eye, also reflects part of it to the prism (e) which in turn reflects into the camera (d). The image of the target is transmitted by the glass plate (b) and the prism (f) to the aimer's eye, and also it is reflected by (f) so as to reach the camera. Both aimer and camera therefore have images of both target and missile in their correct relative angular positions. Operation of the aimer's joystick precesses the mirror so as to simulate missile guidance and thus all necessary conditions are satisfied. The optical arrangements are shown in greater detail in Fig.46.

### 3.3 Missile Simulation

3.3.1 The missile simulation is carried out in the same way as in the laboratory simulator except for two further simplifications: there is no control during boost and the missile is assumed to have a constant forward speed of 705 ft/sec.

### 3.4 Launcher Angle Storage

3.4.1 In the laboratory, the target analogue always approaches from an accurately predictable direction and hence the missile flight path datum can be preset. In field conditions however, the angular position of the (real) target at launch cannot be accurately predicted. Since it is necessary to control the initial angular dispersion of the missile it is necessary to simulate the effect of having a launcher "slaved" to the aimer's binoculars.

3.4.2 The methods used to simulate the tracking launcher are shown diagrammatically in Fig.48. Voltages proportional to sight-line angles in azimuth and elevation are obtained from potentiometers driven by the corresponding angular movements of the aiming stand. These are fed to capacitors  $C_1$  and  $C_2$ . When the firing button is pressed the condensers are isolated from the aiming stand potentiometers and remain charged at voltages proportional to the azimuth and elevation angles at that instant. These voltages are then applied to power amplifiers as demands for mirror angle. The circuits involved are of sufficiently high impedance that the exponential decay of the capacitor charge over a period of one minute is less than 2%.

3.4.3 Dispersions of the missile off the launcher can now be set directly as angles from the launcher datum at the instant of firing. As with the laboratory simulator, provision is made for simulating a launcher displaced some distance from the aimer.

### 3.5 Target aiming point

3.5.1 To facilitate investigations of the effects of target crossing distances an aiming point, in the form of a sodium lamp, is provided for the pilot of the target aircraft. This lamp can be placed on the ground to one side of the trailer at a distance equal to the crossing distance being investigated, in a direction normal to the agreed line of flight.

### 3.6 Communications

One member of the simulator team normally occupies a position from which he is able to observe, through a roof trap, the air traffic in the vicinity and he maintains V.H.F. communication with the target aircraft and Flying Control at all times.

### Conclusions

(1) Studies which have included the use of a simulated missile to attack both simulated and real targets suggest that it is practicable to devise a visual command link with manual guidance, to direct a guided missile against a constant speed, approaching aircraft whose speed is not greater than 900 ft/sec and whose crossing distance is not greater than 900 ft subject to certain provisos. These are

- (i) Miss distances of the order of 15 ft from target centre are acceptable.
- (ii) Launching Dispersions are small.
- (iii) Acquisition ranges are not significantly less than about 15,000 ft.
- (iv) Preparation times  $T_p$  do not exceed 5 seconds.
- (v) A minimum impact range of 4000 ft is acceptable.
- (vi) Some useful measure of control is available during, say, the last second of a 3 second boost.

(2) Given that the other parameters remain unaltered, the minimum impact range could be raised to 4500 ft if the acquisition range were increased by about 1200 ft. Clearly this is a critical parameter for high speed targets. A similar increase gives the requisite 5 seconds of guidance time exclusive of any control during boost. If the acquisition range remains unaltered at 15,000 ft relatively large changes in other parameters would be required to give similar results.

(3) Two systems are available for the guidance. One, which utilizes a single operator, makes use of a special air look-out sight in order to simplify the operator's task. Even so, it is distinctly more difficult than an attack on a fixed target.

(4) The second system uses two men, one of whom, the tracker, is exclusively concerned with tracking the target. By means of electrical generators and networks, a supplementary guidance signal is derived from the motion of the tracking monocular. This involves the use of a stabilized platform for the aiming gear, or else some form of compensation for rolling and pitching, if the aiming point is aboard ship. On the other hand the task of the aimer, who operates the joystick, is rendered very little more difficult than that of attacking a fixed target.

(5) There is little difference in performance to report between the two systems discussed, but it is thought that the two-man system may be potentially more accurate, there being more scope for development.

(6) While the studies described are very encouraging, it would be unwise to assume, without further proof, that a weapon system of this type is bound to be successful. In particular the capabilities of representative operators in controlling a real missile need to be investigated under field conditions.

#### REFERENCES

<u>No.</u>	<u>Author</u>	<u>Title, etc.</u>
1	W. Elfers and D.W. Allen	Simulator Studies of a Command Controlled Anti-tank Missile R.A.E. Tech. Note G.W.218
2	M. Squires and D.W. Allen	An Open-loop Command Link Control System with Application to Project J R.A.E. Tech. Note G.W.325
3	R.J.A. Paul and R. Ball	"G.L.T.V. - Control and Guidance" Quarterly Progress Report No.1 Messrs. Short Bros. and Harland Ltd. Report No. RDC 11
4	R.J. Gossage	A Note on Visual Acquisition and Engagement of High Speed Aircraft A.G.E. Note, February 1955
5	-	"G.L.T.V. - Control and Guidance" Quarterly Progress Report No.2 Messrs. Short Bros. and Harland Ltd. Report No. RD 17
6	C.B. Gibbs and D.W. Allen	An Investigation of Proposed Control and Display Arrangements for Ship to Air G.W. "Green Light" Communicated November 1955 by Applied Psychology Research Unit of the Medical Research Council
7	M. Squires and P.R. Benyon	The use of Negative Feedback for deriving Sharp Limits in Electronic Analogue Computers R.A.E. Tech. Note G.W.361
8	R.W. Holman	The Development and Trials of a Command Link Guidance System R.A.E. Tech. Note G.W.294

REFERENCES (Contd.)

<u>No.</u>	<u>Author</u>	<u>Title, etc.</u>
9	G.B. Longden	Acceleration Requirements of a line of sight course against evading Targets R.R.D.E. Report No.329
10	-	G.L.T.V. Panel Minutes, Meeting No.1, 7-9-54 para.4
11	-	Some Human Factors in the Design of Controls - an evaluation of the literature Naval Motion Study Unit Report No.61 Admiralty Depts. of Physical Research and of the Senior Psychologist, October 1954

Attached:

Appendices A, B, C, D and E  
 Drgs. GW/E/6987 to 7044  
 Negs.124598-124600  
 Detachable Abstract Cards

Advance Distribution:Ministry of Supply

Chief Scientist  
 CGWL  
 DG/GW - 90  
 DLRD(A)  
 DG of A  
 TPA3/TIB - 90

R.A.E.

Director  
 DD(E)  
 DD(A)  
 RFD - 3  
 Radio  
 Arm  
 IAP  
 GWTD  
 GWTW  
 Patents  
 RAE Bedford Library  
 Library

# APPENDIX A

## The Lateral Acceleration of a Missile which is maintained on the Aimer-target Line of Sight

1 Let the aimer-target sight line make an angle  $\theta_T$  with some datum (Fig.1). The missile, whose forward speed is  $v_M$  remains on this sight line as the target moves. In order to do so suppose that instantaneously its flight path makes an angle  $\phi_M$  with the datum. Then if  $r_M$  is the aimer-missile range we have by resolving along and normal to the sight line:

$$r_M \dot{\theta}_T = v_M \sin(\phi_M - \theta_T) \quad (1A)$$

$$\dot{r}_M = v_M \cos(\phi_M - \theta_T) \quad (2A)$$

2 Differentiating (1A) with respect to time:

$$r_M \ddot{\theta}_T + \dot{r}_M \dot{\theta}_T = v_M \cos(\phi_M - \theta_T) [\dot{\phi}_M - \dot{\theta}_T] + \dot{v}_M \sin(\phi_M - \theta_T) \quad (3A)$$

3 The range of tactical situations envisaged makes it justifiable to assume  $\sin(\phi_M - \theta_T) \approx (\phi_M - \theta_T)$  and  $\cos(\phi_M - \theta_T) = 1$ .

Hence from (2A) and (3A)

$$v_M \dot{\phi}_M = 2v_M \dot{\theta}_T + r_M \ddot{\theta}_T - \dot{v}_M(\phi_M - \theta_T) \quad (4A)$$

But  $v_M \dot{\phi}_M$  is the lateral acceleration of the missile.

# APPENDIX B

## Simulator Techniques for Applying Two-operator Guidance

### 1 Networks for Maintaining Sight-line Coincidence by means of Binocular Tracking of the Target

1.1 We consider here the form of pick-off system and network required to give the result referred to in para. 8.1.5 Part I of the main text.

1.2 From equation (4A) Appendix A the lateral acceleration of a missile at range  $r_M$  which remains on the aimer-target sight-line is

$$\ddot{y} = v_M \ddot{\theta}_M = 2v_M \dot{\theta}_T + r_M \ddot{\theta}_T - v_M(\dot{\phi}_M - \dot{\theta}_T) \quad (1B)$$

where  $\theta_T$  is the angle between the aimer-target sight-line and a line through the aiming point parallel to the target flight path (Fig.1).  $(\phi_M - \theta_T)$  is the angle between the sight-line and the instantaneous missile flight path.  $(\dot{\phi}_M - \dot{\theta}_T)$  may be expressed approximately as the ratio between the missile velocity components along and normal to the sight-line; that is, as  $\frac{r_M \dot{\theta}_T}{v_M}$ . Then

$$\ddot{y} = v_M \ddot{\theta}_M = 2v_M \dot{\theta}_T + r_M \ddot{\theta}_T - \frac{\dot{v}_M r_M \dot{\theta}_T}{v_M} \quad (2B)$$

1.3 Equation (2B) defines a relationship between missile motion and the geometry of the situation. To develop the required lateral acceleration  $\ddot{y}$  however, it is necessary to deflect the wings of the missile, and the lateral acceleration corresponding to a given deflection has been assumed proportional to the square of forward speed  $v_M$ . The steady-state lateral acceleration is therefore

$$\ddot{y} = K v_M^2 \delta \quad (3B)$$

where  $K$  is a constant and  $\delta$  the wing deflection.

1.4 The forward speed is in its turn affected by profile drag, also assumed proportional to  $v_M^2$ , one effect of which is to make  $\dot{v}_M$  variable when the thrust is constant. The available data however suggests that  $\dot{v}_M$  during boost is substantially controlled by the boost thrust alone and can therefore be assumed constant. In subsequent flight the forward acceleration, which we will term  $\dot{v}_M'$ , is relatively very small, being about 7 ft/sec<sup>2</sup> in level flight. Having regard to the effects of induced drag, and of gravity when climbing, actual values of  $\dot{v}_M'$  are no doubt considerably smaller in many cases and may be reversed in sign. For example an angle of climb of about 12.5° would suffice to reduce  $\dot{v}_M'$  to zero, and greater angles are likely to arise.  $\dot{v}_M'$  is therefore an indeterminate factor but it will be reasonable to assume  $\left| \frac{\dot{v}_M'}{v_M} \right| \ll 1$  where  $\dot{v}_M$  is the acceleration in boost.

1.5 We arrange the shaping network, to whose input a voltage proportional to  $\dot{\theta}_T$  is applied, quite generally so that the wing angle

$$\delta = \ell \dot{\theta}_T + m \ddot{\theta}_T \quad (4B)$$

The voltage proportional to  $\dot{\theta}_T$  is derived from a generator geared to the tracking binoculars. We do not consider here the problems of axis resolution arising when the guidance problem in three dimensions is considered.

1.6 Eliminating  $\delta$  between (3B) and (4B)

$$\ddot{y} = K v_M^2 (\ell \dot{\theta}_T + m \ddot{\theta}_T) \quad (5B)$$

Equating coefficients in (2B) and (5B), we have during boost:

$$\ell = \frac{2 v_M^2 - v_M r_M}{K v_M^3} \quad (6B)$$

$$m = \frac{r_M}{K v_M^2} \quad (7B)$$

or since  $v_M = v_M t$  and  $r_M = \frac{1}{2} v_M t^2$ ,

$$\ell = \frac{3}{2K v_M t} \quad (8B)$$

$$m = \frac{1}{2K v_M} \quad (9B)$$

1.7 If the demand for wing angle is applied from the generator via a phase-advancing network, we write (4B) in the form

$$\delta = \ell \left( \dot{\theta}_T + \frac{m}{\ell} \ddot{\theta}_T \right) \quad (10B)$$

and the phase-advance time-constant during boost is, from (8B) and (9B)

$$\frac{m}{\ell} = \frac{1}{3} t \quad (11B)$$

where  $t$  is the time from launch. During boost therefore, the phase-advance time-constant should increase at  $1/3$  sec/sec, while the D.C. gain ( $\propto \ell$ ) should vary inversely as the time of flight.

1.8 Subsequent to boost we have from (6B)

$$\ell = \frac{2 v_M^2 - v_M r_M}{K v_M^3} \quad (6B)$$

During this phase, if  $\dot{v}_M^i$  is constant,

$$v_M = \dot{v}_M T_B + \dot{v}_M^i (t - T_B)$$

and

$$r_M = \frac{1}{2} \dot{v}_M T_B^2 + \dot{v}_M T_B (t - T_B) + \frac{1}{2} \dot{v}_M^i (t - T_B)^2$$

Substituting in (6B) for  $v_M$  and  $r_M$ , and dividing numerator and denominator by  $\dot{v}_M^2$  we have

$$\ell = \frac{2 \left\{ T_B^2 + \frac{1}{2} \left( \frac{\dot{v}_M^i}{\dot{v}_M} \right)^2 (t - T_B)^2 + \frac{\dot{v}_M^i}{\dot{v}_M} T_B (t - \frac{3}{2} T_B) \right\}}{K \dot{v}_M \left[ T_B + \frac{\dot{v}_M^i}{\dot{v}_M} (t - T_B) \right]^3}$$

which, since  $\frac{\dot{v}_M^i}{\dot{v}_M} \ll 1$  and  $t$  does not acquire excessive values, reduces very nearly to

$$\ell = \frac{2}{K \dot{v}_M T_B} \quad (12B)$$

where  $T_B$  is the duration of boost. That is,  $\ell$  is constant.

By a similar argument the value of  $m$  is

$$m = \frac{\frac{1}{2} T_B^2 + T_B (t - T_B) + \frac{1}{2} \frac{\dot{v}_M^i}{\dot{v}_M} (t - T_B)^2}{K \dot{v}_M \left( T_B + \frac{\dot{v}_M^i}{\dot{v}_M} (t - T_B) \right)^2} \approx \frac{t - \frac{1}{2} T_B}{K \dot{v}_M T_B} \quad (13B)$$

The phase-advance time-constant is therefore

$$\frac{m}{\ell} = \frac{1}{2} (t - \frac{1}{2} T_B) \quad (14B)$$

so that the phase-advance time-constant should increase at 0.5 sec/sec after boost. A discrete change in value occurs on cessation of boost, from  $\frac{1}{3} T_B$  to  $\frac{1}{4} T_B$ . There is likewise a discrete change in D.C. gain at the end of boost, from  $\frac{3}{2 K \dot{v}_M T_B}$  to  $\frac{2}{K \dot{v}_M T_B}$ , the latter being the constant gain required from this point onwards.

1.9 The appropriate demand for wing deflection may alternatively be obtained by differentiating the voltage generator output and adding the result, to a suitable scale, to the original voltage generator output. This leads to rather different and technically simpler time-variations of the parameters involved (see para. 1.11 below). Fig.7 indicates schematically how this arrangement was realized in the laboratory simulator. From (4B) as before

$$\delta = \ell \dot{\theta}_T + m \ddot{\theta}_T \quad (15B)$$

During boost:

$$\ell = \frac{3}{2K \dot{v}_M t} \quad (16B)$$

$$m = \frac{1}{2K \dot{v}_M} \quad (17B)$$

The signal proportional to  $\dot{\theta}_T$  therefore should be inversely proportional to time of flight while the gain  $m$  in the  $\ddot{\theta}_T$  "channel" is constant.

1.10 Subsequent to boost

$$\ell = \frac{2}{K \dot{v}_M T_B} = \text{constant} \quad (18B)$$

and

$$m = \frac{t - \frac{1}{2} T_B}{K \dot{v}_M T_B} \quad (19B)$$

The gain  $m$  now increases uniformly with time at a rate

$$\dot{m} = \frac{1}{K \dot{v}_M T_B} \quad (20B)$$

1.11 The manner in which  $\ell$  varies is therefore unaffected by the change of circuit. In place of a time-constant  $\ell$  which must undergo a discrete change of value and of rate of change at the end of boost, we now have a gain proportional to  $m$  i.e. one which is constant during boost and thereafter increases at a constant rate without any discrete change of value.

1.12 In practical terms there is little lost by giving  $\ell$  a constant value throughout, equal to  $\frac{2}{K \dot{v}_M T_B}$  since (i) sight-line motion early in the

engagement will be relatively slight; (ii) the gain through an amplifying channel will necessarily be limited in any case, and (iii) the effectiveness of any unduly large signal in producing wing deflection will be limited by mechanical stops.

## 2 To determine the Parameters of a Simulator Shaping Unit for converting Sight-line rates into Missile Acceleration

2.1 Fig.30 shows schematically a suitable simulator arrangement. We have

$$a_2 \delta = \frac{R_3}{R_1} a_1 T \ddot{\theta}_T + \frac{R_3}{R_2} a_1 \dot{\theta}_T \quad (21B)$$

or

$$\delta = \frac{R_3}{R_1} \cdot \frac{a_1}{a_2} \beta T \ddot{\theta}_T + \frac{R_3}{R_2} \cdot \frac{a_1}{a_2} \dot{\theta}_T \quad (22B)$$

If (i) acceleration subsequent to boost is negligible and (ii)  $\epsilon$  is given its post-boost value throughout, then from (15B), (17B), (18B) during boost:

$$\delta = \frac{2}{K v_M} \dot{\theta}_T + \frac{1}{2K \dot{v}_M} \ddot{\theta}_T \quad (23B)$$

and after boost, from (15B), (18B), (19B):

$$\delta = \frac{2}{K v_M} \dot{\theta}_T + \frac{1}{2K \dot{v}_M} \left( 2 \frac{t}{T_B} - 1 \right) \ddot{\theta}_T \quad (24B)$$

where  $\dot{v}_M$  is the forward acceleration during boost.

Equating coefficients in (22B) and (24B)

$$\frac{a_1}{a_2} \cdot \frac{R_3}{R_2} = \frac{2}{K \dot{v}_M} \quad (25B)$$

$$\frac{a_1}{a_2} \cdot \frac{R_3}{R_1} \beta T = \frac{1}{2K \dot{v}_M} \left( 2 \frac{t}{T_B} - 1 \right) \quad (26B)$$

If  $\beta_0$  is the constant value of  $\beta$  during boost, corresponding to the coefficient of  $\ddot{\theta}_T$  in (23B) then

$$\frac{R_3}{R_1} T \beta_0 = \frac{a_2}{a_1} \cdot \frac{1}{2K \dot{v}_M} \quad (27B)$$

Thereafter

$$\frac{R_3}{R_1} T \beta = \frac{a_2}{a_1} \cdot \frac{1}{2K \dot{v}_M} \left( 2 \frac{t}{T_B} - 1 \right) \quad (28B)$$

and

$$\beta = \frac{1}{T} \cdot \frac{R_1}{R_3} \cdot \frac{a_2}{a_1} \cdot \frac{1}{K \dot{v}_M} \quad (29B)$$

Now  $\dot{v}_M \approx 235 \text{ ft/sec}^2$ ,  $K = 2.61 \times 10^{-3}$ ,  $T_B = 3$ ,  
 $a_1 = 38 \text{ volts/rad/sec}$  and  $a_2 = 86.4 \text{ volts/rad}$ . If  $v_M$  is constant = 705 ft/sec then from (25B)

$$\frac{R_3}{R_2} = \frac{2}{K v_M} \cdot \frac{a_2}{a_1} = 2.48 \quad (30B)$$

If  $t_{\max}$  is the maximum contemplated duration of flight, (say 20 seconds) and  $\beta$  is allowed to increase to unity in this time, then from (26B)

$$\frac{R_3}{R_1} T = \frac{a_2}{a_1} \cdot \frac{1}{2K_M} \left[ 2 \frac{t_{\max}}{T_B} - 1 \right]$$

or

$$\frac{R_3}{R_1} T = 23 \text{ secs.} \quad (31B)$$

Then from (27B):

$$\beta_0 = 0.08 \quad (32B)$$

$\beta$  thus runs from 0.08 to unity in  $(t_{\max} - T_B) = 17 \text{ secs.}$

2.2 The maximum value of  $\ddot{\theta}_T$  likely to occur is about  $0.05 \text{ rad/sec}^2$ . The maximum output voltage from the differentiating unit would then be  $38 \times 0.05 T = 1.9 T$ . The simulator units will provide output voltages up to some  $\pm 50$  volts without loss of linearity. It is therefore convenient to choose  $T = 23 \text{ secs}$  and  $\frac{R_3}{R_1} = 1$ . If the input capacitance to the differentiating unit is  $9 \mu\text{f}$ , the feedback resistor should be 2.55 megohms.

Summarizing

$$\frac{R_3}{R_1} = 1; \quad \frac{R_3}{R_2} = 2.48; \quad \beta_0 = 0.08;$$

$$C = 9 \mu\text{f}; \quad R = 2.55 \text{ megohms.}$$

APPENDIX CLateral Acceleration - Total Requirement

1 The manoeuvrability of the missile depends primarily upon the achievable lateral acceleration and upon the rapidity with which this can be built up.

2 The lateral acceleration called for in the present application may be considered in two parts namely (a) the lateral acceleration needed to correct errors i.e. deviations of the missile from the aimer-target sight-line and (b) the lateral acceleration required to maintain the missile on this sight-line assuming no deviations.

3 The lateral acceleration required to correct errors is not easy to establish other than from experience. It is in effect the lateral acceleration required when attacking a fixed target. The missile characteristics assumed in the simulator study of Project "Malkara", an anti-tank device (Ref.2) gave a maximum lateral acceleration of about  $\pm 3g$  at a mean forward speed of 450 f.p.s. There is reason to think that  $\pm 2g$  would have been sufficient, even allowing for the need to gather the missile rapidly on to the line of sight after firing.

4 Again, in the mobile simulator work carried out in the present programme, in which the attacking aircraft made direct approaches to the aimer (i.e. very low rates of sight-line rotation) the records suggest that a maximum lateral acceleration of  $\pm 1-2g$  suffices apart from brief peaks during initial gathering.

5 The lateral accelerations called for in paras. 3 and 4 above are essentially transient and their provision is not inconsistent with the requirements for a guidance loop in which a man can function with a minimum of effort. However, in the present context the aimer-target sight-line is not fixed in direction; in fact its motion is such as to call for sustained missile lateral accelerations and all higher derivatives thereof.

6 Fig.1 depicts a situation in which an attacking aircraft is flying on a straight line at a perpendicular distance  $d$  from the aimer. Its forward speed is  $v_T$  and when the range parallel to the flight path is  $r_T$ , the sight-line elevation is  $\theta_T$ . It is then easy to show that if  $t$  is the time of flight from initial range  $r_{T_0}$

$$\theta_T = \tan^{-1} \frac{d}{(r_{T_0} - v_T t)} \quad (10)$$

$$\dot{\theta}_T = \frac{d v_T}{d^2 + (r_{T_0} - v_T t)^2} \quad (20)$$

$$\ddot{\theta}_T = \frac{2 d v_T^2 (r_{T_0} - v_T t)}{[d^2 + (r_{T_0} - v_T t)^2]^2} \quad (30)$$

If, as in the present context,  $\frac{d^2}{(r_{T_0} - v_T t)^2} \ll 1$  at all times, then

$$\dot{\theta}_T \approx \frac{d v_T}{(r_{T_0} - v_T t)^2} \quad (4C)$$

$$\ddot{\theta}_T \approx \frac{2 d v_T^2}{(r_{T_0} - v_T t)^3} \quad (5C)$$

Hence from equation (2B) Appendix B, since  $\frac{v_M r_M}{v_M} \ll 2 v_M$  subsequent to boost we have very nearly

$$\alpha = v_M \ddot{\theta}_M = 2 v_M \dot{\theta}_T + r_M \ddot{\theta}_T = \frac{2 v_M v_T d \left( r_T + \frac{v_T}{v_M} r_M \right)}{r_T^3} \quad (6C)$$

for  $(r_{T_0} - v_T t) = r_T$  the instantaneous target range.

In a given engagement, if  $v_M$ ,  $v_T$ ,  $d$  are constant,  $\left( r_T + \frac{v_T}{v_M} r_M \right)$  is a constant. The lateral acceleration therefore varies as the inverse cube of the target range and is a maximum at impact.

At impact  $r_T = r_M = r_i$ , say, so that

$$\alpha_{\max} = \frac{2 v_M v_T d \left( 1 + \frac{v_T}{v_M} \right)}{r_i^2} = \frac{2 v_T d (v_M + v_T)}{r_i^2} \quad (7C)$$

The maximum lateral acceleration therefore varies as the inverse square of the impact range.

From para. 2.4 Part I, if  $r_{T_0}$  is the minimum acquisition range,  $T_P = 5$  secs is the preparation time;  $T_B = 3$  secs is the boost duration; and  $v_M$ ,  $v_T$  are taken as 705 ft/sec and 900 ft/sec respectively while  $d = 900$  ft, then we have for the minimum impact range

$$r_{i_{\min}} = 4000 \text{ ft very nearly.}$$

Then in (7C)

$$\alpha_{\max} \approx 160 \text{ ft/sec}^2 \approx 5g \quad (8C)$$

Taking the result of equation (8C) in conjunction with the observed acceleration requirements for error correction, we conclude that a total lateral acceleration capacity, less the requirement of gravity correction, is about 7g. The missile analogue provided in the laboratory simulator was capable of about 8g at the end of boost, rising to some 10g after a further 14.5 secs of level flight (Fig.2).

APPENDIX DThe Validity of "Demand Storage"1 General

1.1 Experiments have shown that for the human operator, the type of guidance system most likely to combine a well damped dynamic response with a capacity to provide a measure of sustained lateral acceleration is one in which, in principle, the joystick demands lateral acceleration directly, but in which this demand is heavily phase-advanced. In producing this phase advance it is convenient to incorporate also a small exponential lag so that in response to very rapid, or even step motions of the joystick, the instantaneous demand is bounded and known.

1.2 The equivalent of a step of joystick deflection may occur in a system where the joystick is energized suddenly at a time when it is being held away from its neutral position. The demand  $\delta_D$  applied to the wing actuator may therefore take the form

$$\delta_D = K J \left( \frac{1+p T_F}{1+p T'} \right)$$

where  $J$  is the joystick deflection and  $K$  is constant. The time constant  $T'$  is generally required to be small since it forms part of the overall response lag of the system, which if excessive, adversely affects operation.

1.3 Having regard to the scaling usually necessary, the ratio  $T_F/T'$  may well be such that for large and rapid joystick movements, missile control surface deflections are demanded which exceed their capacity. In that case the resulting lateral acceleration will fall short of what is demanded. It is important to avoid this. We therefore discuss the validity of an arrangement recommended for Project Malkara, whereby if an instantaneous demand is so large that under linear operating conditions an excess of wing deflection would be demanded, the demand is automatically kept within the limits of possible wing response, but extended in time as necessary, to give the demanded total time-integral of acceleration, that is, the demanded change in lateral velocity.

1.4 In Fig.35 we have a voltage limiter in a closed loop, together with a Miller integrator across whose condenser a resistor  $R_2$  is connected. The signal from the joystick is  $AJ$  and the limiter experiences an error input  $\epsilon$  which, for  $\epsilon < \bar{\epsilon}$  it transmits to the wing actuator. For  $\epsilon > \bar{\epsilon}$  the demand, and also the input to the integrator is limited to  $\pm \bar{\epsilon}$ .

2 Linear Operation

2.1 For  $\epsilon < \bar{\epsilon}$  the system is a linear, phase-advanced acceleration control, and

$$\epsilon = AJ - \frac{R_2}{R_1} \cdot \frac{1}{1+pCR_2} \epsilon \quad (1D)$$

or

$$\epsilon = AJ \left( \frac{R_1}{R_1+R_2} \right) \left( \frac{1+p T_F}{1+p T'} \right) \quad (2D)$$

where  $T_F = CR_2$  and  $T' = C \left( \frac{R_1 R_2}{R_1+R_2} \right)$ .

The time-relation corresponding to (2D) for a step input  $AJ$ , is

$$\epsilon = AJ \left( \frac{R_1}{R_1 + R_2} \right) \left\{ 1 - \left( 1 - \frac{T_F}{T_I} \right) \exp \left( - \frac{t}{T_I} \right) \right\} . \quad (3D)$$

2.2 This response can be divided into a steady state response  $\epsilon_S$  giving a constant acceleration proportional to  $J$  and a transient response  $\epsilon_T$  which gives rise to a change in lateral velocity.

Then

$$\epsilon_S = AJ \left( \frac{R_1}{R_1 + R_2} \right) \quad (4D)$$

$$\epsilon_T = AJ \left( \frac{R_1}{R_1 + R_2} \right) \left( \frac{T_F}{T_I} - 1 \right) \exp \left( - \frac{t}{T_I} \right) . \quad (5D)$$

The corresponding wing deflections are

$$\frac{\epsilon_S}{a_1} = \delta_S$$

and

$$\frac{\epsilon_T}{a_1} = \delta_T$$

where  $\frac{1}{a_1} =$  radians of wing deflection per unit voltage applied (assumed instantaneous).

2.3 The corresponding lateral accelerations (assumed instantaneously proportional to wing deflection) are  $\ddot{y}_S = K \delta_S$  and  $\ddot{y}_T = K \delta_T$  where  $K =$  lateral acceleration per unit wing deflection. Hence in (4D)

$$\frac{a_1 \ddot{y}_S}{K} = AJ \left( \frac{R_1}{R_1 + R_2} \right)$$

and in (5D)

$$\frac{a_1 \ddot{y}_T}{K} = AJ \left( \frac{R_1}{R_1 + R_2} \right) \left( \frac{T_F}{T_I} - 1 \right) \exp \left( - \frac{t}{T_I} \right)$$

or

$$a_1 \ddot{y}_S = AJK \left( \frac{R_1}{R_1 + R_2} \right) \quad (4Da)$$

$$a_1 \ddot{y}_T = AJK \left( \frac{R_1}{R_1 + R_2} \right) \left( \frac{T_F}{T_I} - 1 \right) \exp \left( - \frac{t}{T_I} \right) . \quad (5Da)$$

2.4 The total change of lateral velocity due to the transient component i.e. to phase advance is

$$a_1(\dot{y}-\dot{y}_0) = AJK \left( \frac{R_1}{R_1+R_2} \right) \left( \frac{T_F}{T_1} - 1 \right) \int_0^\infty \exp \left( -\frac{t}{T_1} \right) dt \quad (5Db)$$

$$= AJK \left( \frac{R_1}{R_1+R_2} \right) (T_F - T_1) \quad (6D)$$

When, as we consider below, demand limits are brought into operation, equation (6D) must continue to be satisfied if the terms of para. 1.3 of this Appendix are to be met.

### 3 Operation of Limits

3.1 The initial joystick demand is here assumed to be such that for a time,  $|\epsilon| > |\bar{\epsilon}|$ . Divide the interval during which a demand for wing deflection is made into two parts viz:

- (a)  $|\epsilon| > |\bar{\epsilon}|$  during which the limits operate, and
- (b)  $|\epsilon| < |\bar{\epsilon}|$  i.e. the linear regime.

#### 3.2 $|\epsilon| > |\bar{\epsilon}|$

3.2.1 From Fig.35,

$$\epsilon = AJ - \bar{\epsilon} \frac{R_2}{R_1} \left( \frac{1}{1+p T_F} \right) \quad (7D)$$

Hence in response to a stepwise input,

$$\epsilon = AJ - \bar{\epsilon} \frac{R_2}{R_1} + \bar{\epsilon} \frac{R_2}{R_1} \exp \left( -\frac{t}{T_F} \right) \quad (8D)$$

$$a_1 \ddot{y} = AJK - K \bar{\epsilon} \frac{R_2}{R_1} + K \bar{\epsilon} \frac{R_2}{R_1} \exp \left( -\frac{t}{T_F} \right) \quad (9D)$$

3.2.2 If in (8D)  $AJ - \bar{\epsilon} \frac{R_2}{R_1} > \bar{\epsilon}$  i.e.  $AJ > \bar{\epsilon} \left( \frac{R_1+R_2}{R_1} \right)$  i.e. if

$\frac{AJ R_1}{R_1+R_2} > \bar{\epsilon}$ , then the limiting maximum value of demand voltage  $\bar{\epsilon}$  will persist indefinitely. If however  $\frac{AJ R_1}{R_1+R_2} < \bar{\epsilon}$ , then after some time  $t_L$  say, the system will restore to the linear regime. We now determine  $t_L$ .

#### 3.3 Time for which Limits remain in Operation

3.3.1 The limits remain in operation until  $\epsilon$  falls to  $\bar{\epsilon}$ . The condition in (8D) is then

$$AJ - \bar{\epsilon} \frac{R_2}{R_1} \left( 1 - \exp \left[ -\frac{t_L}{T_F} \right] \right) = \bar{\epsilon}$$

(see para. 3.2.2 above).

This gives

$$t_L = -T_F \log_e \left[ 1 - \frac{R_1}{R_2} \left( \frac{AJ}{\bar{\epsilon}} - 1 \right) \right] \quad (10D)$$

### 3.4 Change in Lateral Velocity during Limiting, due to Transient Demand

3.4.1 During this period we may subdivide the constant demand voltage  $\bar{\epsilon}$  into (1) a component  $\epsilon_S$  as in para. 2.2 of this Appendix, which remains in being after all transients have disappeared, and (2) a component  $\epsilon_{T_1}$  due to the transient component in the demand. We then have

$$\epsilon_S + \epsilon_{T_1} = \bar{\epsilon}$$

and from (4D):

$$\epsilon_S = AJ \left( \frac{R_1}{R_1 + R_2} \right)$$

Hence

$$\epsilon_{T_1} = \bar{\epsilon} - AJ \left( \frac{R_1}{R_1 + R_2} \right)$$

and the corresponding demand for lateral acceleration is

$$\frac{K \epsilon_{T_1}}{a_1} = \frac{K}{a_1} \left[ \bar{\epsilon} - AJ \left( \frac{R_1}{R_1 + R_2} \right) \right] \quad (11D)$$

3.4.2 The change in lateral velocity due to  $\epsilon_{T_1}$  is the product of  $\epsilon_{T_1}$  and the time for which the demand persists, that is,  $\epsilon_{T_1} \cdot t_L$ . From (10D) and (11D) therefore the change in lateral velocity is

$$\begin{aligned} \dot{y}_L - \dot{y}_0 &= -\epsilon_{T_1} T_F \log_e \left[ 1 - \frac{R_1}{R_2} \left( \frac{AJ}{\bar{\epsilon}} - 1 \right) \right] \\ &= T_F \log_e \left[ 1 - \frac{R_1}{R_2} \left( \frac{AJ}{\bar{\epsilon}} - 1 \right) \right] \left\{ \frac{AJK}{a_1} \left( \frac{R_1}{R_1 + R_2} \right) - \frac{\bar{\epsilon}K}{a_1} \right\} \quad (12D) \end{aligned}$$

### 3.5 Change in Lateral Velocity subsequent to Limiting, due to Transient Demand

3.5.1 The total velocity change due to phase advance is obtained by adding to  $\dot{y}_L - \dot{y}_0$  as obtained in para. 3.4.2 above, the change  $(\dot{y} - \dot{y}_L)$  which occurs in the subsequent linear phase i.e. when  $|\epsilon| < |\bar{\epsilon}|$ .

3.5.2 The transition to the linear regime occurs when  $|\epsilon| = |\bar{\epsilon}|$ . We may therefore use (6D) to determine  $(\dot{y} - \dot{y}_L)$  if in that equation we replace  $AJ$  by  $\bar{\epsilon}$ , the nett input at the moment of transition. Then

$$(\dot{y} - \dot{y}_L) = \frac{\bar{\epsilon}K}{a_1} \left( \frac{R_1}{R_1 + R_2} \right) (T_F - T') \quad (13D)$$

### 3.6 Total change in Lateral Velocity due to Transient Demand

3.6.1 The total effect of the transient in producing a change of lateral velocity is, from (12D) and (13D):

$$\begin{aligned} (\dot{y} - \dot{y}_0) &= (\dot{y}_L - \dot{y}_0) + (\dot{y} - \dot{y}_L) \\ &= \frac{\bar{\epsilon}K}{a_1} \left( \frac{R_1}{R_1 + R_2} \right) (T_F - T') + \frac{K T_F}{a_1} \left\{ A_J \frac{R_1}{R_1 + R_2} - \bar{\epsilon} \right\} \log_e \left[ 1 - \frac{R_1}{R_2} \left( \frac{A_J}{\bar{\epsilon}} - 1 \right) \right] \end{aligned}$$

..... (14D)

If demand storage were to produce the desired result, namely a change of lateral velocity due to phase advancing the joystick signal, which is independent of limiting action, then equations (6D) and (14D) should show

the same result. This is evidently not the case unless  $\frac{R_1}{R_2} \left( \frac{A_J}{\bar{\epsilon}} - 1 \right) \rightarrow 0$ .

That is in effect, unless  $R_2 \rightarrow \infty$  for if  $\left( \frac{A_J}{\bar{\epsilon}} - 1 \right)$  were zero the limits would not be called into play.

3.6.2 Elimination of  $R_2$  results in a demand which, for a stepwise joystick movement, tends to zero with time. That is, there is pure velocity control with a time lag, in the linear regime, of  $CR_1$ . The achieved velocity is given by taking the R.H.S. of equation (14D) to the limit as  $R_2 \rightarrow \infty$ , and it is

$$\dot{y} - \dot{y}_0 = \frac{A_J K C R_1}{a_1} \quad (14Da)$$

3.6.3 As would be expected, the same result is obtained by applying the process to equation (6D). Thus in the absence of  $R_2$ , a demanded change in lateral velocity is produced irrespective of the action of demand limits, although the limits extend the process in time. The conditions for demand storage are therefore satisfied.

## 4 Phase-advanced Acceleration Control with Demand Storage

4.1 We have now seen that the "demand storage" process is only completely effective when operating so as to give, in the linear regime, the time-derivative of joystick deflection alone, although small accretions of acceleration control ( $R_2$  great but not necessarily infinite) can be tolerated with small resulting error. Such an arrangement is therefore immediately applicable in principle, where the acceleration demand is only a second order effect as in "Malkara".

4.2 More generally a phase-advanced acceleration demand with demand storage is achieved by removing  $R_2$  in Fig.36, and applying to the wing actuator an additional demand obtained directly from the joystick output. This latter provides a sustained demand for control surface deflection when the joystick is deflected. The two demands may then be combined to suitable scales by means of a summing amplifier or the like. The additional connections are shown dotted in Fig.36.

## 5 Control of Limiting Amplitude $\bar{\epsilon}$

5.1 The control surface deflection available for response to the demand storage circuit depends at any instant on the sum total of demands from other sources to which the control surfaces are called upon to respond. Strictly therefore, the limiting amplitude  $\bar{\epsilon}$  in the demand storage circuit should be reduced whenever there are demands from other quarters. For example in the case of the arrangement shown in Fig.36, if  $\bar{\epsilon}$  demands full control surface deflection, (that is  $\bar{\epsilon}/a_1$  is full deflection) and the direct demand via the dotted connection is for a deflection  $\delta'$  in the same direction, then in order to produce full response the limiting amplitude should be reduced from  $\bar{\epsilon}$  to  $\bar{\epsilon} - a_1\delta'$ . The limiting amplitude should therefore be controlled continuously by the extraneous demands.

5.2 This implies that the limiting amplitude could easily vary during the non-linear operation of the demand storage unit. We have not attempted in this survey to examine the probable effects of this complication.

## 6 Minimum Velocity Response Time

6.1 If we consider only that part of the system which is designed to produce a change in lateral velocity, i.e. the "demand storage" circuit, we may readily ascertain the conditions in which this velocity is most rapidly achieved. Quite generally, the most rapid velocity build-up would occur if on deflecting the joystick, maximum lateral acceleration demand were applied, this demand being fully maintained until the desired lateral velocity was achieved. Thereupon the demand for control surface deflection would be instantly removed.

6.2 From para. 3.4.2 of this Appendix, the lateral velocity build-up consists of two parts. In the first, the demand limits are in operation i.e. maximum lateral acceleration occurs; in the second, linear operation supervenes and the lateral acceleration falls off exponentially with time. Minimum time of lateral velocity build-up will therefore be achieved to the extent that the first or non-linear phase can be made to preponderate over the second.

6.3 We have from equation (13D) that the lateral velocity change during the limiting phase is

$$\dot{y}_L - \dot{y}_0 = T_F \log_e \left[ 1 - \frac{R_1}{R_2} \left( \frac{AJ}{\bar{\epsilon}} - 1 \right) \right] \left[ \frac{AJK}{a_1} \left( \frac{R_1}{R_1 + R_2} \right) - \frac{\bar{\epsilon}K}{a_1} \right]. \quad (13D)$$

On proceeding to the limit as  $R_2 \rightarrow \infty$  this becomes

$$\lim_{R_2 \rightarrow \infty} (\dot{y}_L - \dot{y}_0) = CR_1 \frac{\bar{\epsilon}K}{a_1} \left( \frac{AJ}{\bar{\epsilon}} - 1 \right) \quad (16D)$$

and similarly for the linear phase

$$\lim_{R_2 \rightarrow \infty} (\dot{y} - \dot{y}_L) = \frac{\bar{\epsilon}K}{a_1} CR_1. \quad (17D)$$

6.4 If now we progressively reduce  $CR_1$  (the integration time-constant), and at the same time increase  $A$  (the voltage per unit joystick deflection) so as

to keep the total change in lateral velocity  $\dot{y} - \dot{y}_0 = \frac{AJKCR_1}{a_1}$  constant, then the value of  $\dot{y}_L - \dot{y}_0$  tends to  $\frac{AJKCR_1}{a_1}$  while  $\dot{y} - \dot{y}_L$  tends to zero.

6.5 That is, an increasing proportion of the total change in lateral velocity is developed during the limiting phase. But it is characteristic of this phase that maximum permissible lateral acceleration is present and hence lateral velocity grows at the maximum permissible rate. Hence to the extent that we carry out the process described in para. 6.4 above, we achieve a demanded velocity change in a reduced time. In the limit, this time is sensibly the time  $t_L$  for which the limits remain in operation.

This is given by equation (12D) after taking to the limit as  $R_2 \rightarrow \infty$ , as

$$t_L = \frac{CR_1 AJ}{\bar{\epsilon}} \quad (18D)$$

As might be expected therefore, the time required is linearly proportional to the demand  $J$ , and inversely proportional to the limiting amplitude  $\bar{\epsilon}$ .

APPENDIX EA Relation between Guidance Parameters and Missile Speed

1 In applying the guidance parameters arrived at for one missile to another, it is necessary to consider what changes may be required in order to ensure true equivalence. The criterion with which we are concerned here is the dynamic stability; that is, in effect, the response observed by the aimer to a given joystick deflection. It is necessary that this be the same for both cases.

2 The quantities expressing the observer's impressions are angular sight-line displacements. It is therefore necessary, if two systems are to be equivalent, for a joystick displacement to affect the sight-line orientation in the same way for both missiles, at any given time after launching. Fig.47 illustrates the implications of this.

3 We assume an idealized guidance system in which the joystick output signal is applied, phase-advanced, to the missile so as to produce instant proportional lateral acceleration. The effect of a step of joystick deflection then produces an instantaneous change in flight direction (i.e. of velocity normal to the initial flight path) and a steady lateral acceleration. If the change in lateral velocity is  $v_A$  and the missile's forward velocity is  $v_M$  ( $v_M \gg v_A$ ), the change in flight path direction is  $\phi_A \approx v_A/v_M$ .

4 If the missile's range is  $r_0$  when the demand is applied and the boost duration is  $T_B$  seconds, we have

$$r_0 = v_M (t - \frac{1}{2} T_B) \quad (1E)$$

at  $t$  seconds from launch.

The consequent angular rate of the sight-line is, after a short further interval  $\delta t$  ( $\delta t \ll t - T_B$ )

$$\dot{\theta}_{M_1} = \frac{v_A}{r_0 + v_M \delta t} \approx \frac{v_A}{v_M (t - \frac{1}{2} T_B)} \quad (2E)$$

The angular rate of the sight-line due to a lateral acceleration  $\ddot{v}_A$  is similarly

$$\dot{\theta}_{M_2} = \frac{\ddot{v}_A \delta t}{v_M (t - \frac{1}{2} T_B)} \quad (3E)$$

5 From (2E) and (3E), to produce the same sight-line rate at a given time after launch for missiles of different forward speeds but for which  $T_B$  is the same it should be arranged that the lateral velocity and/or lateral acceleration demanded by a given joystick deflection should vary in proportion to the forward speed.

6 If one considers the problem of translating the missile on to a new flight path which intersects the initial flight path at the aiming point, the same conclusion is reached. In applying "Malkara" (Ref.2) guidance parameters to G.L.T.V., it follows that the former should be multiplied by  $\frac{690}{450}$ , that is by 1.5 approximately.

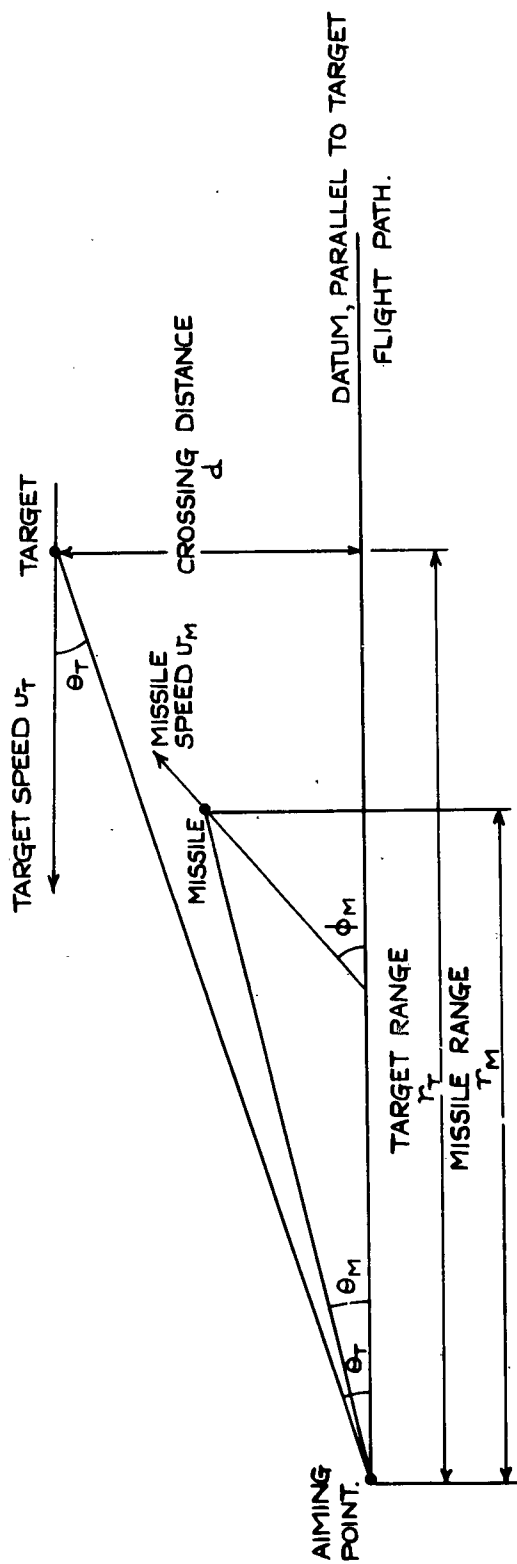
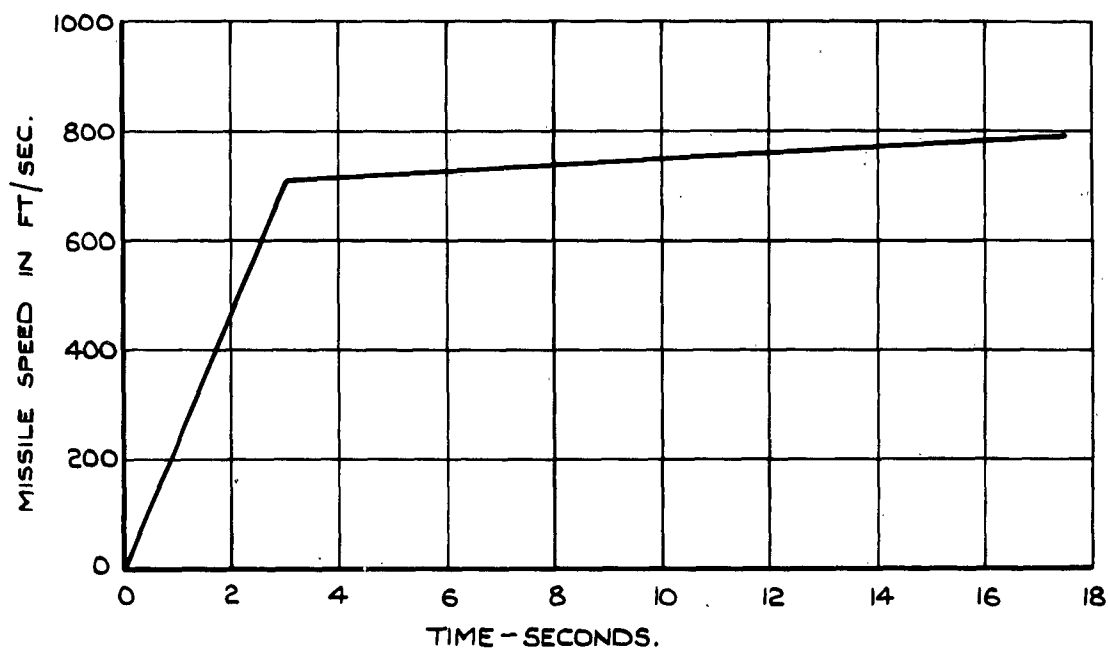


FIG.1. ATTACK ON A CONSTANT VELOCITY TARGET.



ESTIMATED THRUST AND WEIGHT FIGURES  
FOR GL.T.V.

BOOST THRUST	1360 LB.
SUSTAINER THRUST	200 LB.
ALL UP WEIGHT	210 LB.
ALL BURNT WEIGHT	170 LB.
DURATION OF BOOST	3 SECS.
DURATION OF SUSTAINER	14½ SECS.

FIG.2. ESTIMATED VELOCITY/TIME CHARACTERISTIC  
FOR GL.T.V. IN HORIZONTAL FLIGHT.

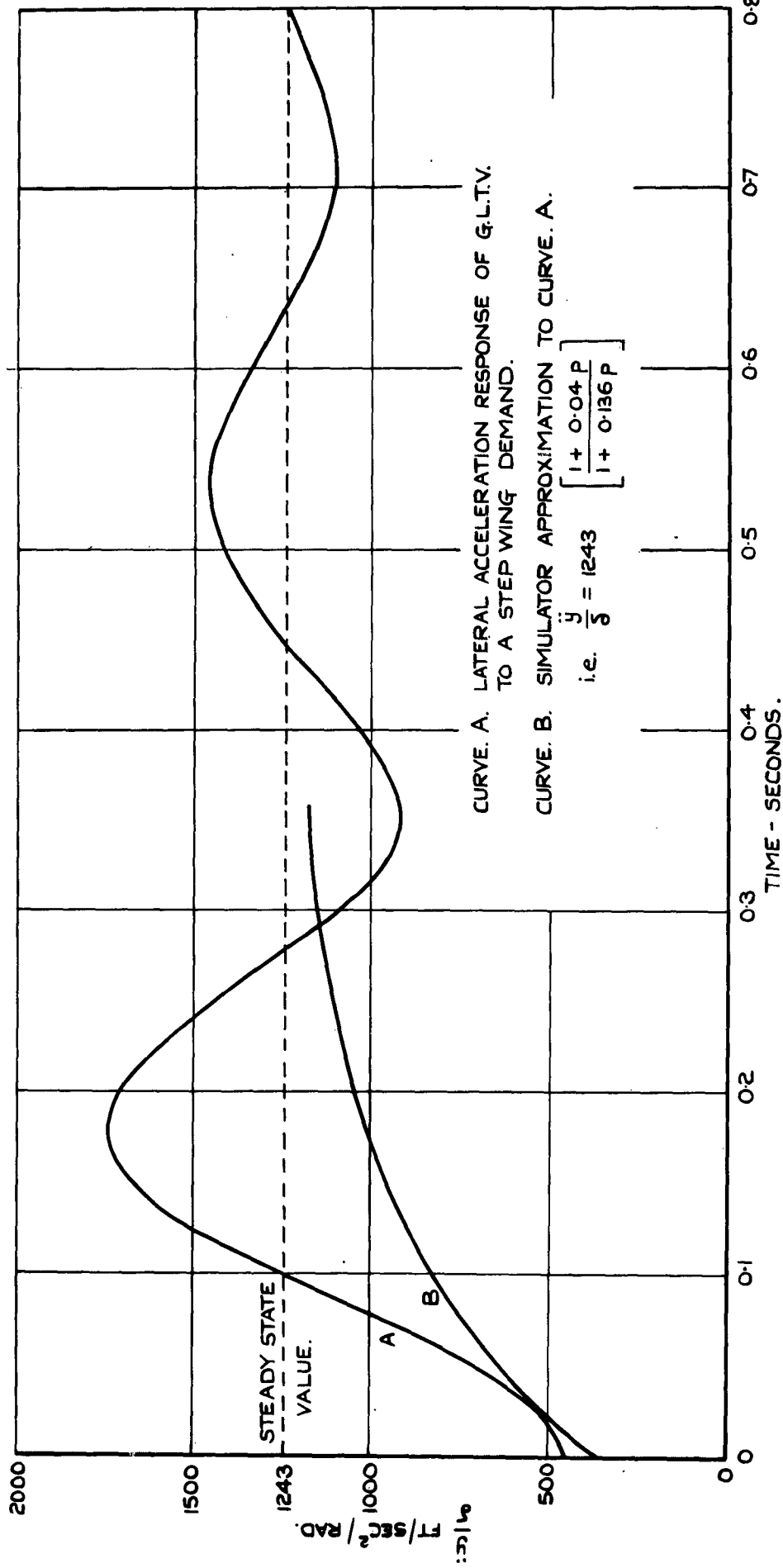


FIG.3. LATERAL ACCELERATION RESPONSE OF G.L.T.V. AND THE MISSILE ANALOGUE.

$U_M = 705 \text{ FT/SEC.}$

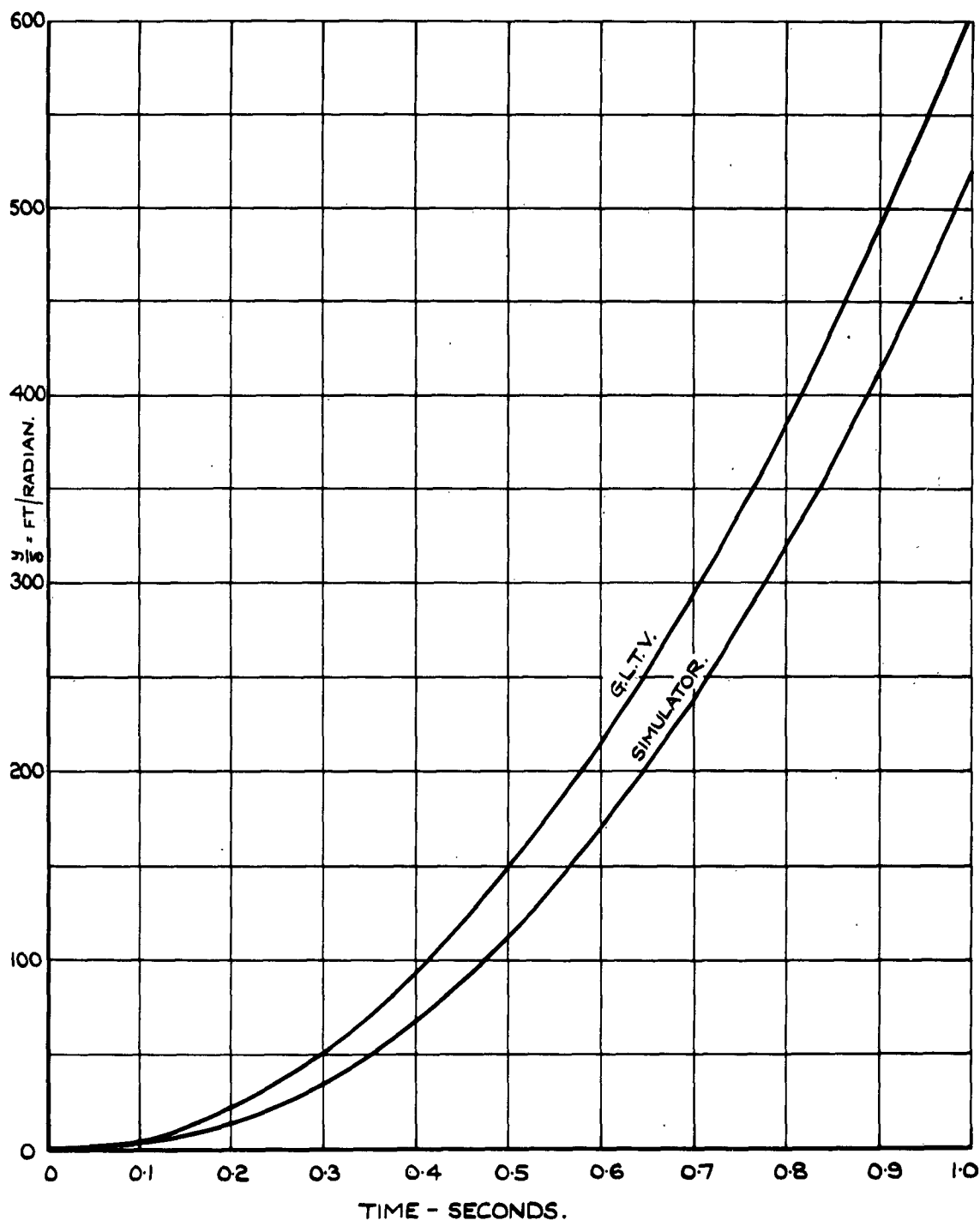


FIG.4. COMPARISON OF G.L.T.V. AND SIMULATOR  
LATERAL DISPLACEMENT RESPONSES FOR  
UNIT STEP WING DEFLECTION.  
 $U_M = 705$  FT/SEC.

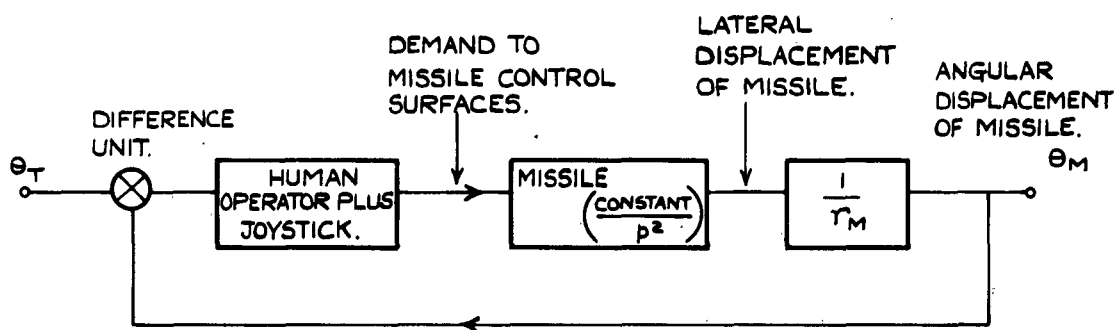


FIG.5. SIMPLIFIED BLOCK SCHEMATIC OF GUIDANCE LOOP.

x x x EXPERIMENTAL RUNS IN WHICH THERE WAS FAILURE TO ENGAGE OWING TO THE JOYSTICK COMING AGAINST ITS STOPS.

o o o EXPERIMENTAL RUNS IN WHICH THERE WAS EITHER SUCCESSFUL ENGAGEMENT, OR FAILURE WAS DUE TO HUMAN ERRORS.

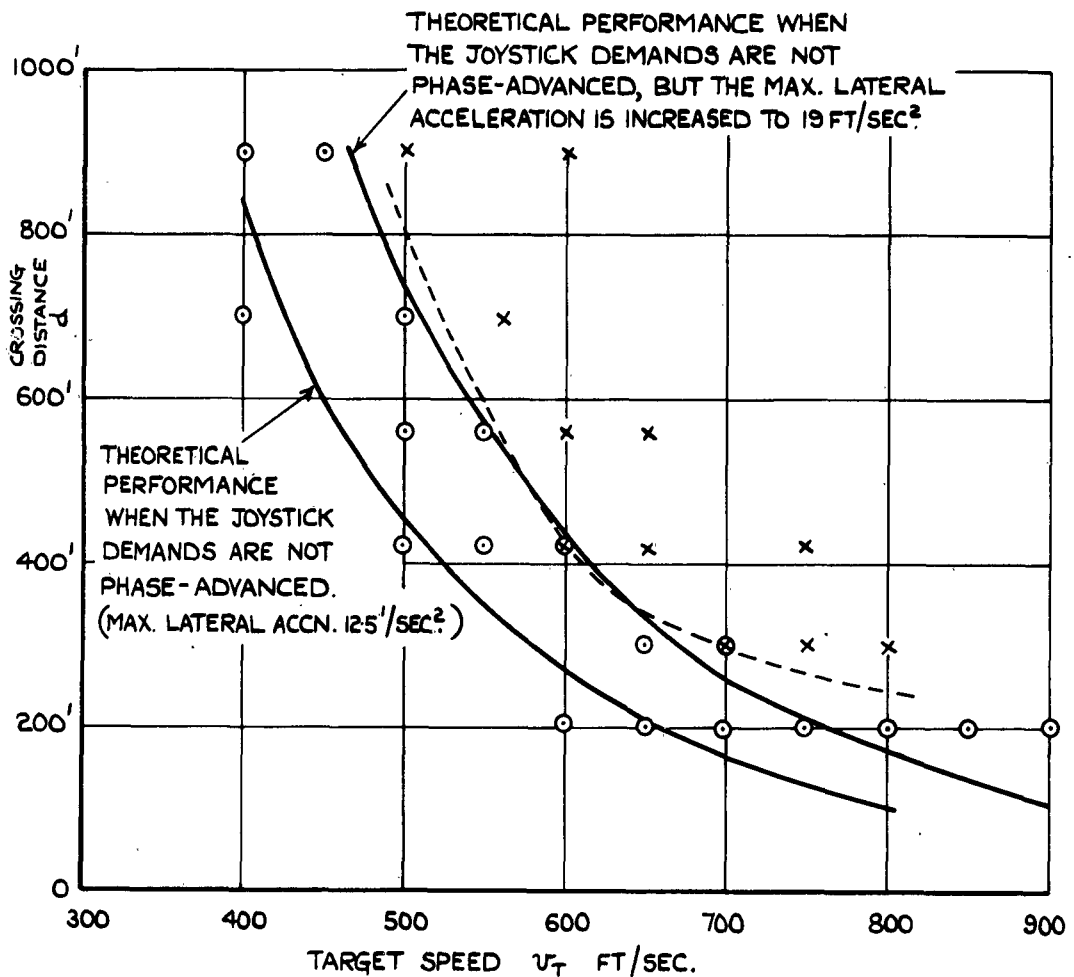


FIG.6. COMBINATIONS OF CROSSING DISTANCE  $d$  AND TARGET SPEEDS  $U_T$  FOR WHICH THE MISSILE LATERAL ACCN. AT IMPACT IS 12.5 FT/SEC<sup>2</sup>. THE MISSILE IS FIRED 5 SECS. AFTER THE TARGET IS SIGHTED AT 15,000 FT. IT IS THEN ACCELERATED UNIFORMLY TO 690'/SEC. IN 3 SECS. AND THEREAFTER FLIES AT 690'/SEC.

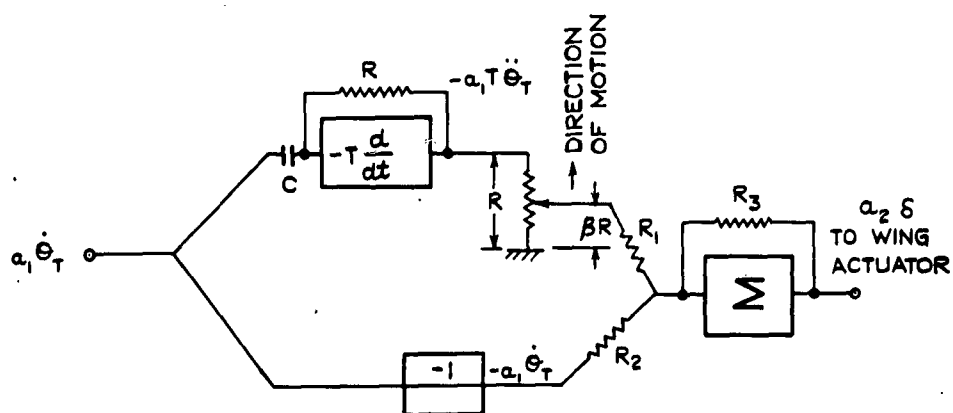


FIG.7. SCHEMATIC ARRANGEMENT FOR MAINTAINING MISSILE ON AIMER-TARGET SIGHT LINE.

FIG. 8.

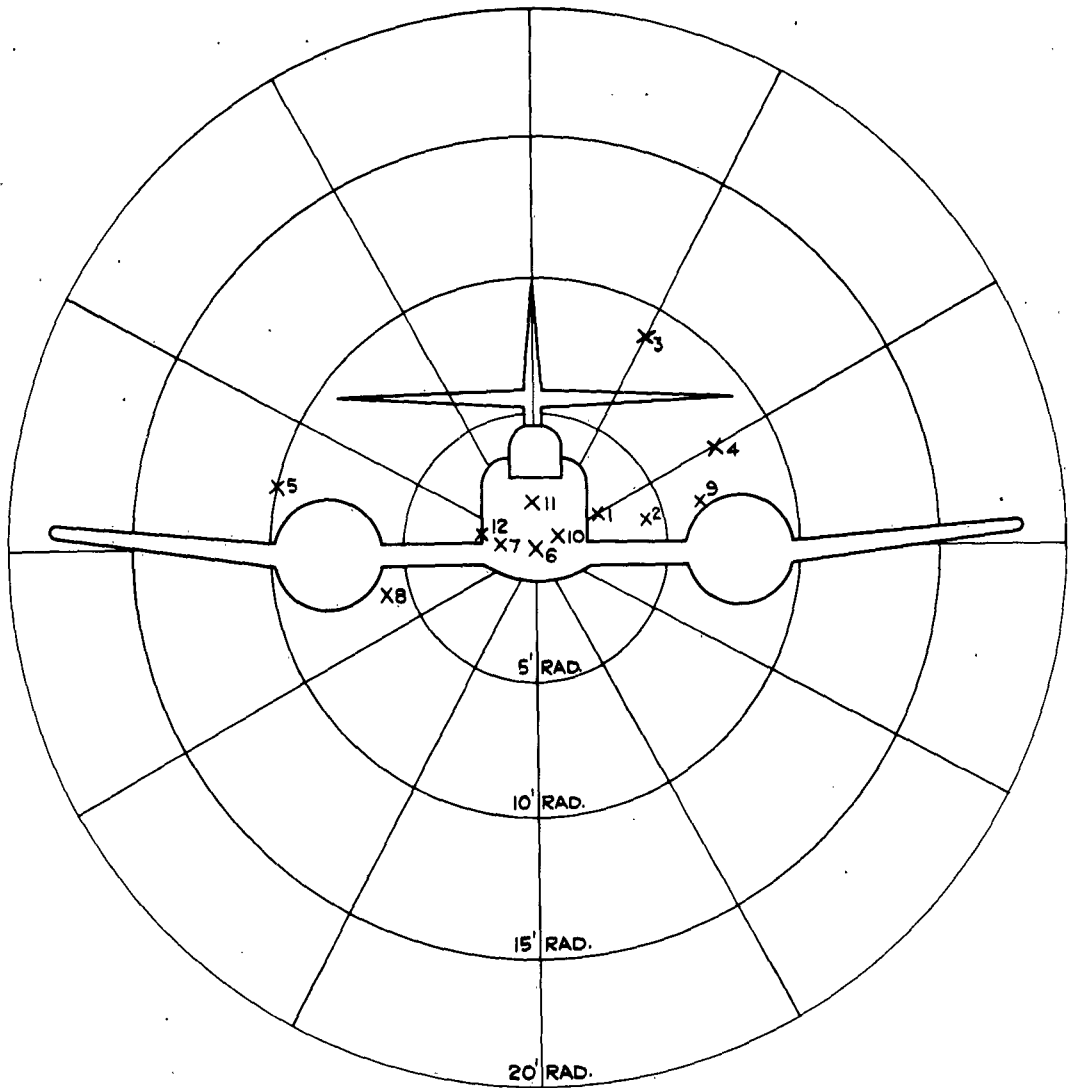


FIG. 8. RESULTS, OF DUMMY ATTACKS  
ON A 'METEOR' AIRCRAFT USING THE  
FIELD SIMULATOR.

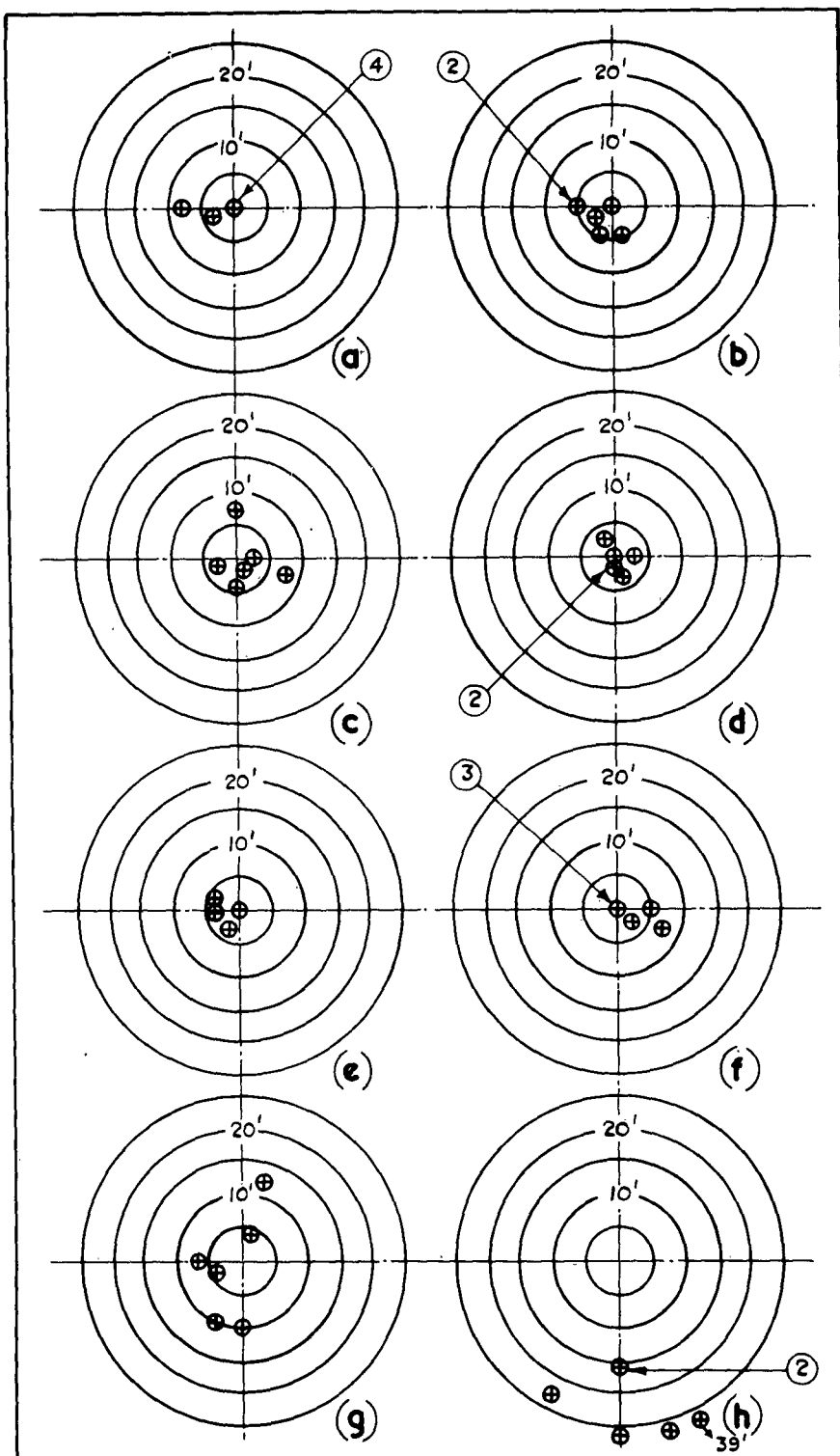
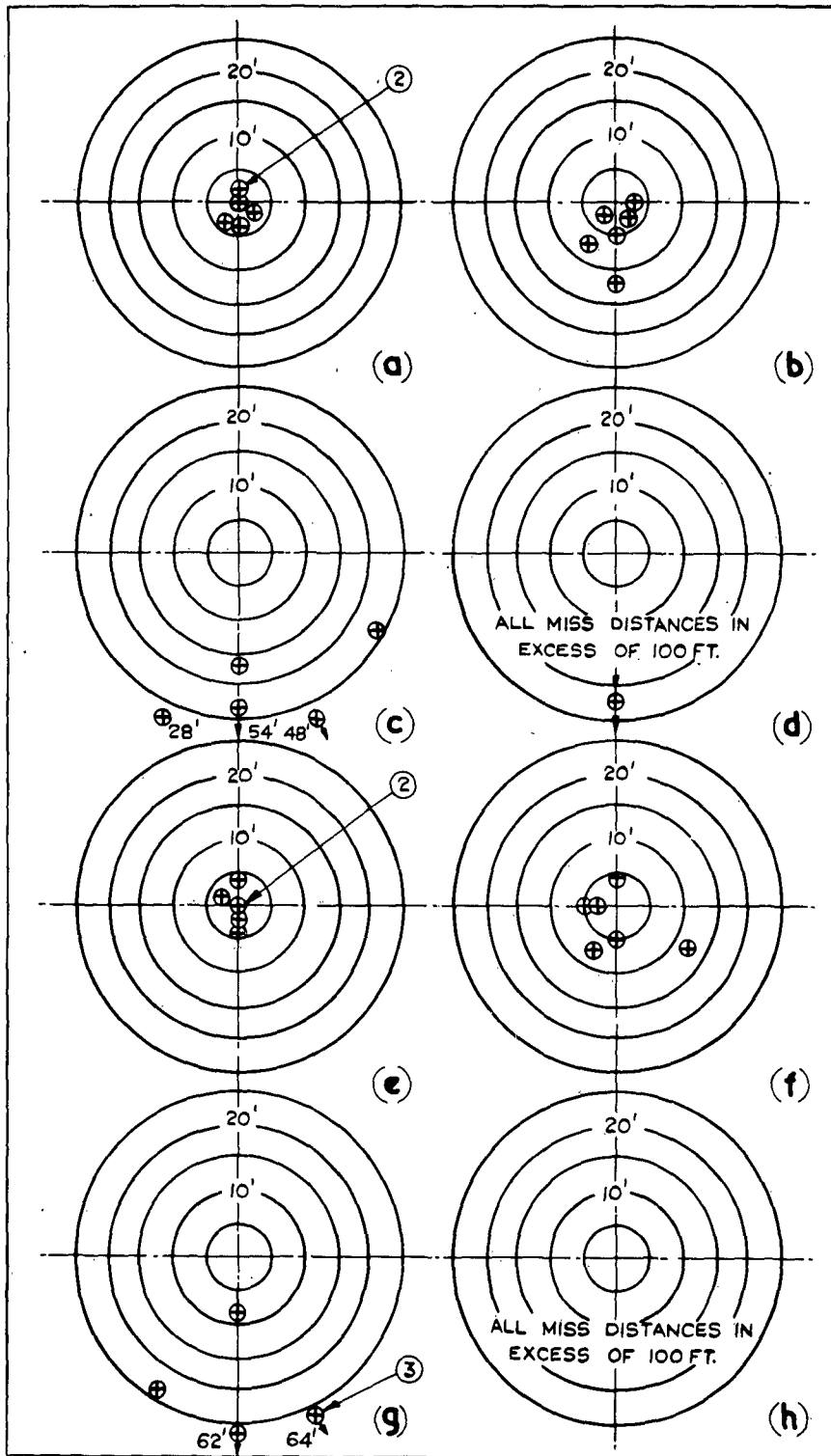


FIG. 9. CONTROL STIFFNESS= $12.5 \text{ FT/SEC}^2$  AND  $T_f = 4 \text{ SECS.}$

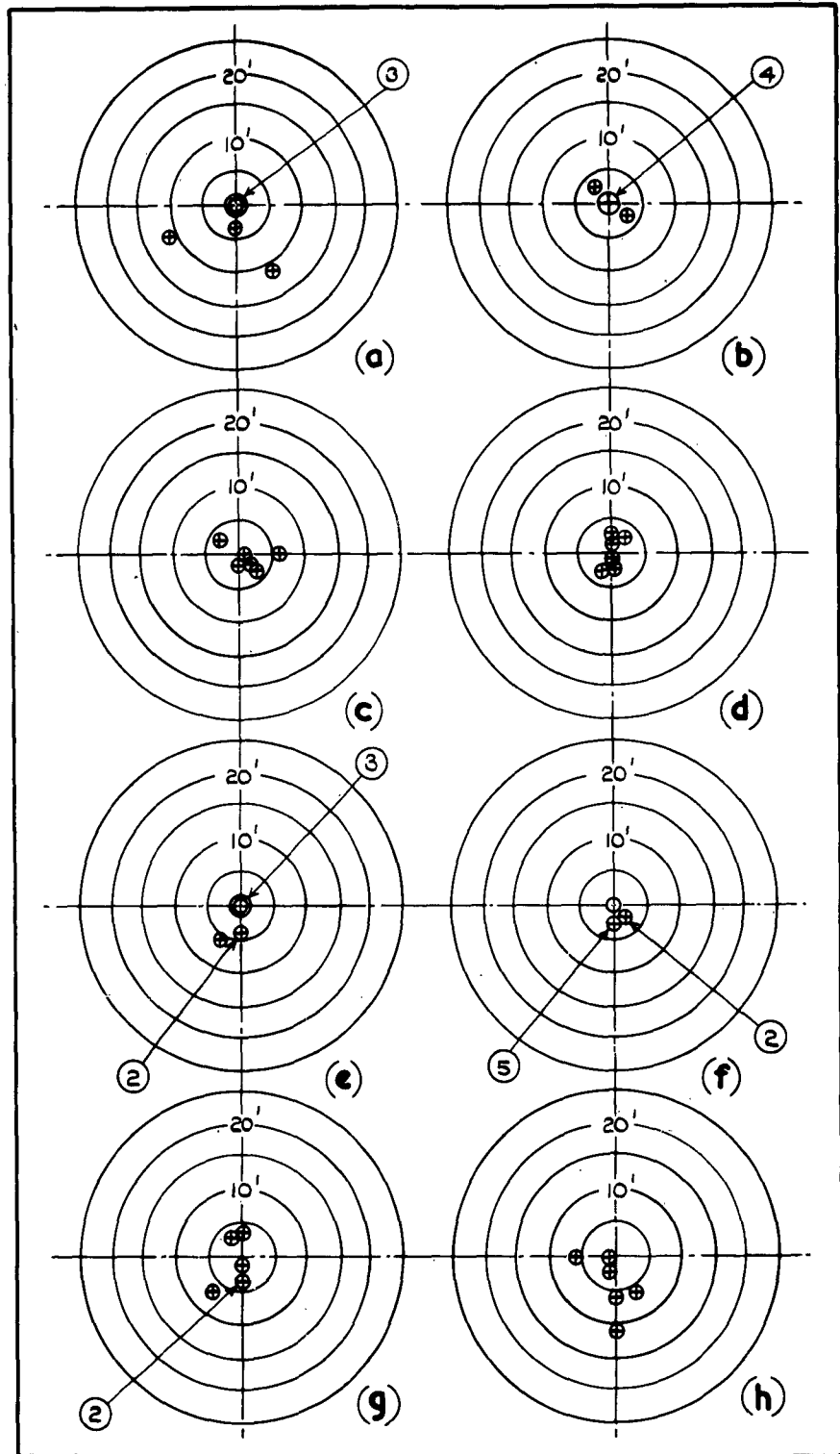
- (a) TARGET VEL. 200 F/S. CROSSING DIST. ZERO. (e) TARGET VEL. 200 F/S. CROSSING DIST. 300'  
 (b) TARGET VEL. 500 F/S. CROSSING DIST. ZERO. (f) TARGET VEL. 500 F/S. CROSSING DIST. 300'  
 (c) TARGET VEL. 700 F/S. CROSSING DIST. ZERO. (g) TARGET VEL. 700 F/S. CROSSING DIST. 300'  
 (d) TARGET VEL. 900 F/S. CROSSING DIST. ZERO. (h) TARGET VEL. 900 F/S. CROSSING DIST. 300'

FIG. 9. (a)



**FIG. 9(a) CONTROL STIFFNESS =  $12.5 \text{ FT/SEC}^2$  AND  $T_F = 4 \text{ SECS.}$**

- (a) TARGET VEL. 200 F/S. CROSSING DIST. 600' (e) TARGET VEL. 200 F/S. CROSSING DIST. 900'  
 (b) TARGET VEL. 500 F/S. CROSSING DIST. 600' (f) TARGET VEL. 500 F/S. CROSSING DIST. 900'  
 (c) TARGET VEL. 700 F/S. CROSSING DIST. 600' (g) TARGET VEL. 700 F/S. CROSSING DIST. 900'  
 (d) TARGET VEL. 900 F/S. CROSSING DIST. 600' (h) TARGET VEL. 900 F/S. CROSSING DIST. 900'



**FIG.10. CONTROL STIFFNESS = 25 FT/SEC<sup>2</sup> AND T<sub>F</sub> = 2 SECS**

- |   |   |
|---|---|
| (a) TARGET VEL. 200 F/S. CROSSING DIST. 0 | (e) TARGET VEL. 200 F/S. CROSSING DIST. 300 FT. |
| (b) TARGET VEL. 500 F/S. CROSSING DIST. 0 | (f) TARGET VEL. 500 F/S. CROSSING DIST. 300 FT. |
| (c) TARGET VEL. 700 F/S. CROSSING DIST. 0 | (g) TARGET VEL. 700 F/S. CROSSING DIST. 300 FT. |
| (d) TARGET VEL. 900 F/S. CROSSING DIST. 0 | (h) TARGET VEL. 900 F/S. CROSSING DIST. 300 FT. |

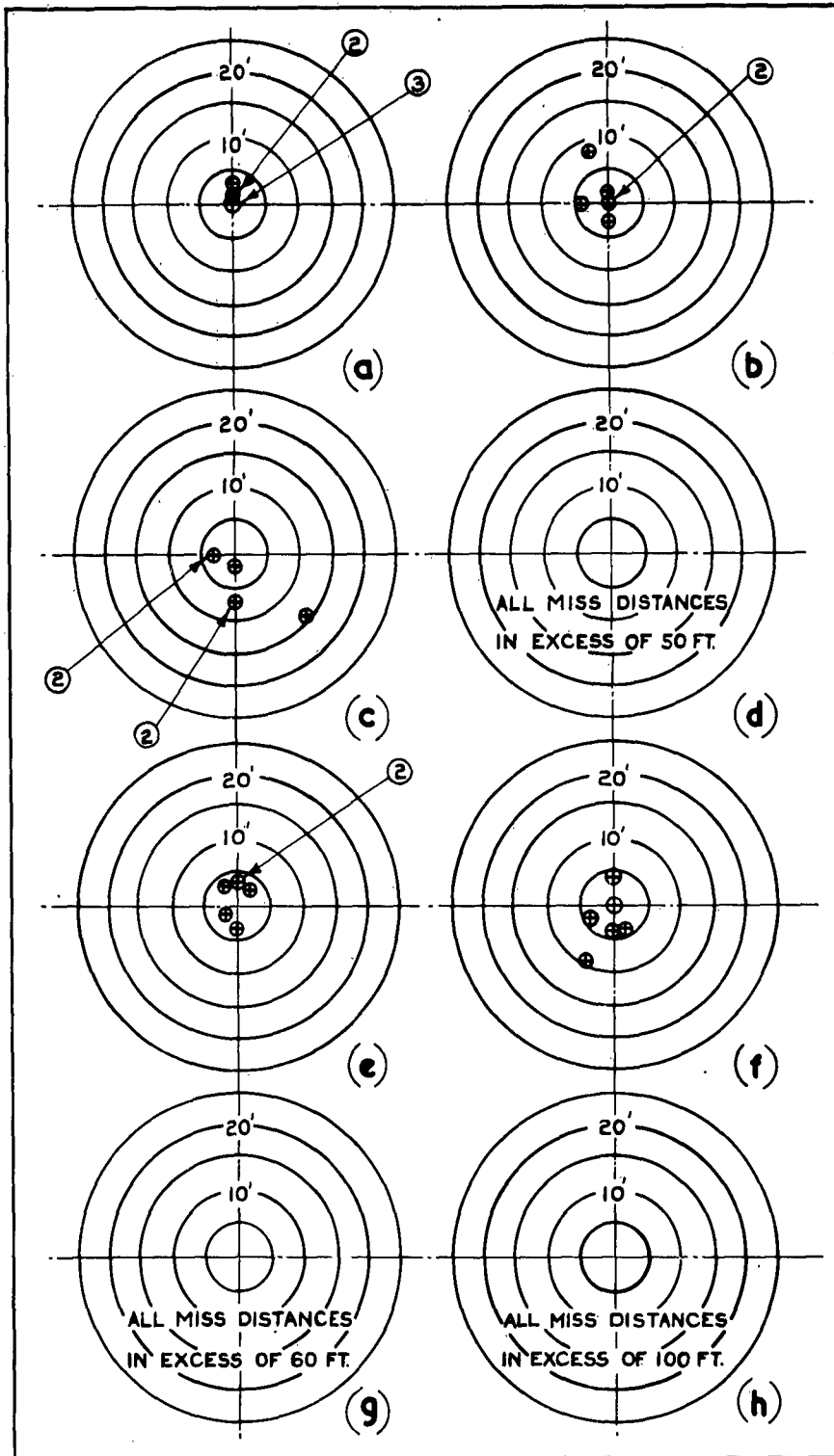
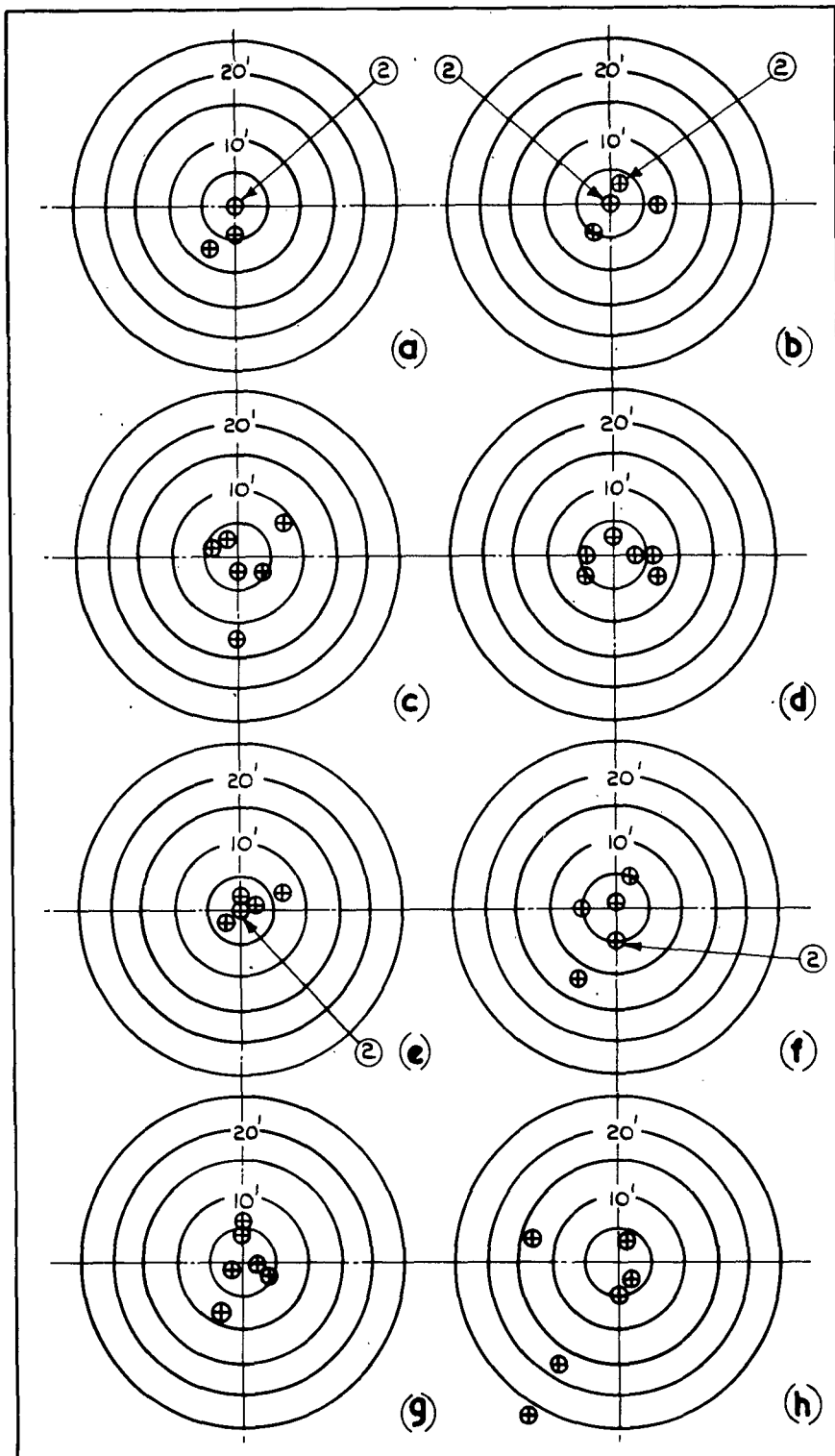


FIG. 10a. CONTROL STIFFNESS=25 FT/SEC<sup>2</sup> AND  $T_F = 2$  SECS.

- (a) TARGET VEL. 200 FT/SEC. CROSSING DIST. 600 FT. (e) TARGET VEL. 200 FT/SEC. CROSSING DIST. 900 FT.  
 (b) TARGET VEL. 500 FT/SEC. CROSSING DIST. 600 FT. (f) TARGET VEL. 500 FT/SEC. CROSSING DIST. 900 FT.  
 (c) TARGET VEL. 700 FT/SEC. CROSSING DIST. 600 FT. (g) TARGET VEL. 700 FT/SEC. CROSSING DIST. 900 FT.  
 (d) TARGET VEL. 900 FT/SEC. CROSSING DIST. 600 FT. (h) TARGET VEL. 900 FT/SEC. CROSSING DIST. 900 FT.



**FIG. 11. CONTROL STIFFNESS = 25 FT/SEC<sup>2</sup> AND  $T_f = 4$  SECS.**

- (a) TARGET VEL. 200 F/S. CROSSING DIST. ZERO. (e) TARGET VEL. 200 F/S. CROSSING DIST. 300 FT.  
 (b) TARGET VEL. 500 F/S. CROSSING DIST. ZERO. (f) TARGET VEL. 500 F/S. CROSSING DIST. 300 FT.  
 (c) TARGET VEL. 700 F/S. CROSSING DIST. ZERO. (g) TARGET VEL. 700 F/S. CROSSING DIST. 300 FT.  
 (d) TARGET VEL. 900 F/S. CROSSING DIST. ZERO. (h) TARGET VEL. 900 F/S. CROSSING DIST. 300 FT.

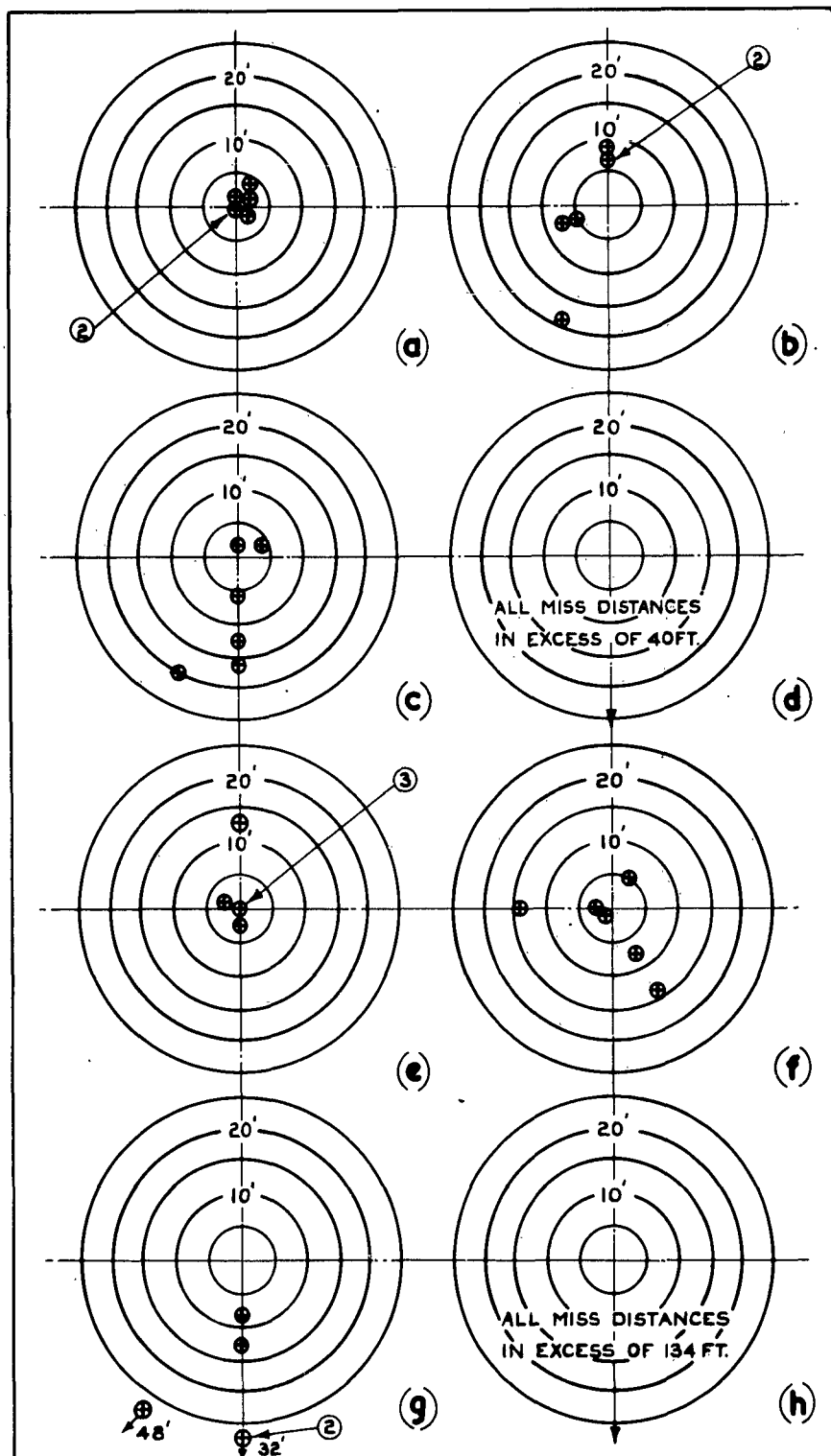


FIG. 11(a) CONTROL STIFFNESS =  $25 \text{ FT/SEC}^2$  AND  $T_f = 4 \text{ SECS.}$

- |   |   |
|---|---|
| (a) TARGET VEL. 200 F/S. CROSSING DIST. 600 FT. | (e) TARGET VEL. 200 F/S. CROSSING DIST. 900 FT. |
| (b) TARGET VEL. 500 F/S. CROSSING DIST. 600 FT. | (f) TARGET VEL. 500 F/S. CROSSING DIST. 900 FT. |
| (c) TARGET VEL. 700 F/S. CROSSING DIST. 600 FT. | (g) TARGET VEL. 700 F/S. CROSSING DIST. 900 FT. |
| (d) TARGET VEL. 900 F/S. CROSSING DIST. 600 FT. | (h) TARGET VEL. 900 F/S. CROSSING DIST. 900 FT. |

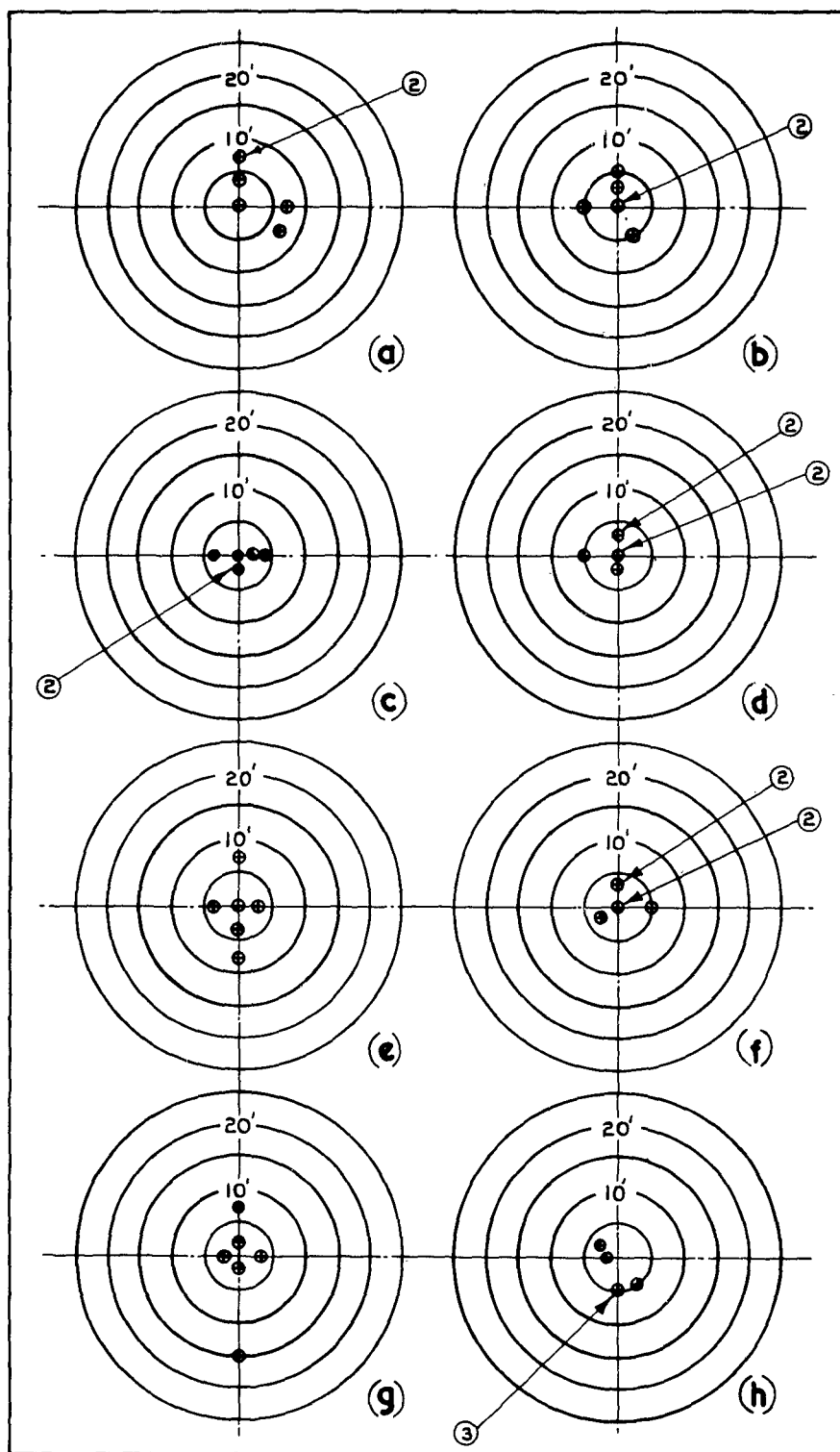
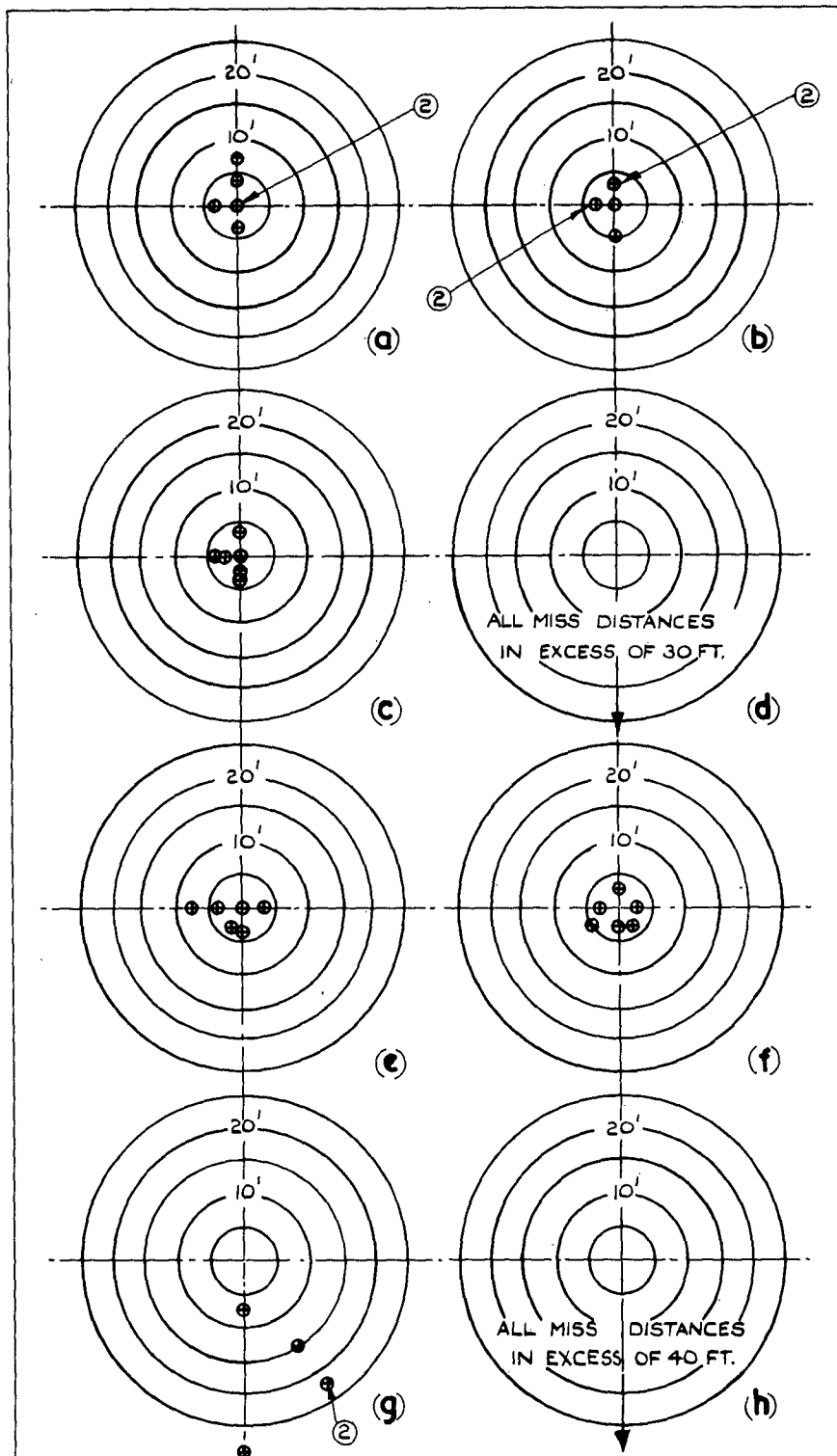


FIG. 12. CONTROL STIFFNESS =  $50 \text{ FT/SEC}^2$  AND  $T_F = 1.0 \text{ SEC}$ .

- (a) TARGET VEL. 200 FT/SEC. CROSSING DIST. 0 FT. (e) TARGET VEL. 200 FT/SEC. CROSSING DIST. 300 FT.  
 (b) TARGET VEL. 500 FT/SEC. CROSSING DIST. 0 FT. (f) TARGET VEL. 500 FT/SEC. CROSSING DIST. 300 FT.  
 (c) TARGET VEL. 700 FT/SEC. CROSSING DIST. 0 FT. (g) TARGET VEL. 700 FT/SEC. CROSSING DIST. 300 FT.  
 (d) TARGET VEL. 900 FT/SEC. CROSSING DIST. 0 FT. (h) TARGET VEL. 900 FT/SEC. CROSSING DIST. 300 FT.

FIG. 12.(a)

FIG. 12.(a) CONTROL STIFFNESS = 50 FT/SEC<sup>2</sup> & T<sub>F</sub> = 1.0 SECS.

- (a) TARGET VEL. 200 F/S. CROSSING DIST. 600 FT. (e) TARGET VEL. 200 F/S. CROSSING DIST. 900 FT.  
 (b) TARGET VEL. 500 F/S. CROSSING DIST. 600 FT. (f) TARGET VEL. 500 F/S. CROSSING DIST. 900 FT.  
 (c) TARGET VEL. 700 F/S. CROSSING DIST. 600 FT. (g) TARGET VEL. 700 F/S. CROSSING DIST. 900 FT.  
 (d) TARGET VEL. 900 F/S. CROSSING DIST. 600 FT. (h) TARGET VEL. 900 F/S. CROSSING DIST. 900 FT.

FIG. 13.

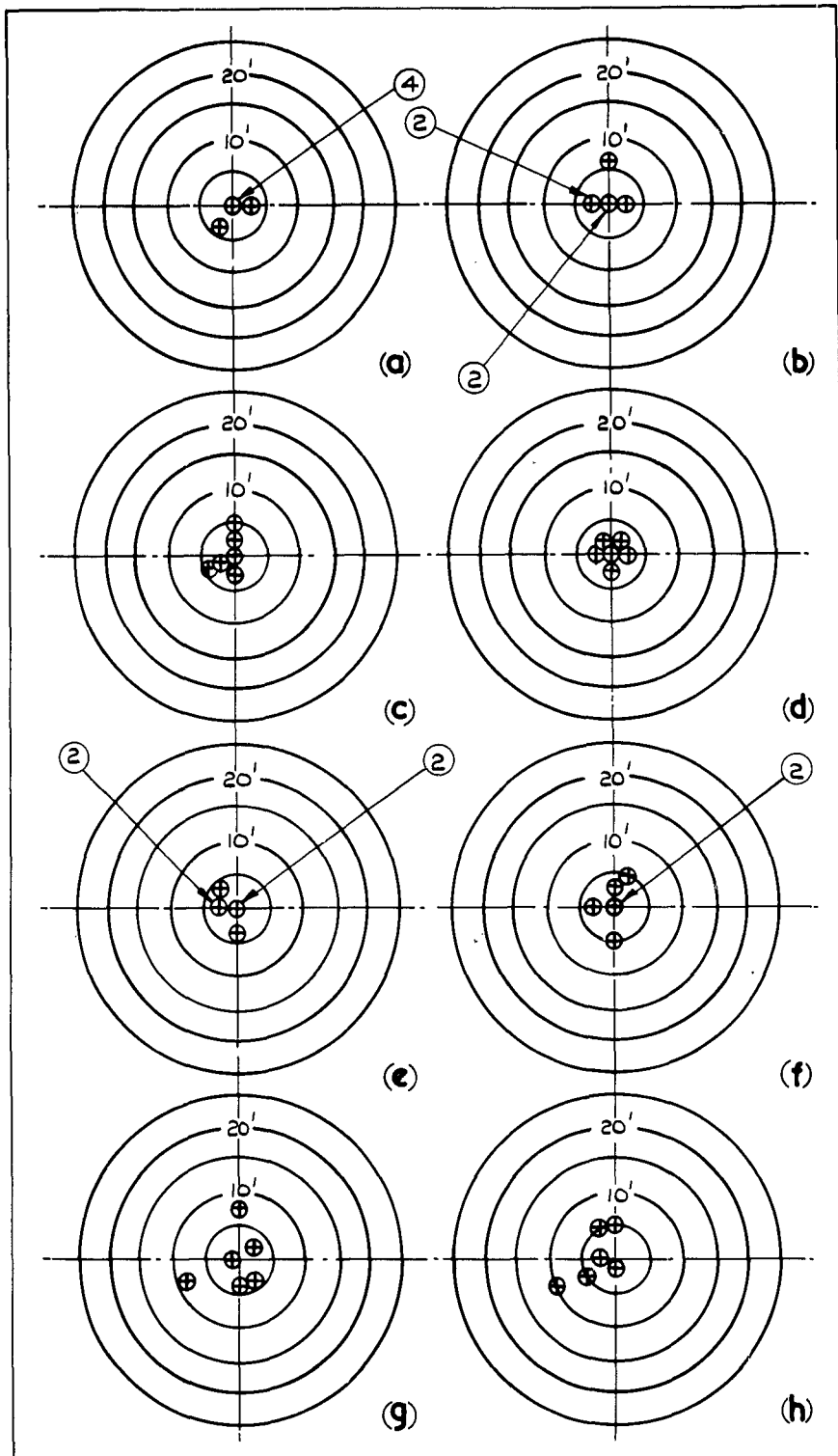


FIG. 13. CONTROL STIFFNESS =  $50 \text{ FT/SEC}^2$  AND  $T_F = 2 \text{ SECS}$ .

- (a) TARGET VEL. 200 F/S. CROSSING DIST. ZERO. (e) TARGET VEL. 200 F/S. CROSSING DIST. 300 FT.  
 (b) TARGET VEL. 500 F/S. CROSSING DIST. ZERO. (f) TARGET VEL. 500 F/S. CROSSING DIST. 300 FT.  
 (c) TARGET VEL. 700 F/S. CROSSING DIST. ZERO. (g) TARGET VEL. 700 F/S. CROSSING DIST. 300 FT.  
 (d) TARGET VEL. 900 F/S. CROSSING DIST. ZERO. (h) TARGET VEL. 900 F/S. CROSSING DIST. 300 FT.

FIG.13(a)

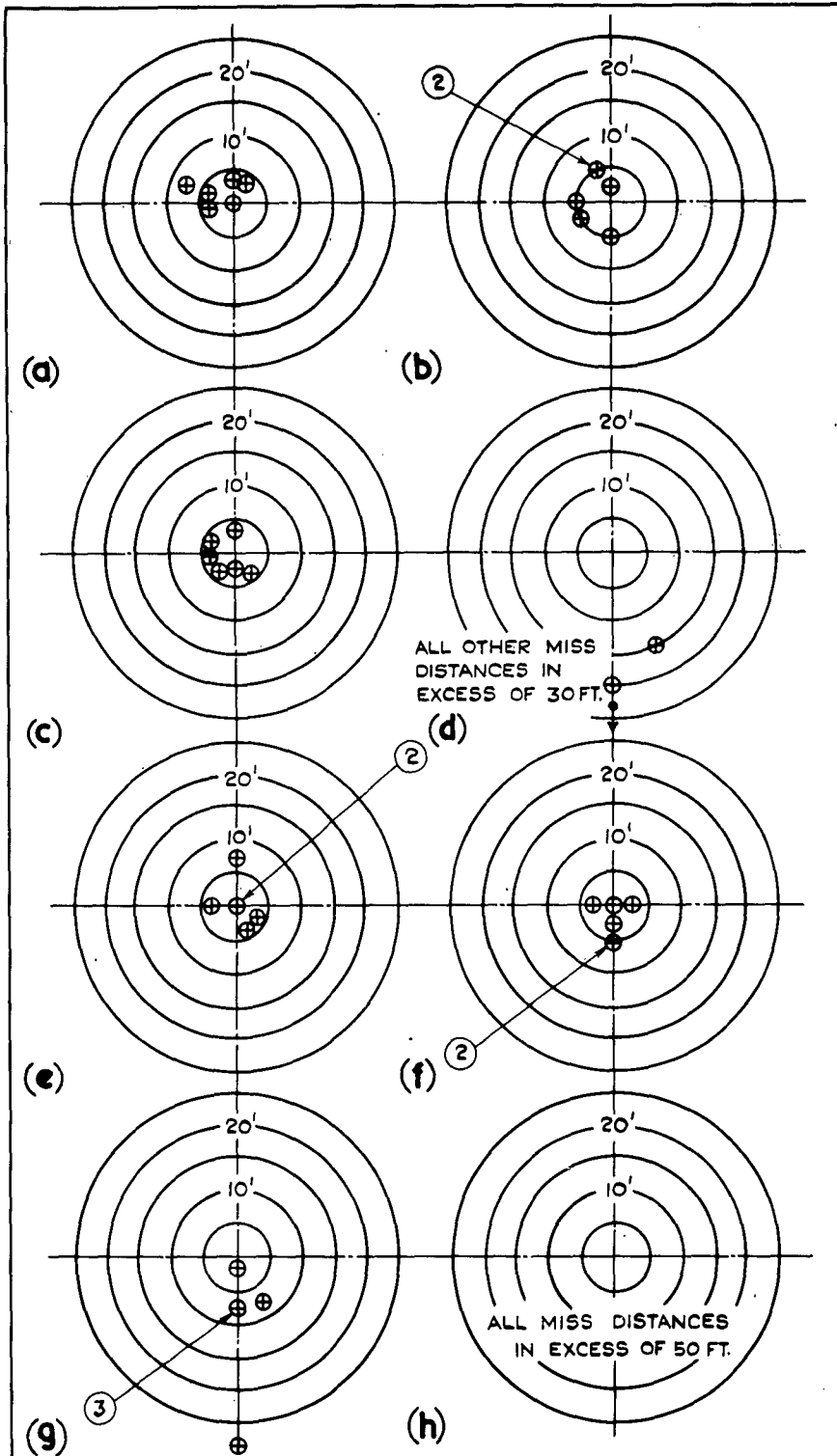


FIG.13(a) CONTROL STIFFNESS = 50 FT/SEC<sup>2</sup> & T<sub>F</sub> = 2 SECS.

- (a) TARGET VEL. 200 F/S. CROSSING DIST. 600' (e) TARGET VEL. 200 F/S. CROSSING DIST. 900'
- (b) TARGET VEL. 500 F/S. CROSSING DIST. 600' (f) TARGET VEL. 500 F/S. CROSSING DIST. 900'
- (c) TARGET VEL. 700 F/S. CROSSING DIST. 600' (g) TARGET VEL. 700 F/S. CROSSING DIST. 900'
- (d) TARGET VEL. 900 F/S. CROSSING DIST. 600' (h) TARGET VEL. 900 F/S. CROSSING DIST. 900'

FIG.14.

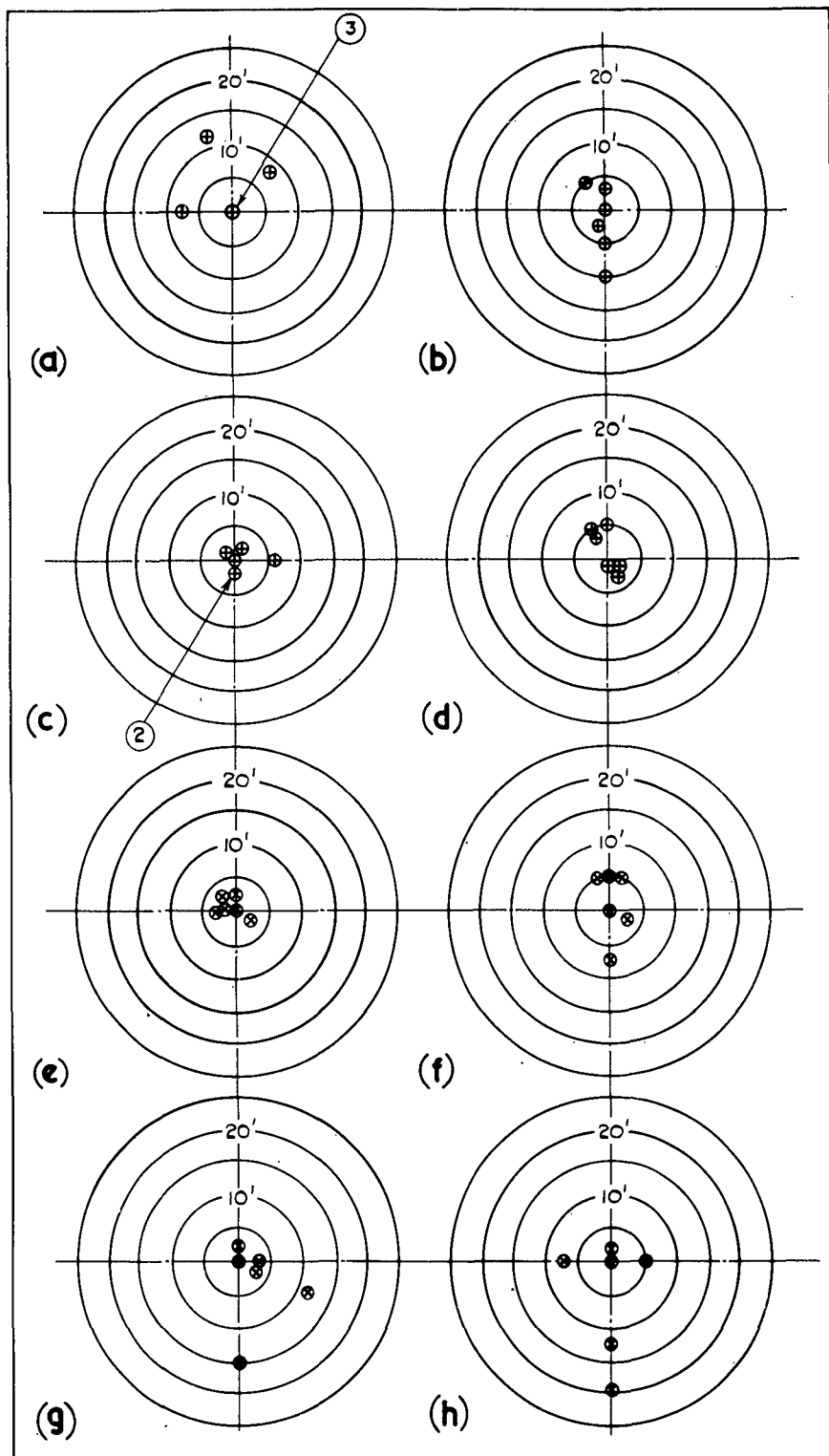


FIG.14. CONTROL STIFFNESS =  $50 \text{ FT/SEC}^2$  &  $T_F = 4 \text{ SECS.}$

- (a) TARGET VEL. 200 F/S. CROSSING DIST. ZERO. (e) TARGET VEL. 200 F/S. CROSSING DIST. 300'  
 (b) TARGET VEL. 500 F/S. CROSSING DIST. ZERO. (f) TARGET VEL. 500 F/S. CROSSING DIST. 300'  
 (c) TARGET VEL. 700 F/S. CROSSING DIST. ZERO. (g) TARGET VEL. 700 F/S. CROSSING DIST. 300'  
 (d) TARGET VEL. 900 F/S. CROSSING DIST. ZERO. (h) TARGET VEL. 900 F/S. CROSSING DIST. 300'



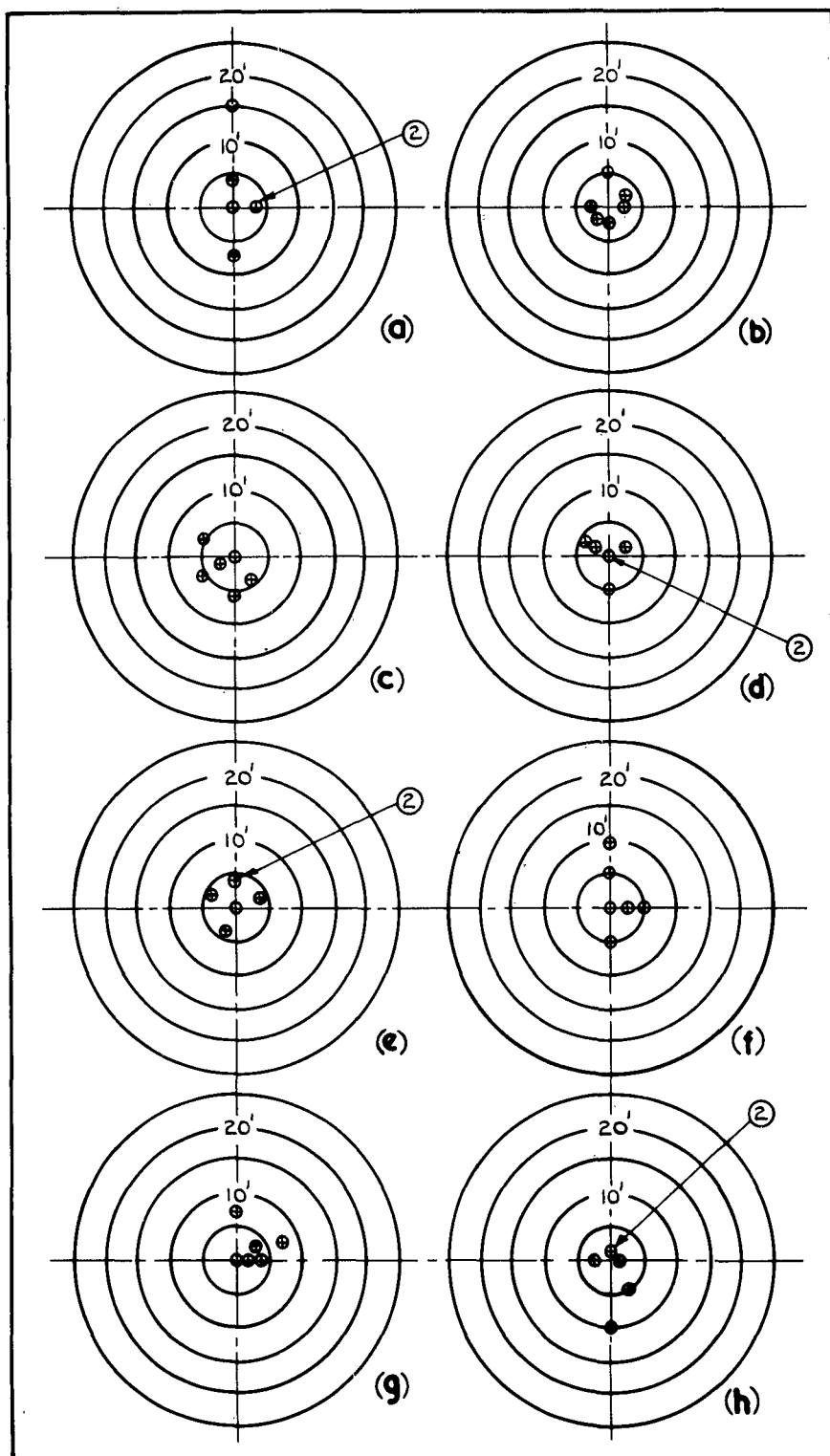


FIG.15. CONTROL STIFFNESS =  $100 \text{ FT/SEC}^2$  &  $T_r = 0.5 \text{ SEC}$ .

- (a) TARGET VEL.  $200 \text{ F/5}$ . CROSSING DIST. 0 FT. (e) TARGET VEL.  $200 \text{ F/5}$ . CROSSING DIST. 300 FT.  
 (b) TARGET VEL.  $500 \text{ F/5}$ . CROSSING DIST. 0 FT. (f) TARGET VEL.  $500 \text{ F/5}$ . CROSSING DIST. 300 FT.  
 (c) TARGET VEL.  $700 \text{ F/5}$ . CROSSING DIST. 0 FT. (g) TARGET VEL.  $700 \text{ F/5}$ . CROSSING DIST. 300 FT.  
 (d) TARGET VEL.  $900 \text{ F/5}$ . CROSSING DIST. 0 FT. (h) TARGET VEL.  $900 \text{ F/5}$ . CROSSING DIST. 300 FT.

FIG. 15(a)

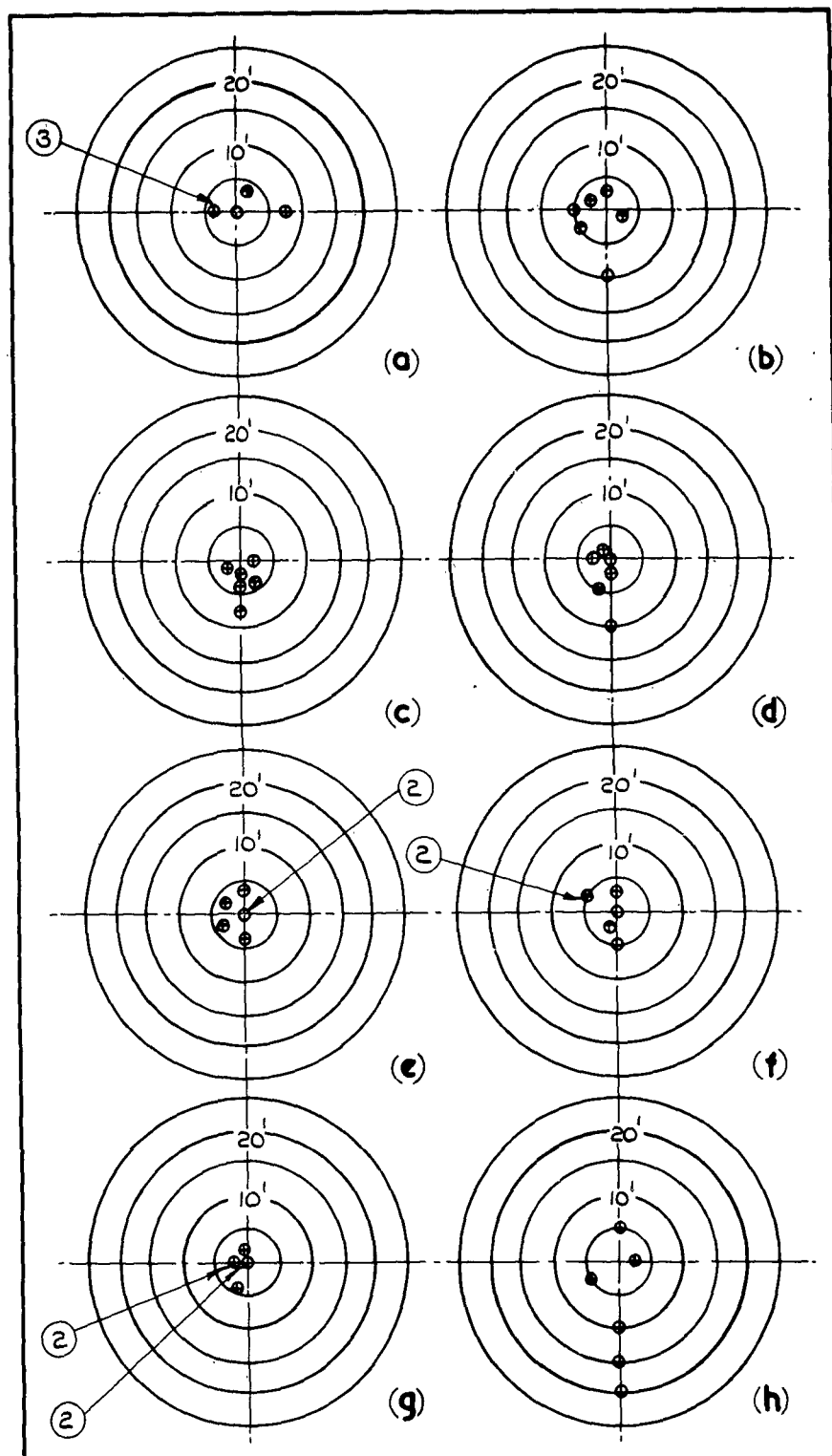


FIG.15(a) CONTROL STIFFNESS = 100 FT/SEC.<sup>2</sup> &  $T_F = 0.5$  SEC.

- (a) TARGET VEL. 200 F/S. CROSSING DIST. 600 FT. (e) TARGET VEL. 200 F/S. CROSSING DIST. 900 FT.  
 (b) TARGET VEL. 500 F/S. CROSSING DIST. 600 FT. (f) TARGET VEL. 500 F/S. CROSSING DIST. 900 FT.  
 (c) TARGET VEL. 700 F/S. CROSSING DIST. 600 FT. (g) TARGET VEL. 700 F/S. CROSSING DIST. 900 FT.  
 (d) TARGET VEL. 900 F/S. CROSSING DIST. 600 FT. (h) TARGET VEL. 900 F/S. CROSSING DIST. 900 FT.

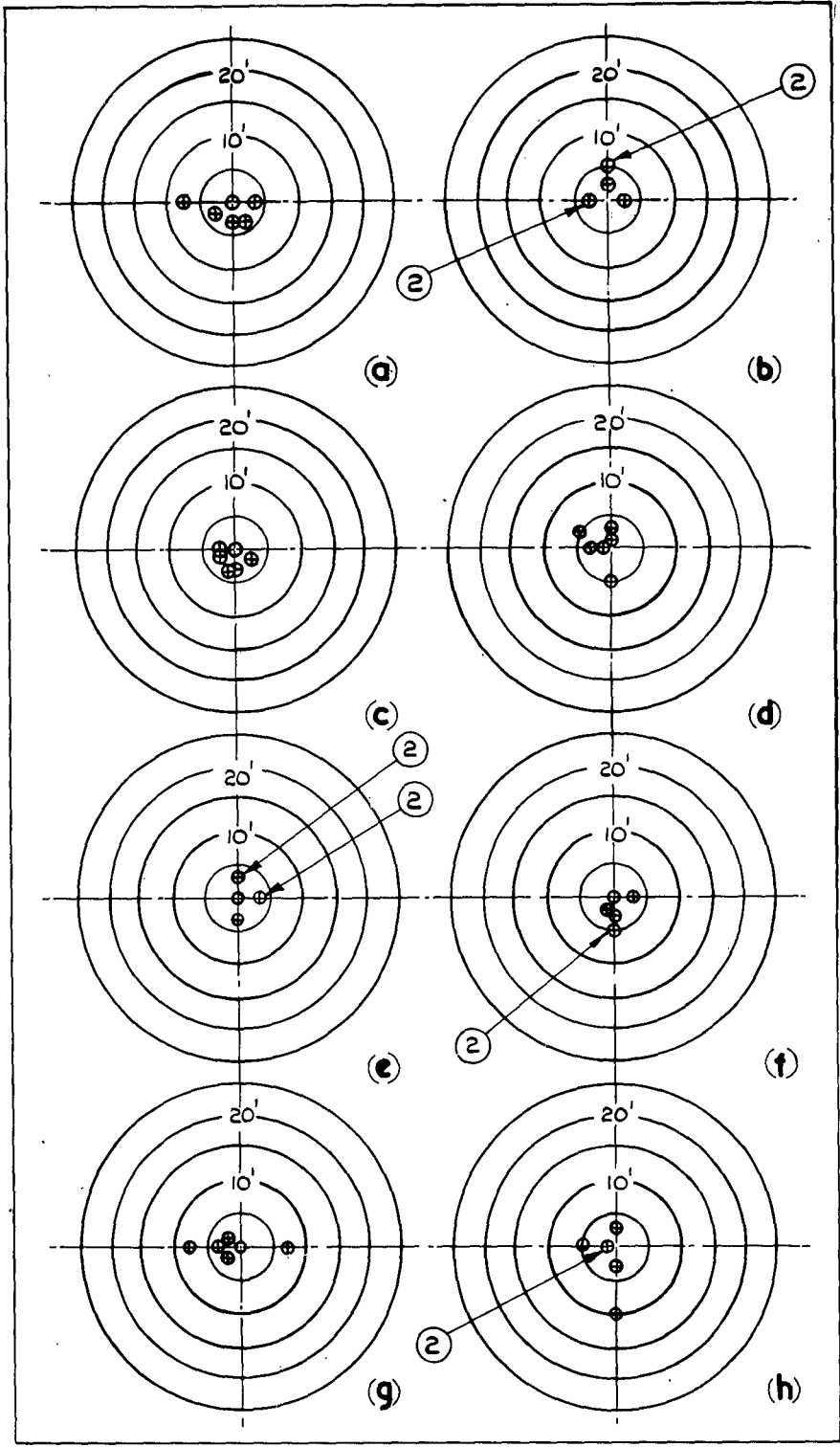
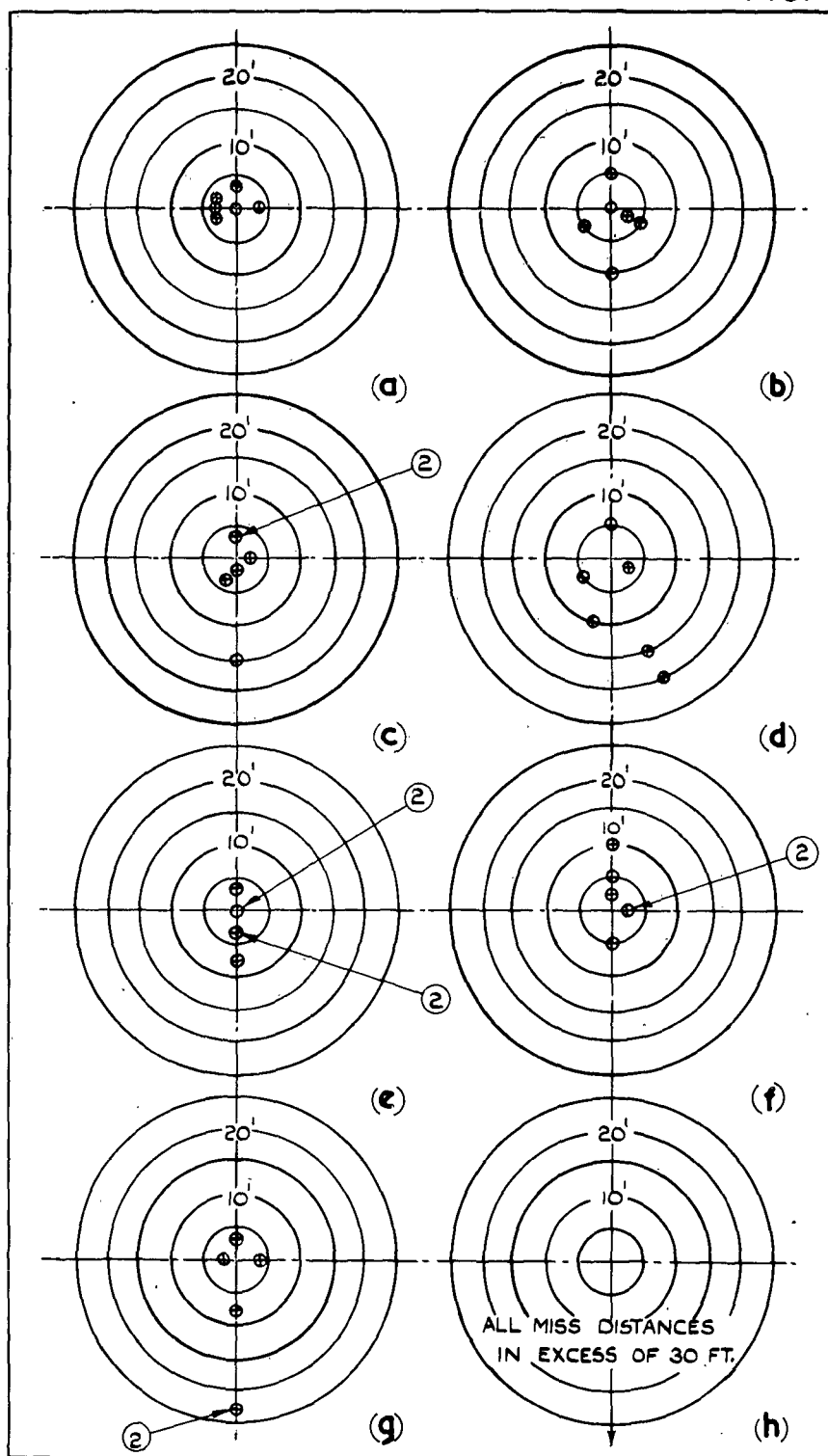


FIG. 16. CONTROL STIFFNESS = 100 FT/SEC<sup>2</sup> AND T<sub>F</sub> = 1 SEC.

- |   |   |
|---|---|
| (a) TARGET VEL. 200 F/S. CROSSING DIST. 0 | (e) TARGET VEL. 200 F/S. CROSSING DIST. 300 FT. |
| (b) TARGET VEL. 500 F/S. CROSSING DIST. 0 | (f) TARGET VEL. 500 F/S. CROSSING DIST. 300 FT. |
| (c) TARGET VEL. 700 F/S. CROSSING DIST. 0 | (g) TARGET VEL. 700 F/S. CROSSING DIST. 300 FT. |
| (d) TARGET VEL. 900 F/S. CROSSING DIST. 0 | (h) TARGET VEL. 900 F/S. CROSSING DIST. 300 FT. |

FIG. 16. (a)

FIG. 16(a) CONTROL STIFFNESS = 100 FT/SEC<sup>2</sup> AND  $T_F = 1$  SEC.

- (a) TARGET VEL. 200 F/S. CROSSING DIST. 600 FT. (e) TARGET VEL. 200 F/S. CROSSING DIST. 900 FT.  
 (b) TARGET VEL. 500 F/S. CROSSING DIST. 600 FT. (f) TARGET VEL. 500 F/S. CROSSING DIST. 900 FT.  
 (c) TARGET VEL. 700 F/S. CROSSING DIST. 600 FT. (g) TARGET VEL. 700 F/S. CROSSING DIST. 900 FT.  
 (d) TARGET VEL. 900 F/S. CROSSING DIST. 600 FT. (h) TARGET VEL. 900 F/S. CROSSING DIST. 900 FT.

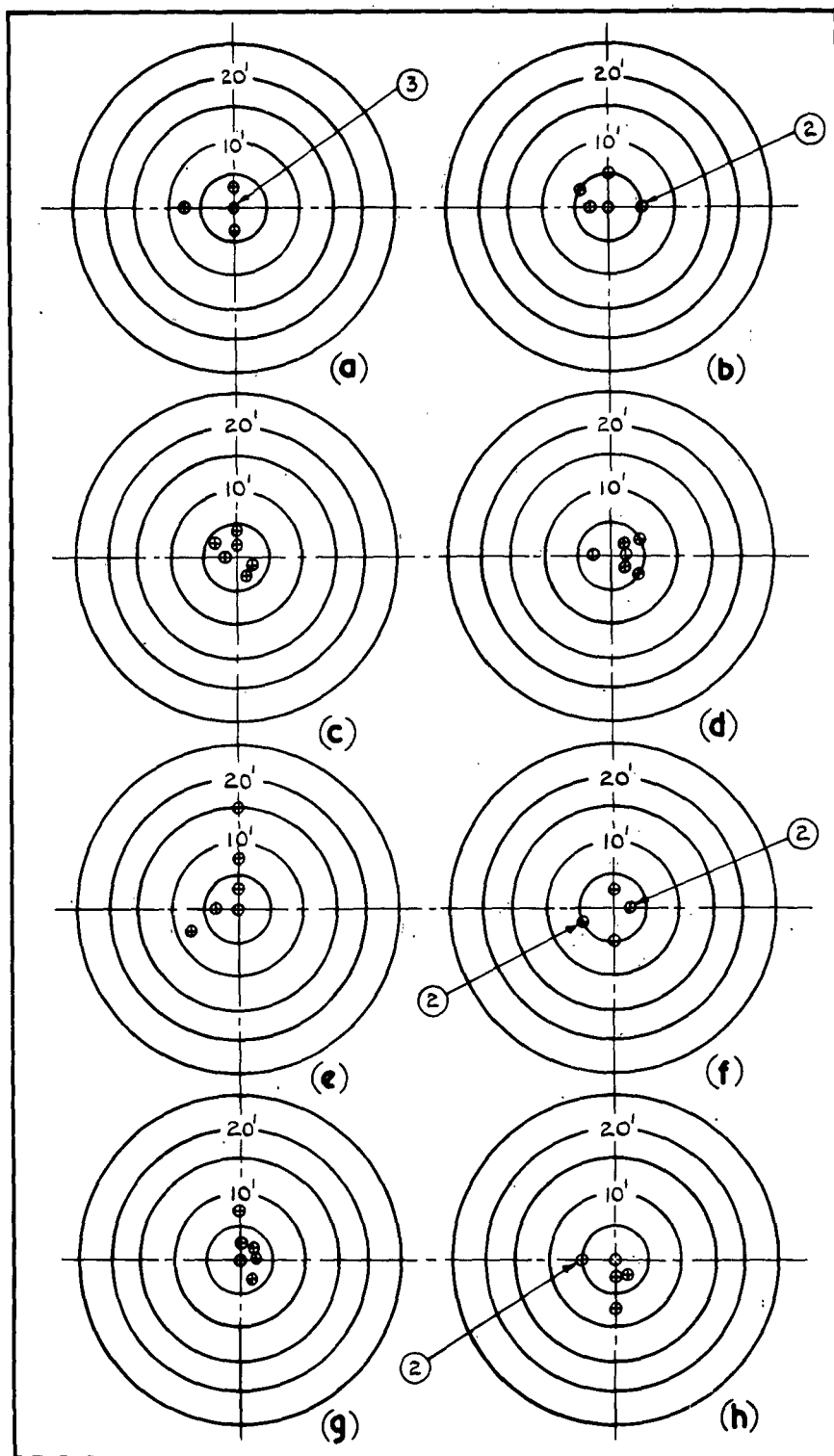


FIG.17. CONTROL STIFFNESS =  $100\text{FT/SEC}^2$  AND  $T_f = 2$  SECS.

- (a) TARGET VEL.  $200\text{F/S}$ . CROSSING DIST. 0 FT. (e) TARGET VEL.  $200\text{F/S}$ . CROSSING DIST. 300 FT.  
 (b) TARGET VEL.  $500\text{F/S}$ . CROSSING DIST. 0 FT. (f) TARGET VEL.  $500\text{F/S}$ . CROSSING DIST. 300 FT.  
 (c) TARGET VEL.  $700\text{F/S}$ . CROSSING DIST. 0 FT. (g) TARGET VEL.  $700\text{F/S}$ . CROSSING DIST. 300 FT.  
 (d) TARGET VEL.  $900\text{F/S}$ . CROSSING DIST. 0 FT. (h) TARGET VEL.  $900\text{F/S}$ . CROSSING DIST. 300 FT.

FIG. 17 (a)

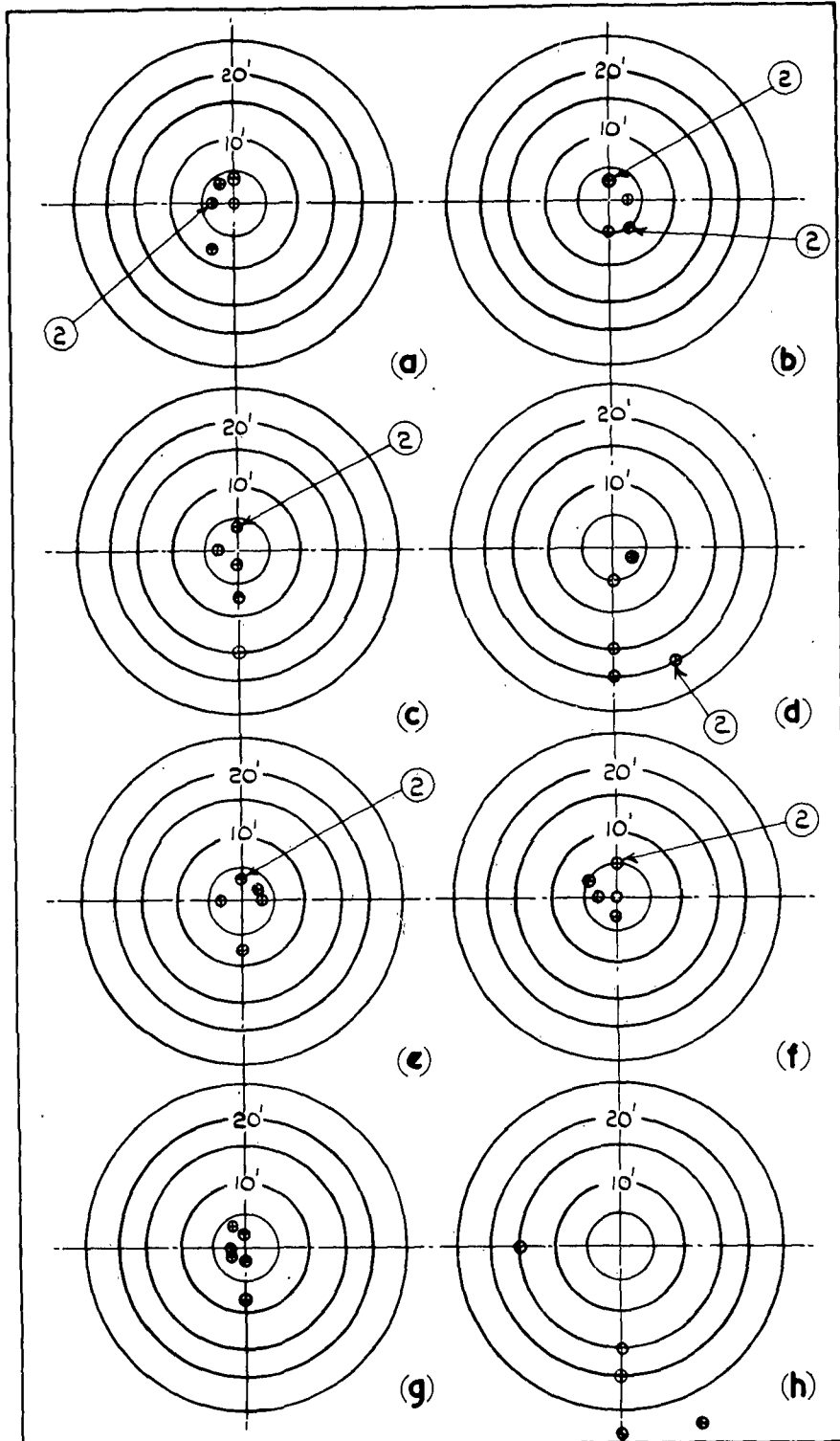


FIG. 17(a) CONTROL STIFFNESS = 100 FT/SEC.<sup>2</sup> AND  $T_F = 2$  SECS

- (a) TARGET VEL. 200 F/S. CROSSING DIST. 600 FT. (e) TARGET VEL. 200 F/S. CROSSING DIST. 900 FT.  
 (b) TARGET VEL. 500 F/S. CROSSING DIST. 600 FT. (f) TARGET VEL. 500 F/S. CROSSING DIST. 900 FT.  
 (c) TARGET VEL. 700 F/S. CROSSING DIST. 600 FT. (g) TARGET VEL. 700 F/S. CROSSING DIST. 900 FT.  
 (d) TARGET VEL. 900 F/S. CROSSING DIST. 600 FT. (h) TARGET VEL. 900 F/S. CROSSING DIST. 900 FT.

FIG. 18.

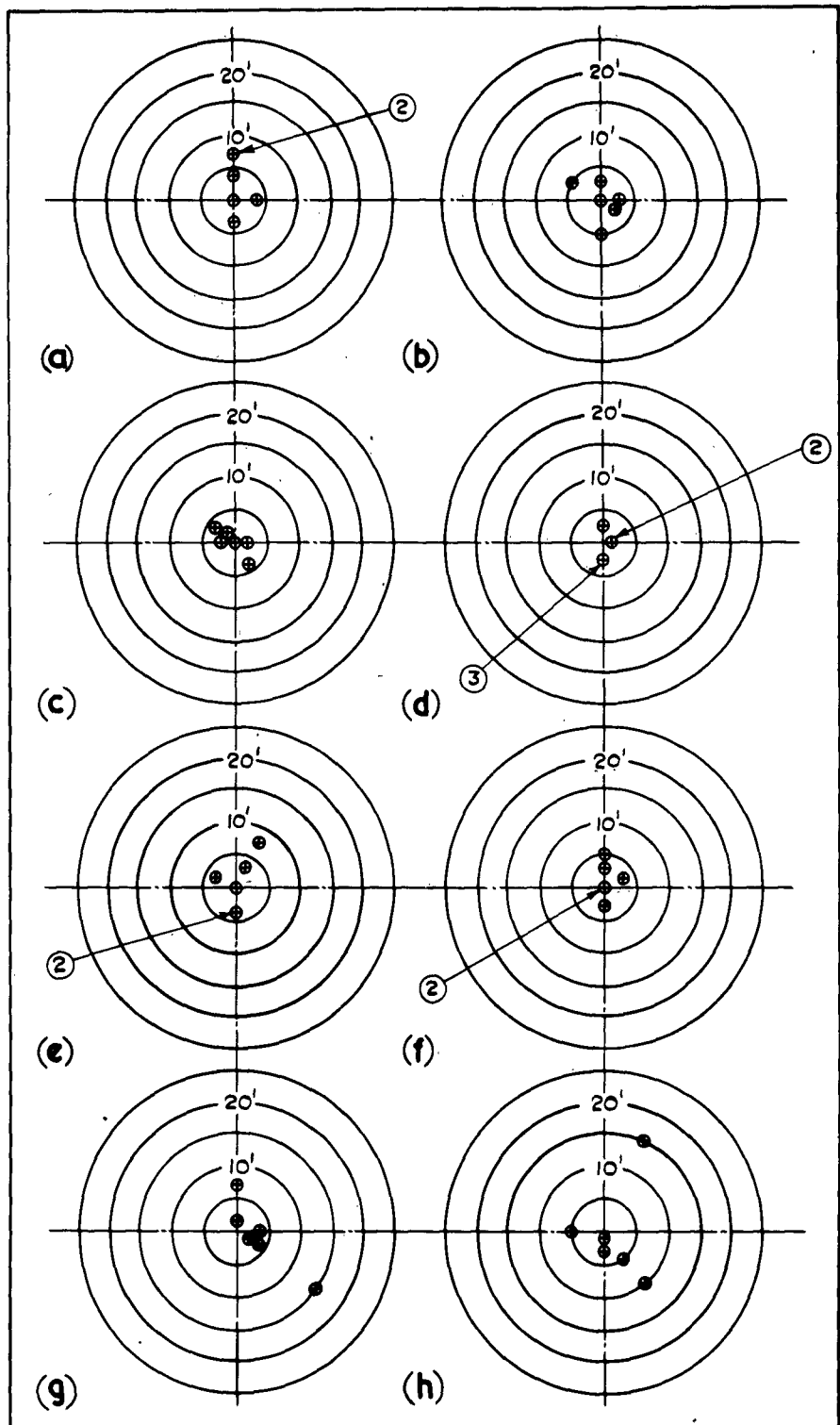
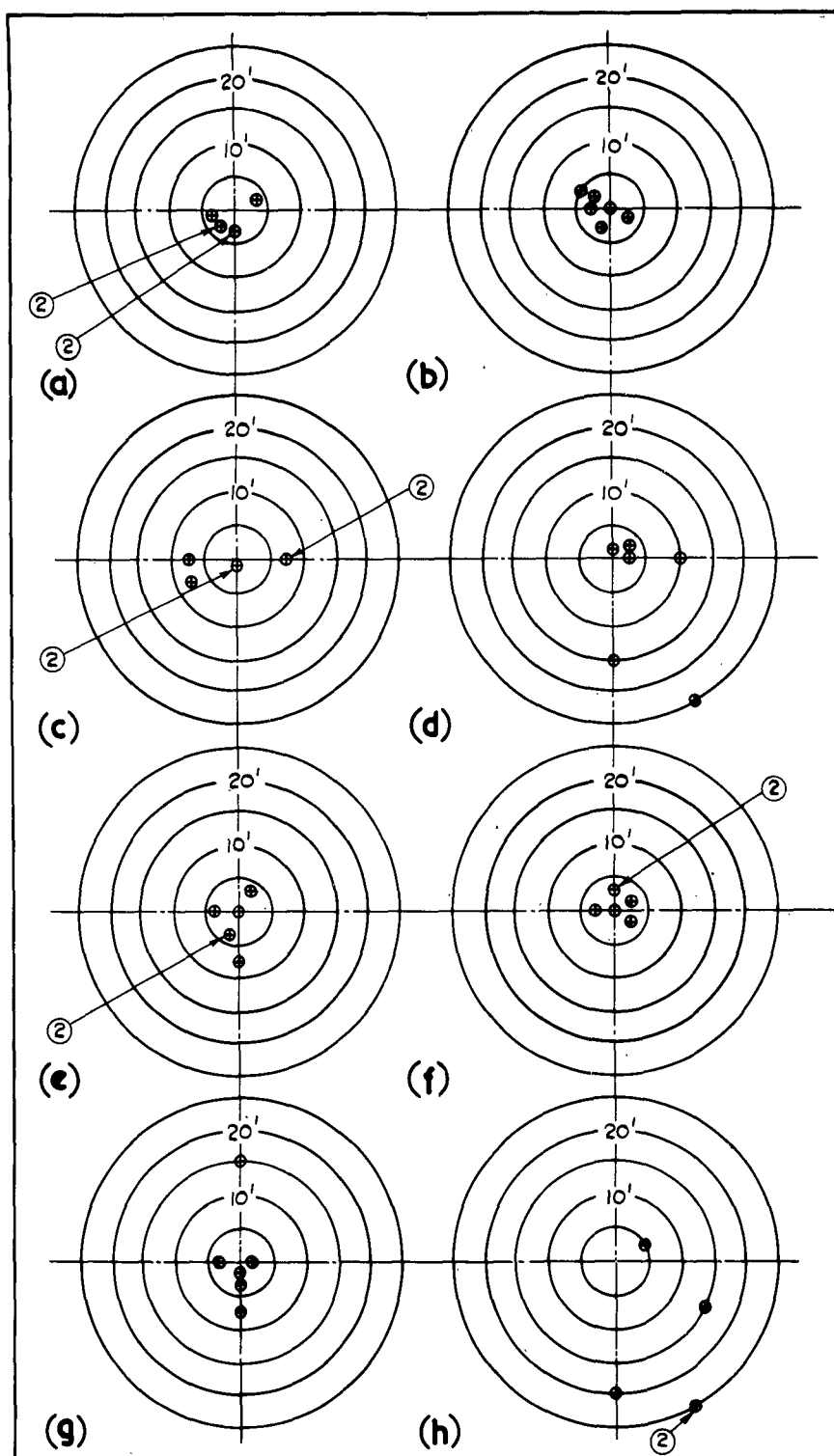


FIG. 18. CONTROL STIFFNESS =  $200 \text{ FT/SEC}^2$  &  $T_F = 0.5 \text{ SEC.}$

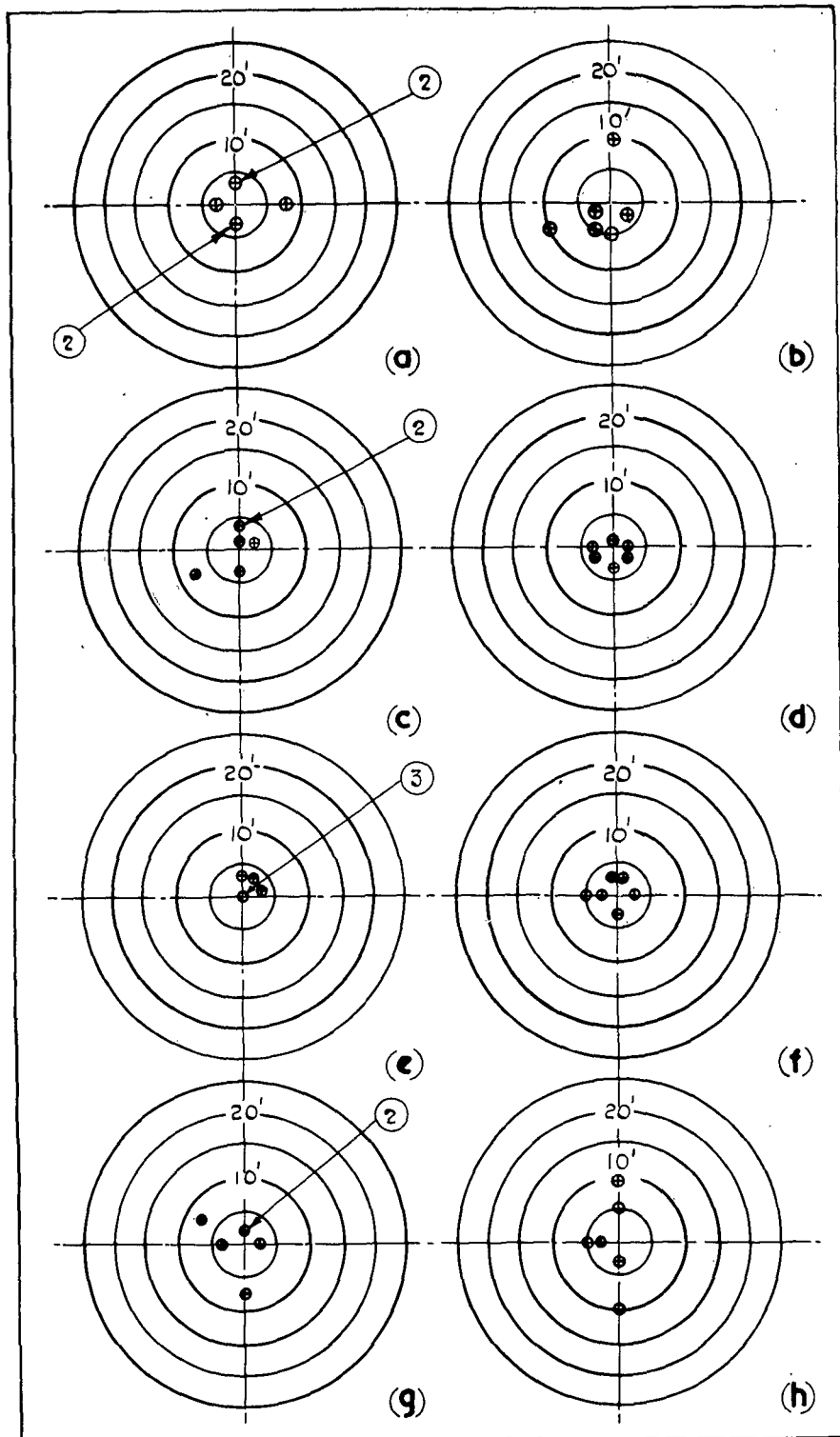
- |   |  |
|---|--|
| (a) TARGET VEL. 200 F/S. CROSSING DIST. 0 | (e) TARGET VEL. 200 F/S. CROSSING DIST. 300' |
| (b) TARGET VEL. 500 F/S. CROSSING DIST. 0 | (f) TARGET VEL. 500 F/S. CROSSING DIST. 300' |
| (c) TARGET VEL. 700 F/S. CROSSING DIST. 0 | (g) TARGET VEL. 700 F/S. CROSSING DIST. 300' |
| (d) TARGET VEL. 900 F/S. CROSSING DIST. 0 | (h) TARGET VEL. 900 F/S. CROSSING DIST. 300' |

FIG. 18(a)



**FIG. 18(a) CONTROL STIFFNESS =  $200 \text{ FT/SEC}^2$  &  $T_F = 0.5 \text{ SEC}$ .**

- (a) TARGET VEL. 200 F/S. CROSSING DIST. 600' (e) TARGET VEL. 200 F/S. CROSSING DIST. 900'  
 (b) TARGET VEL. 500 F/S. CROSSING DIST. 600' (f) TARGET VEL. 500 F/S. CROSSING DIST. 900'  
 (c) TARGET VEL. 700 F/S. CROSSING DIST. 600' (g) TARGET VEL. 700 F/S. CROSSING DIST. 900'  
 (d) TARGET VEL. 900 F/S. CROSSING DIST. 600' (h) TARGET VEL. 900 F/S. CROSSING DIST. 900'



**FIG.19. CONTROL STIFFNESS = 200 FT./SEC.<sup>2</sup> AND  $T_F = 1.0$  SEC.**

- |   |   |
|---|---|
| (a) TARGET VEL. 200 F/S. CROSSING DIST. 0 | (e) TARGET VEL. 200 F/S. CROSSING DIST. 300 FT. |
| (b) TARGET VEL. 500 F/S. CROSSING DIST. 0 | (f) TARGET VEL. 500 F/S. CROSSING DIST. 300 FT. |
| (c) TARGET VEL. 700 F/S. CROSSING DIST. 0 | (g) TARGET VEL. 700 F/S. CROSSING DIST. 300 FT. |
| (d) TARGET VEL. 900 F/S. CROSSING DIST. 0 | (h) TARGET VEL. 900 F/S. CROSSING DIST. 300 FT. |

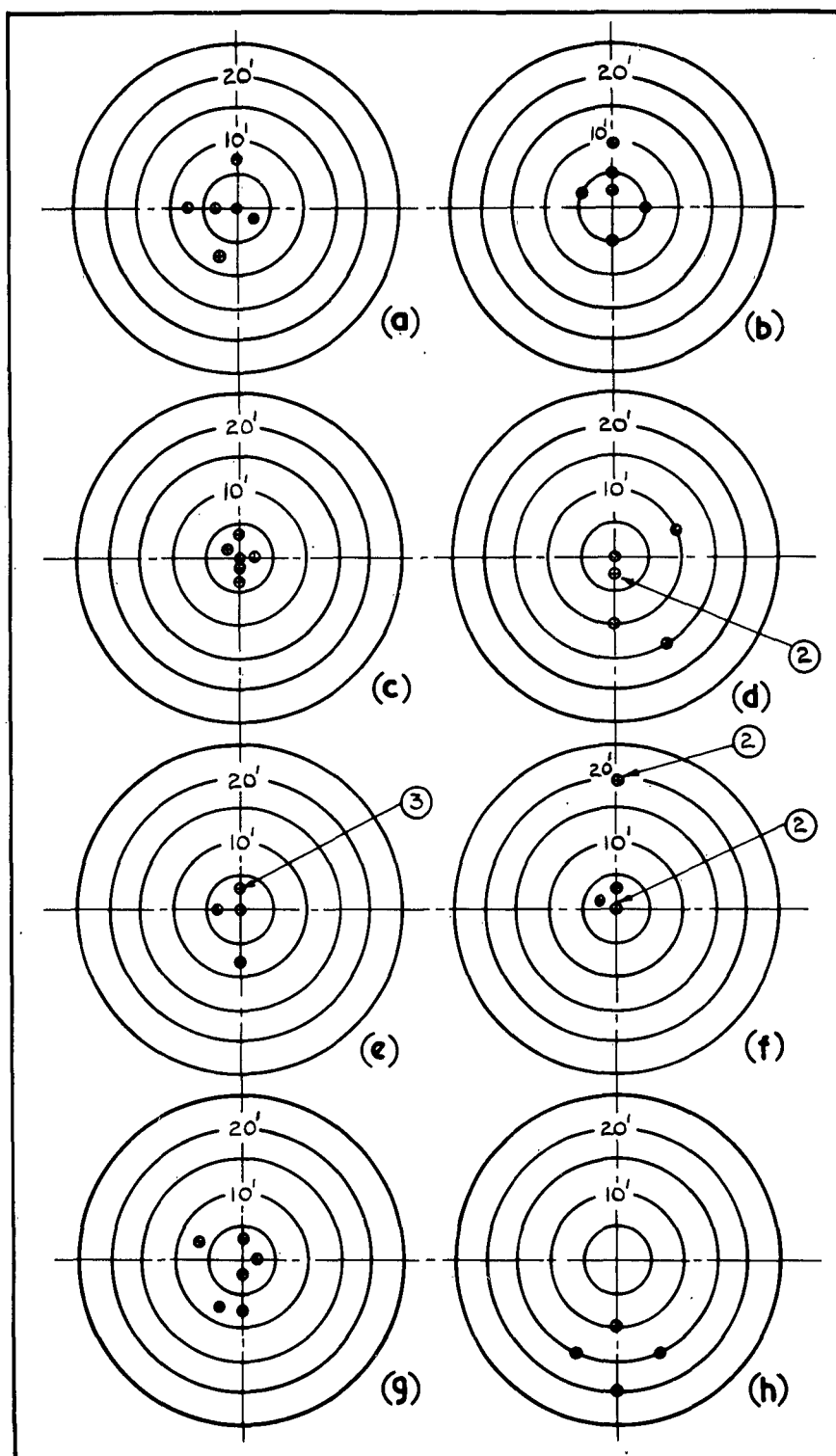
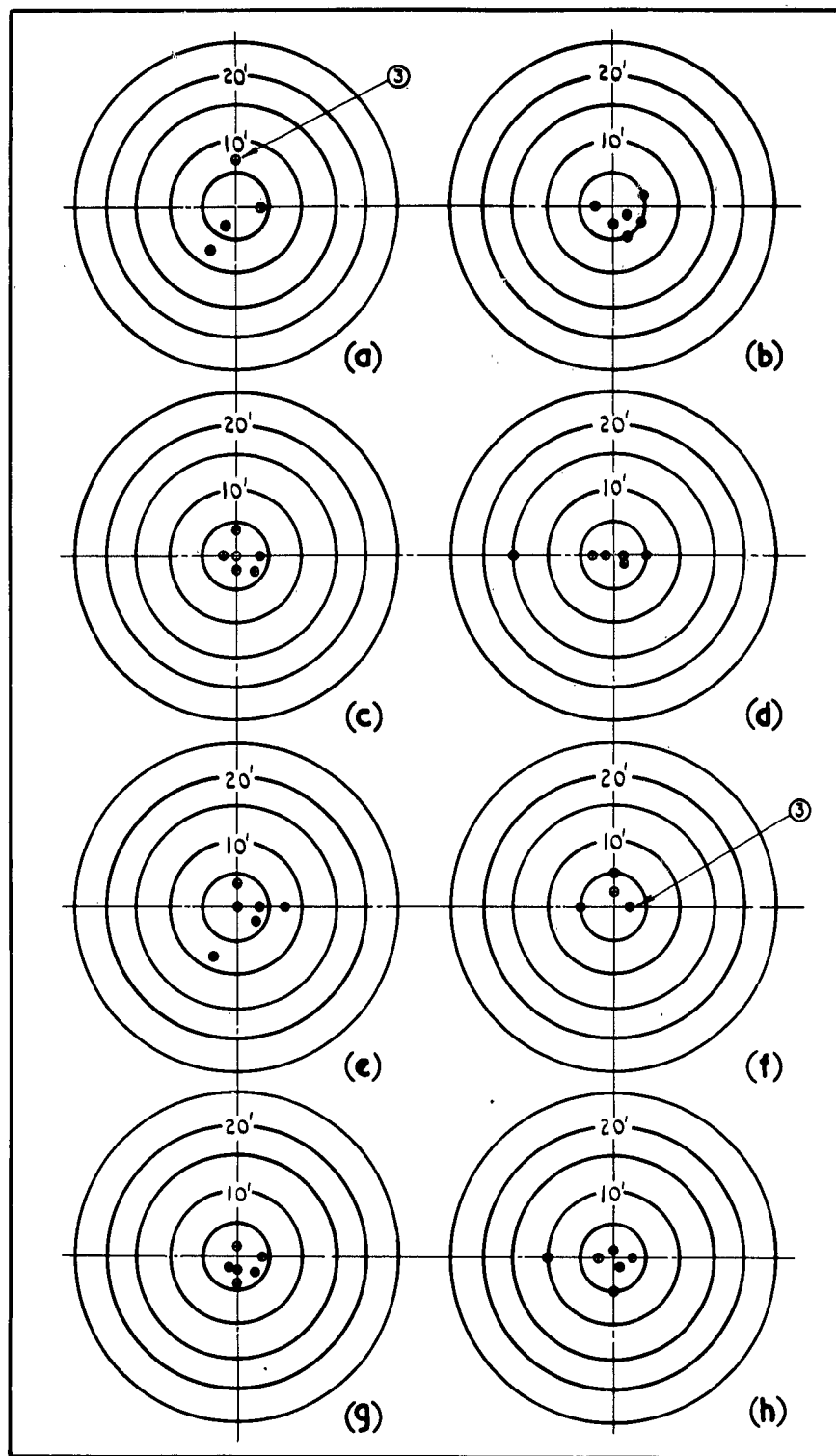


FIG.19(a) CONTROL STIFFNESS =  $200 \text{ FT/SEC}^2$  &  $T_r = 1.0 \text{ SEC}$ .

- (a) TARGET VEL.  $200 \text{ F/S}$  CROSSING DIST.  $600 \text{ FT}$ . (e) TARGET VEL.  $200 \text{ F/S}$  CROSSING DIST.  $900 \text{ FT}$ .  
 (b) TARGET VEL.  $500 \text{ F/S}$  CROSSING DIST.  $600 \text{ FT}$ . (f) TARGET VEL.  $500 \text{ F/S}$  CROSSING DIST.  $900 \text{ FT}$ .  
 (c) TARGET VEL.  $700 \text{ F/S}$  CROSSING DIST.  $600 \text{ FT}$ . (g) TARGET VEL.  $700 \text{ F/S}$  CROSSING DIST.  $900 \text{ FT}$ .  
 (d) TARGET VEL.  $900 \text{ F/S}$  CROSSING DIST.  $600 \text{ FT}$ . (h) TARGET VEL.  $900 \text{ F/S}$  CROSSING DIST.  $900 \text{ FT}$ .



**FIG. 20. CONTROL STIFFNESS =  $400 \text{ FT/SEC}^2$  &  $T_f = 0.5 \text{ SEC}$ .**

- |   |   |
|---|---|
| (a) TARGET VEL. 200 f/s. CROSSING DIST. 0 | (e) TARGET VEL. 200 f/s. CROSSING DIST. 300 FT. |
| (b) TARGET VEL. 500 f/s. CROSSING DIST. 0 | (f) TARGET VEL. 500 f/s. CROSSING DIST. 300 FT. |
| (c) TARGET VEL. 700 f/s. CROSSING DIST. 0 | (g) TARGET VEL. 700 f/s. CROSSING DIST. 300 FT. |
| (d) TARGET VEL. 900 f/s. CROSSING DIST. 0 | (h) TARGET VEL. 900 f/s. CROSSING DIST. 300 FT. |

FIG. 20.(a)

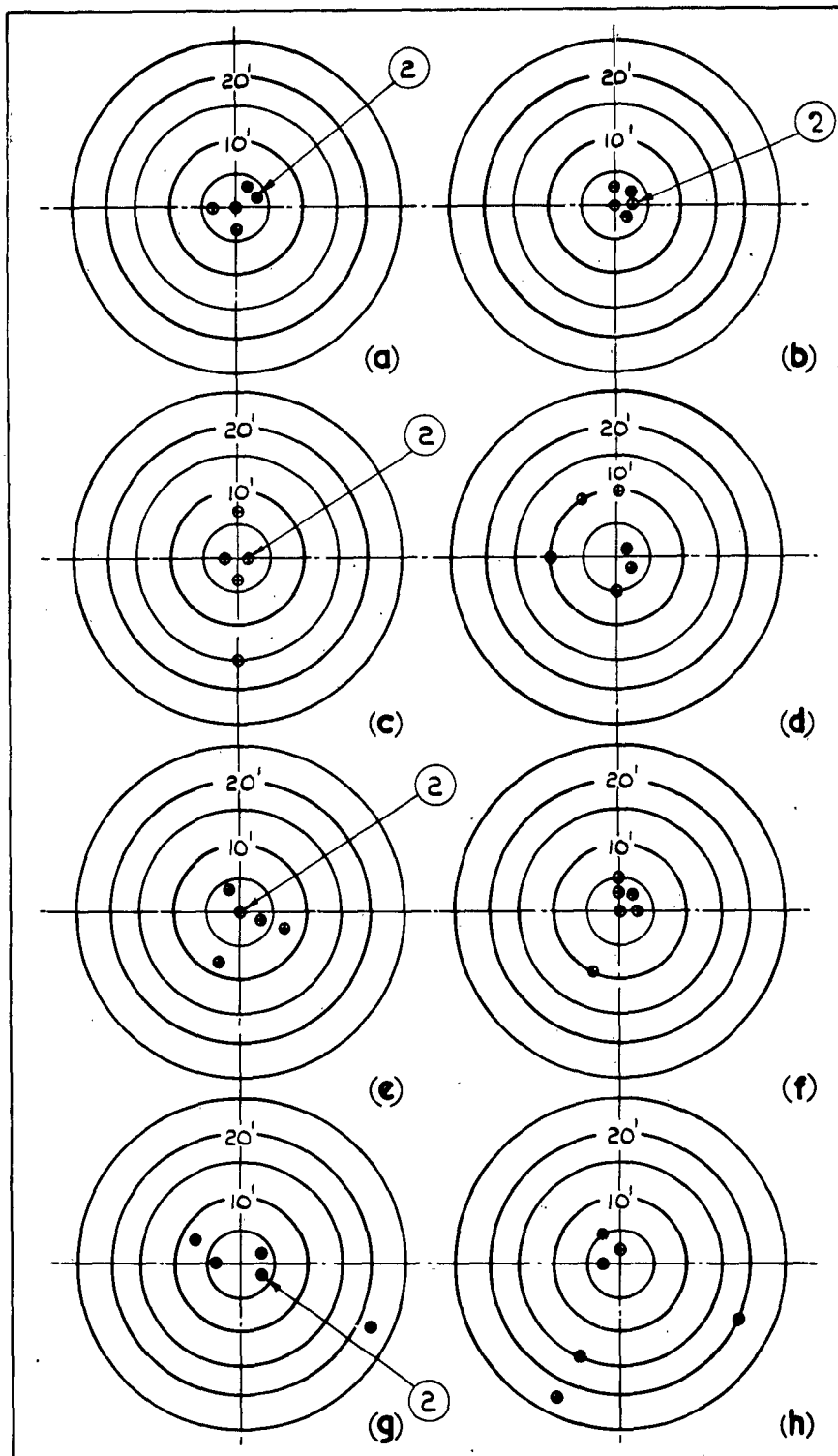


**FIG. 20.(a) CONTROL STIFFNESS = 400 FT/SEC<sup>2</sup> & T<sub>F</sub> = 0.5 SEC.**

(a) TARGET VEL. 200 F/S. CROSSING DIST. 600 FT. (e) TARGET VEL. 200 F/S. CROSSING DIST. 900 FT.

(b) TARGET VEL. 500 F/S. CROSSING DIST. 600 FT. (f) TARGET VEL. 500 F/S. CROSSING DIST. 900 FT.

(c) TARGET VEL. 700 F/S. CROSSING DIST. 600 FT. (g) TARGET VEL. 700 F/S. CROSSING DIST. 900 FT.

(d) TARGET VEL. 900 F/S. CROSSING DIST. 600 FT. (h) TARGET VEL. 900 F/S. CROSSING DIST. 900 FT.

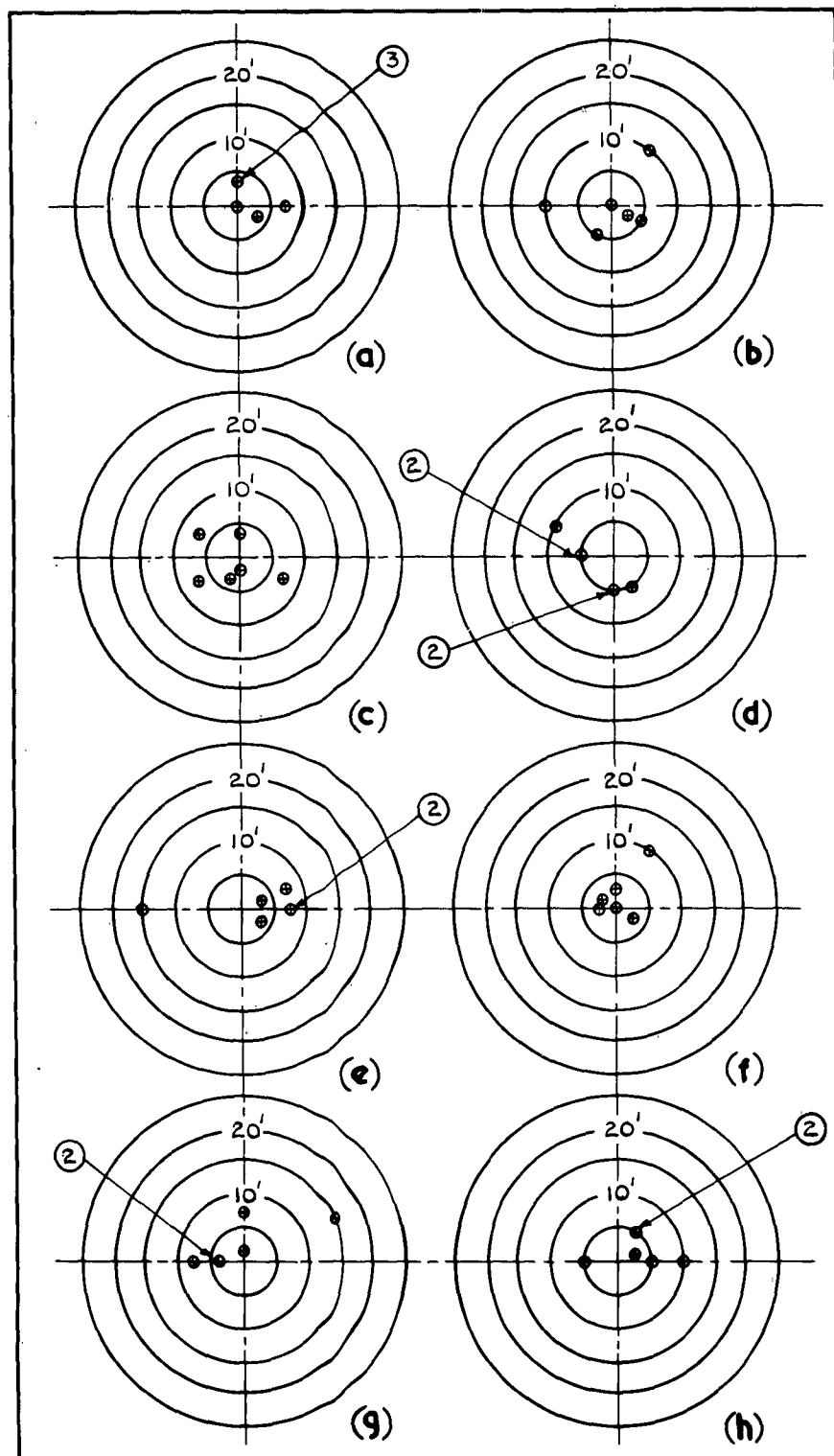
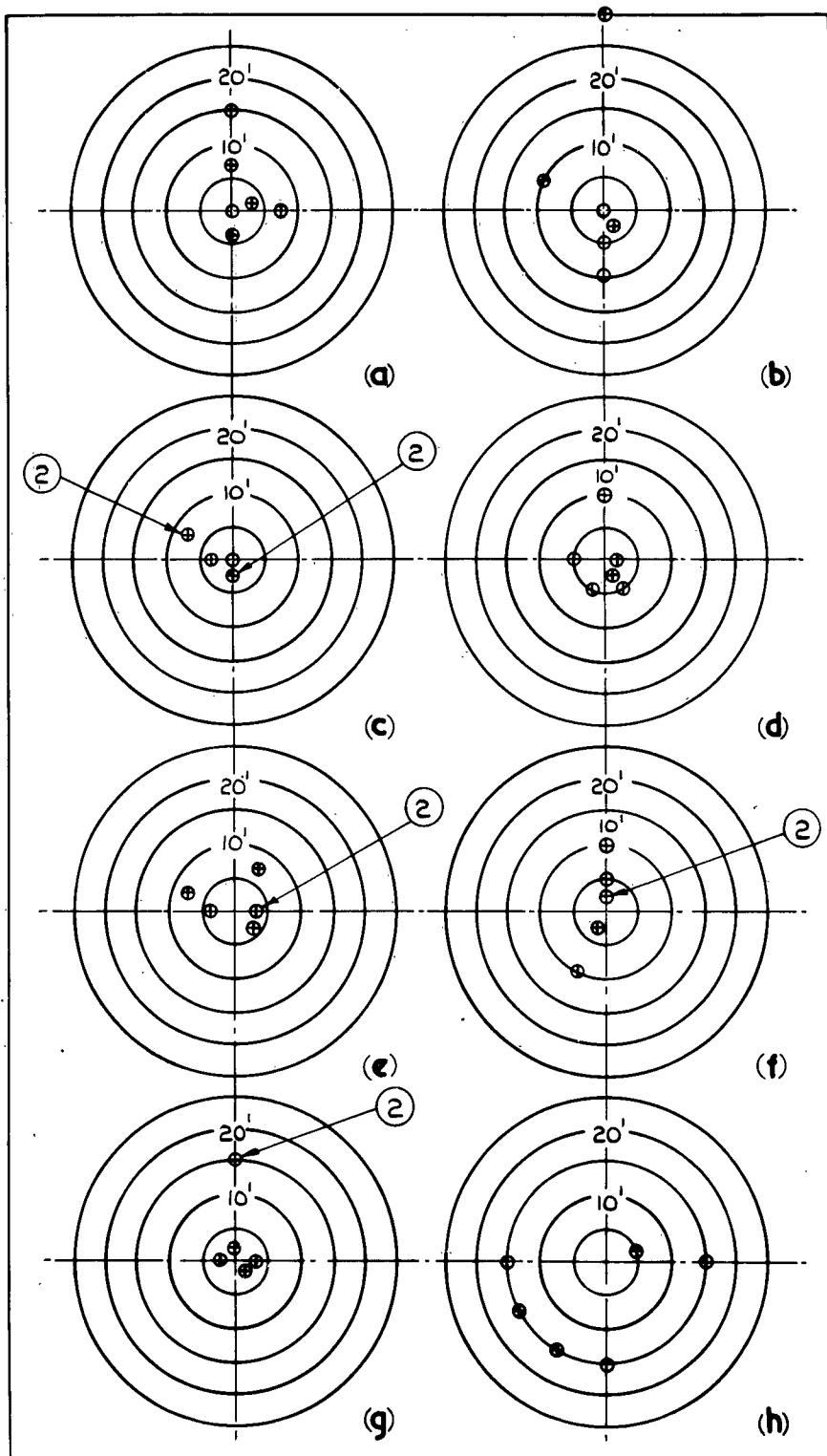


FIG.21. CONTROL STIFFNESS =  $600\text{FT/SEC}^2$  AND  $T_f = 0.5\text{ SEC.}$

- (a) TARGET VEL.  $200\text{F/S.}$  CROSSING DIST. 0 FT. (e) TARGET VEL.  $200\text{F/S.}$  CROSSING DIST. 300 FT.  
 (b) TARGET VEL.  $500\text{F/S.}$  CROSSING DIST. 0 FT. (f) TARGET VEL.  $500\text{F/S.}$  CROSSING DIST. 300 FT.  
 (c) TARGET VEL.  $700\text{F/S.}$  CROSSING DIST. 0 FT. (g) TARGET VEL.  $700\text{F/S.}$  CROSSING DIST. 300 FT.  
 (d) TARGET VEL.  $900\text{F/S.}$  CROSSING DIST. 0 FT. (h) TARGET VEL.  $900\text{F/S.}$  CROSSING DIST. 300 FT.

FIG. 21. (a)

FIG. 21. (a) CONTROL STIFFNESS =  $600 \text{ FT/SEC.}^2$  &  $T_F = 0.5 \text{ SEC.}$ 

(a) TARGET VEL. 200 F/S. CROSSING DIST. 600 FT. (e) TARGET VEL. 200 F/S. CROSSING DIST. 900 FT.

(b) TARGET VEL. 500 F/S. CROSSING DIST. 600 FT. (f) TARGET VEL. 500 F/S. CROSSING DIST. 900 FT.

(c) TARGET VEL. 700 F/S. CROSSING DIST. 600 FT. (g) TARGET VEL. 700 F/S. CROSSING DIST. 900 FT.

(d) TARGET VEL. 900 F/S. CROSSING DIST. 600 FT. (h) TARGET VEL. 900 F/S. CROSSING DIST. 900 FT.

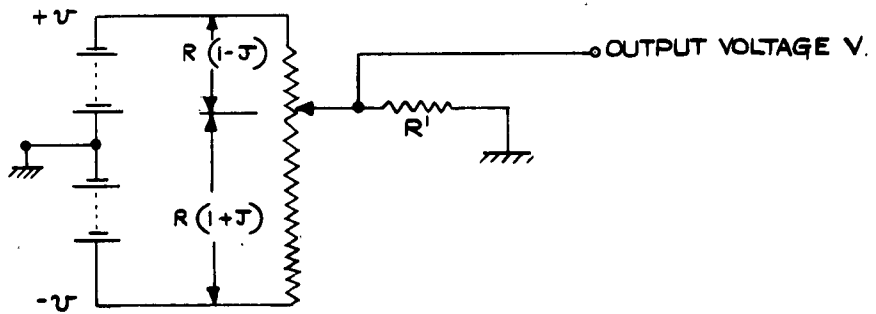
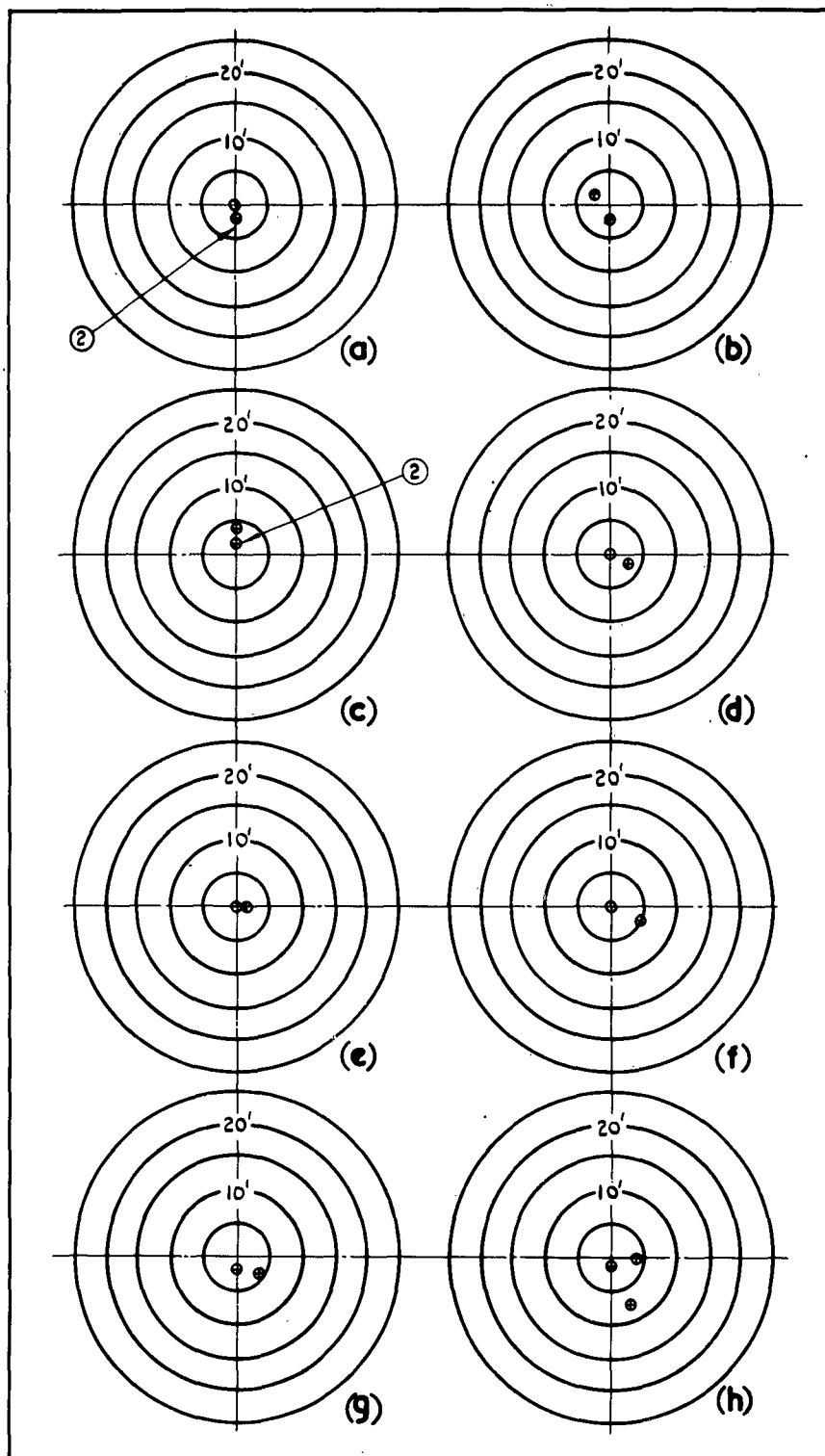
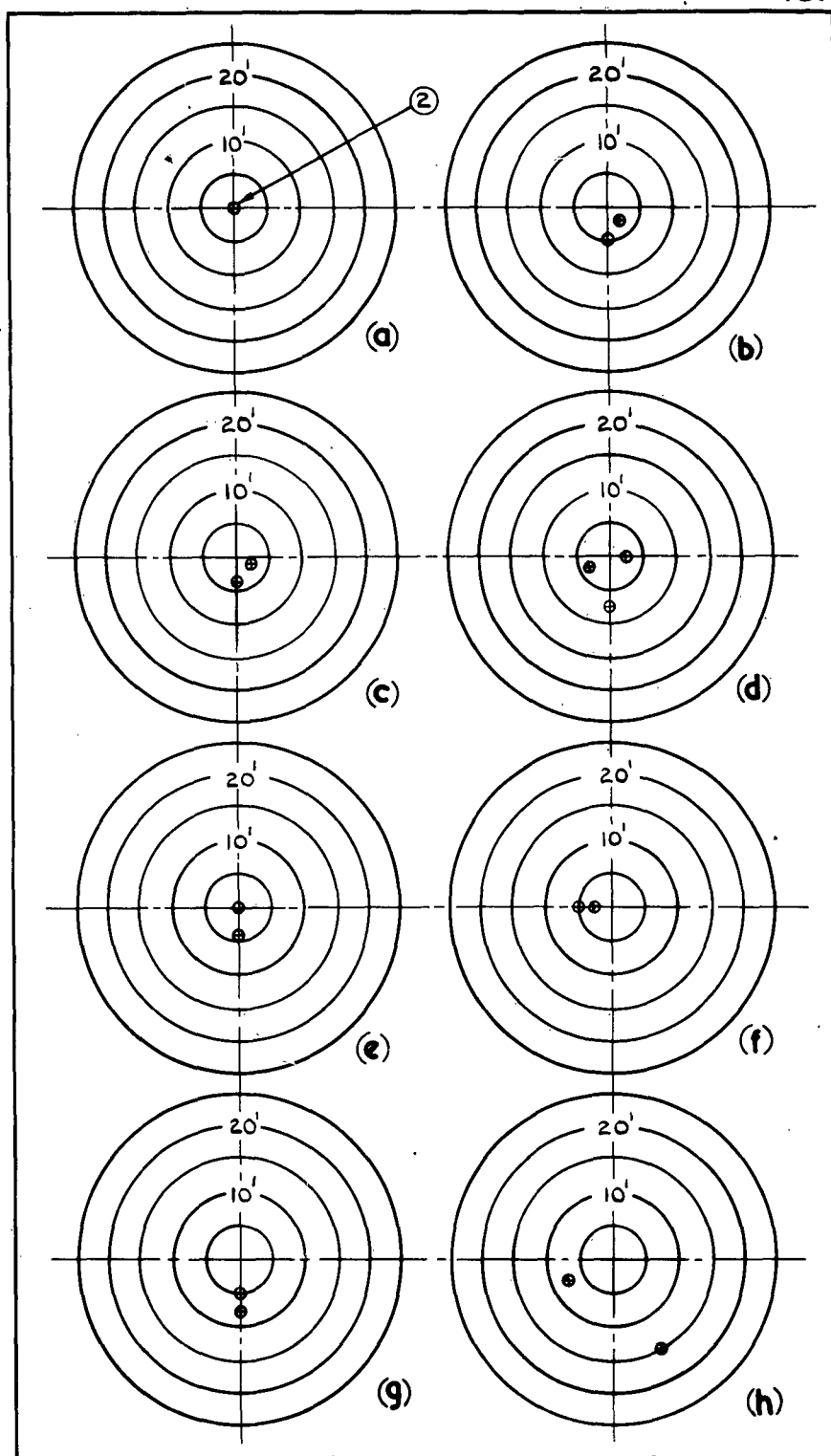


FIG. 22. ARRANGEMENT FOR GIVING  
NON-LINEAR JOYSTICK  
DEFLECTION-OUTPUT RELATION.



**FIG. 23. MAX. ACCN. DEMAND=100 FT/SEC<sup>2</sup>. NON-LINEAR JOYSTICK LAW :  $\frac{R}{R_1} = 4$  &  $T_F = 4$  SEC.**

- |   |   |
|---|---|
| (a) TARGET VEL. 200 f/s. CROSSING DIST. 0 | (e) TARGET VEL. 200 f/s. CROSSING DIST. 300 FT. |
| (b) TARGET VEL. 500 f/s. CROSSING DIST. 0 | (f) TARGET VEL. 500 f/s. CROSSING DIST. 300 FT. |
| (c) TARGET VEL. 700 f/s. CROSSING DIST. 0 | (g) TARGET VEL. 700 f/s. CROSSING DIST. 300 FT. |
| (d) TARGET VEL. 900 f/s. CROSSING DIST. 0 | (h) TARGET VEL. 900 f/s. CROSSING DIST. 300 FT. |



**FIG. 23(a) MAX. ACCN. DEMAND = 100 FT/SEC<sup>2</sup> NON - LINEAR JOYSTICK LAW:  $\frac{R}{R_0} = 4$  AND  $T_f = 4$  SECS.**

- (a) TARGET VEL. 200 F/S. CROSSING DIST. 600 FT. (e) TARGET VEL. 200 F/S. CROSSING DIST. 900 FT.  
 (b) TARGET VEL. 500 F/S. CROSSING DIST. 600 FT. (f) TARGET VEL. 500 F/S. CROSSING DIST. 900 FT.  
 (c) TARGET VEL. 700 F/S. CROSSING DIST. 600 FT. (g) TARGET VEL. 700 F/S. CROSSING DIST. 900 FT.  
 (d) TARGET VEL. 900 F/S. CROSSING DIST. 600 FT. (h) TARGET VEL. 900 F/S. CROSSING DIST. 900 FT.

FIG. 24.

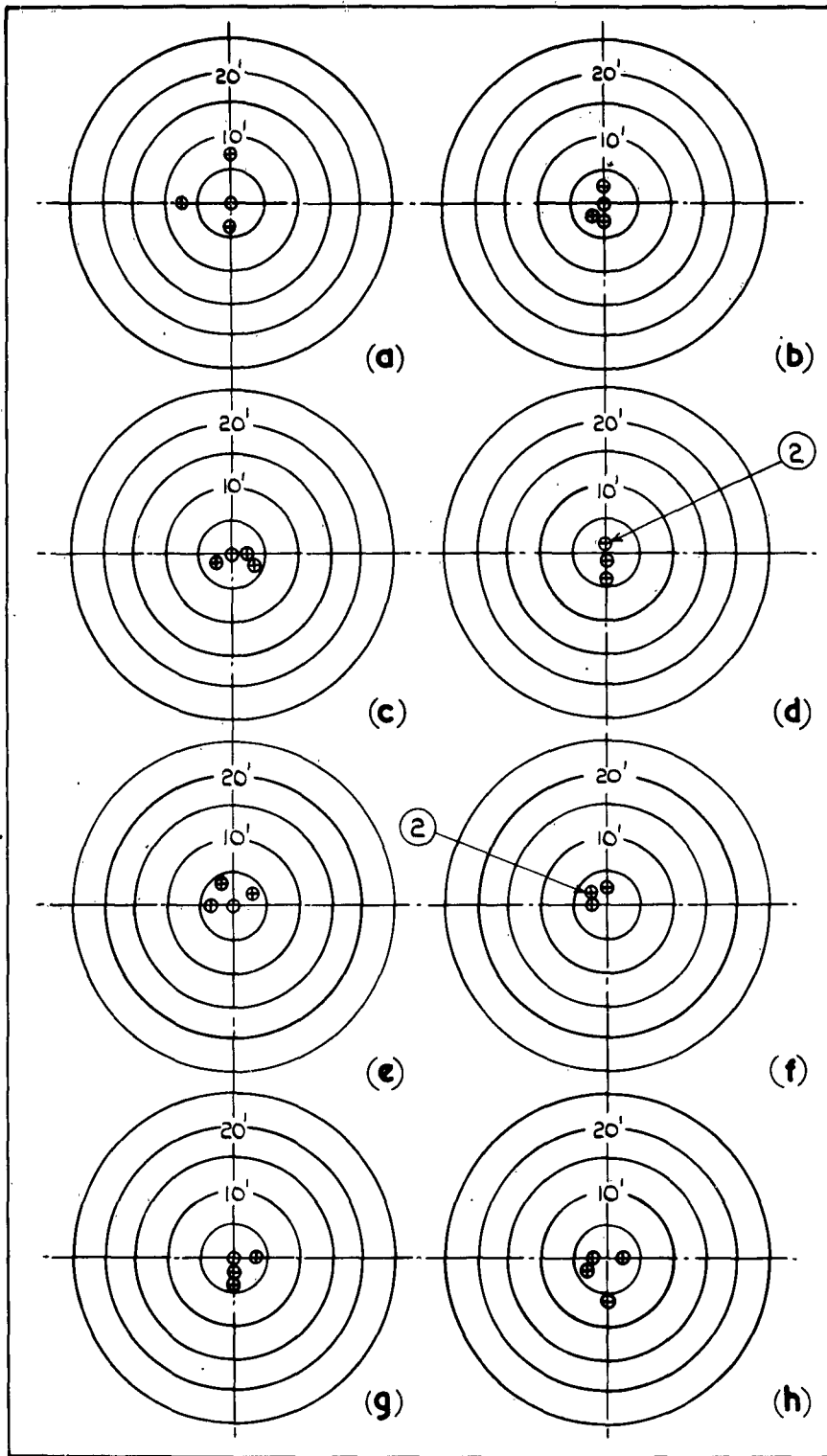


FIG. 24. MAX. ACCN. DEMAND=150 FT/SEC.<sup>2</sup> NON-LINEAR JOYSTICK LAW:  $\frac{R}{R_1}=4$  &  $T_F=2$  SECS.

- |   |   |
|---|---|
| (a) TARGET VEL. 200 F/S. CROSSING DIST. 0 | (e) TARGET VEL. 200 F/S. CROSSING DIST. 300 FT. |
| (b) TARGET VEL. 500 F/S. CROSSING DIST. 0 | (f) TARGET VEL. 500 F/S. CROSSING DIST. 300 FT. |
| (c) TARGET VEL. 700 F/S. CROSSING DIST. 0 | (g) TARGET VEL. 700 F/S. CROSSING DIST. 300 FT. |
| (d) TARGET VEL. 900 F/S. CROSSING DIST. 0 | (h) TARGET VEL. 900 F/S. CROSSING DIST. 300 FT. |

FIG. 24(a)

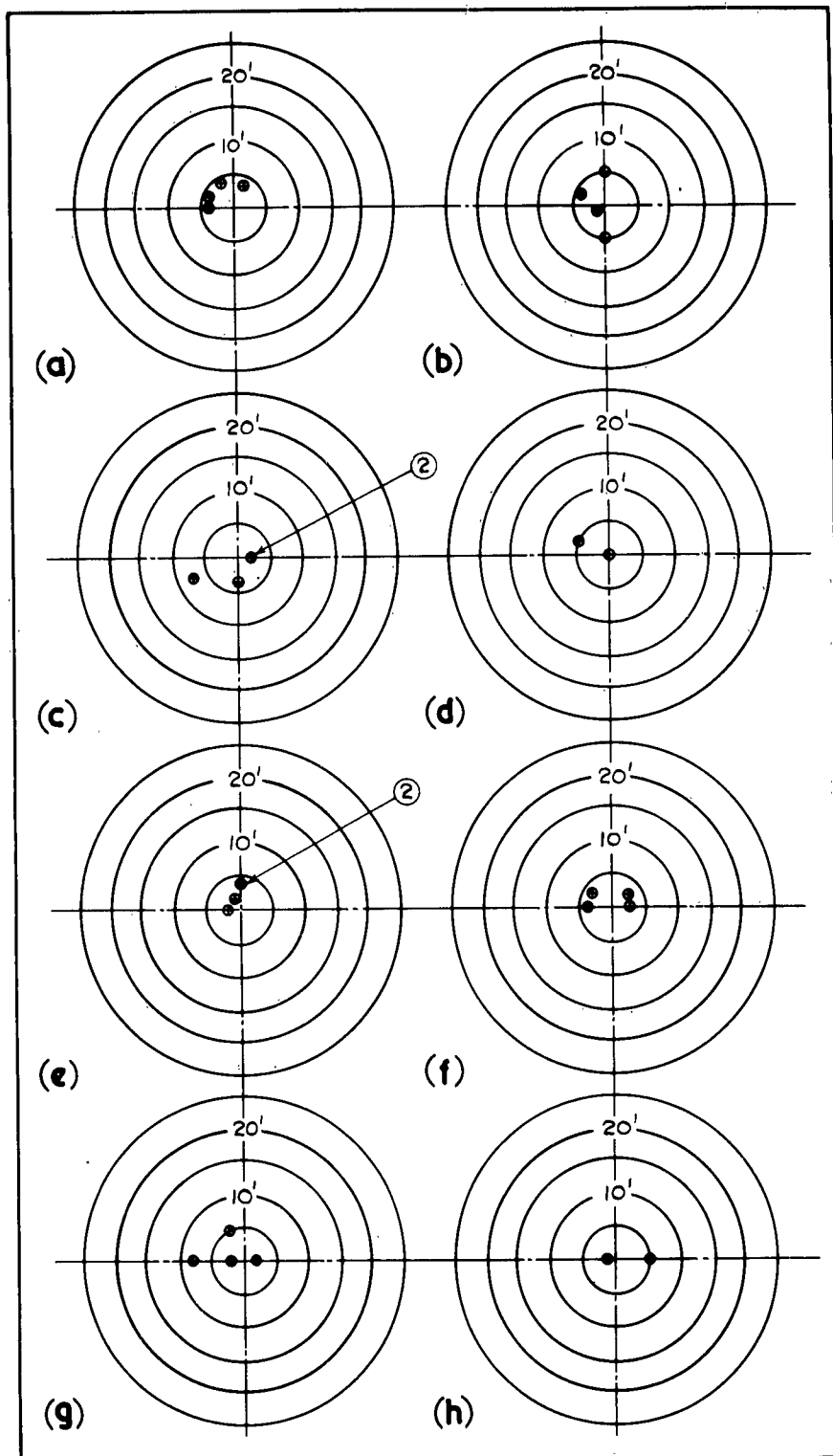
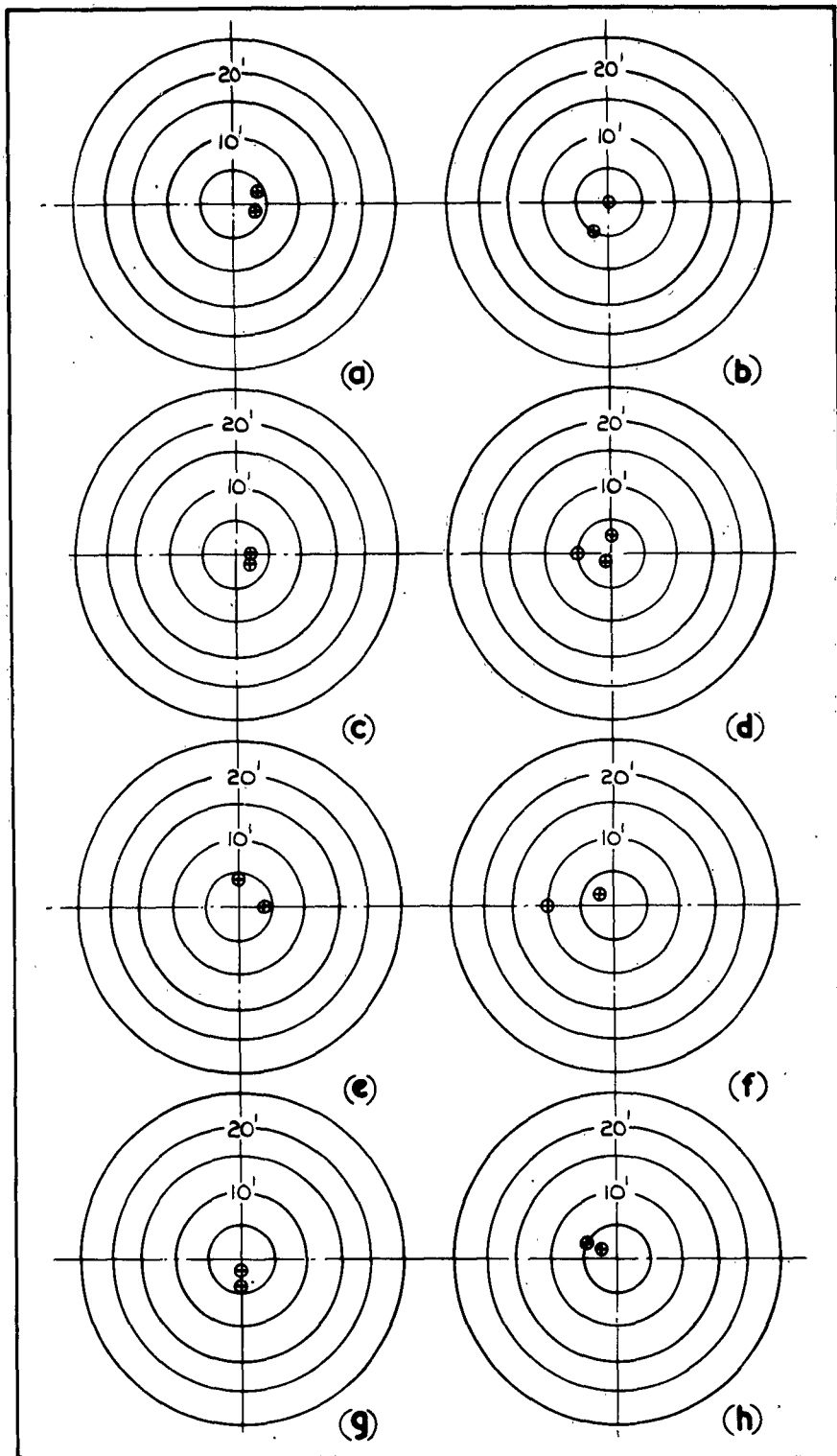


FIG. 24(a) MAX. ACC<sup>n</sup>. DEMAND = 150 FT/ SEC.<sup>2</sup>  
 NON - LINEAR JOYSTICK LAW:  $\frac{R}{R'} = 4$  &  $T_F = 2$  SECS.

- (a) TARGET VEL. 200 F/S. CROSSING DIST. 600' (e) TARGET VEL. 200 F/S. CROSSING DIST. 900'  
 (b) TARGET VEL. 500 F/S. CROSSING DIST. 600' (f) TARGET VEL. 500 F/S. CROSSING DIST. 900'  
 (c) TARGET VEL. 700 F/S. CROSSING DIST. 600' (g) TARGET VEL. 700 F/S. CROSSING DIST. 900'  
 (d) TARGET VEL. 900 F/S. CROSSING DIST. 600' (h) TARGET VEL. 900 F/S. CROSSING DIST. 900'



**FIG.25. MAX. ACCN. DEMAND=300 FT/SEC<sup>2</sup> NON-LINEAR JOYSTICK LAW:  $\frac{R}{R'} = 4$  AND  $T_F = 1.0$  SEC.**

(a) TARGET VEL. 200 F/S. CROSSING DIST. 0

(e) TARGET VEL. 200 F/S. CROSSING DIST. 300 FT.

(b) TARGET VEL. 500 F/S. CROSSING DIST. 0

(f) TARGET VEL. 500 F/S. CROSSING DIST. 300 FT.

(c) TARGET VEL. 700 F/S. CROSSING DIST. 0

(g) TARGET VEL. 700 F/S. CROSSING DIST. 300 FT.

(d) TARGET VEL. 900 F/S. CROSSING DIST. 0

(h) TARGET VEL. 900 F/S. CROSSING DIST. 300 FT.

FIG.25(a).

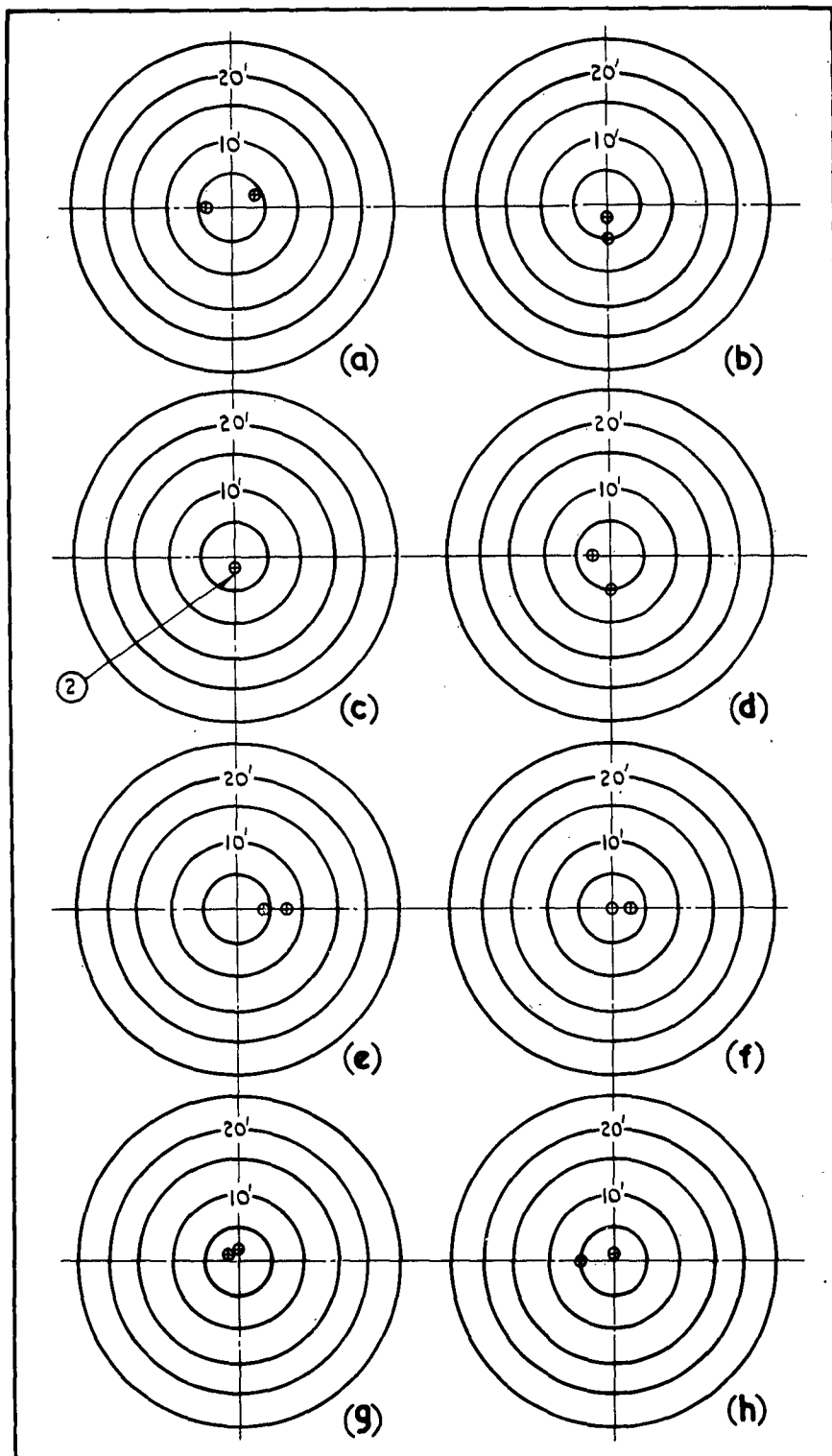


FIG.25(a). MAX. ACCN. DEMAND =  $300 \text{ FT/SEC}^2$  NON-LINEAR  
JOYSTICK LAW :  $\frac{R}{R_i} = 4$  &  $T_F = 1.0 \text{ SEC.}$

- (a) TARGET VEL. 200 f/s. CROSSING DIST. 600 FT. (e) TARGET VEL. 200 f/s. CROSSING DIST. 900 FT.  
 (b) TARGET VEL. 500 f/s. CROSSING DIST. 600 FT. (f) TARGET VEL. 500 f/s. CROSSING DIST. 900 FT.  
 (c) TARGET VEL. 700 f/s. CROSSING DIST. 600 FT. (g) TARGET VEL. 700 f/s. CROSSING DIST. 900 FT.  
 (d) TARGET VEL. 900 f/s. CROSSING DIST. 600 FT. (h) TARGET VEL. 900 f/s. CROSSING DIST. 900 FT.

FIG. 26.

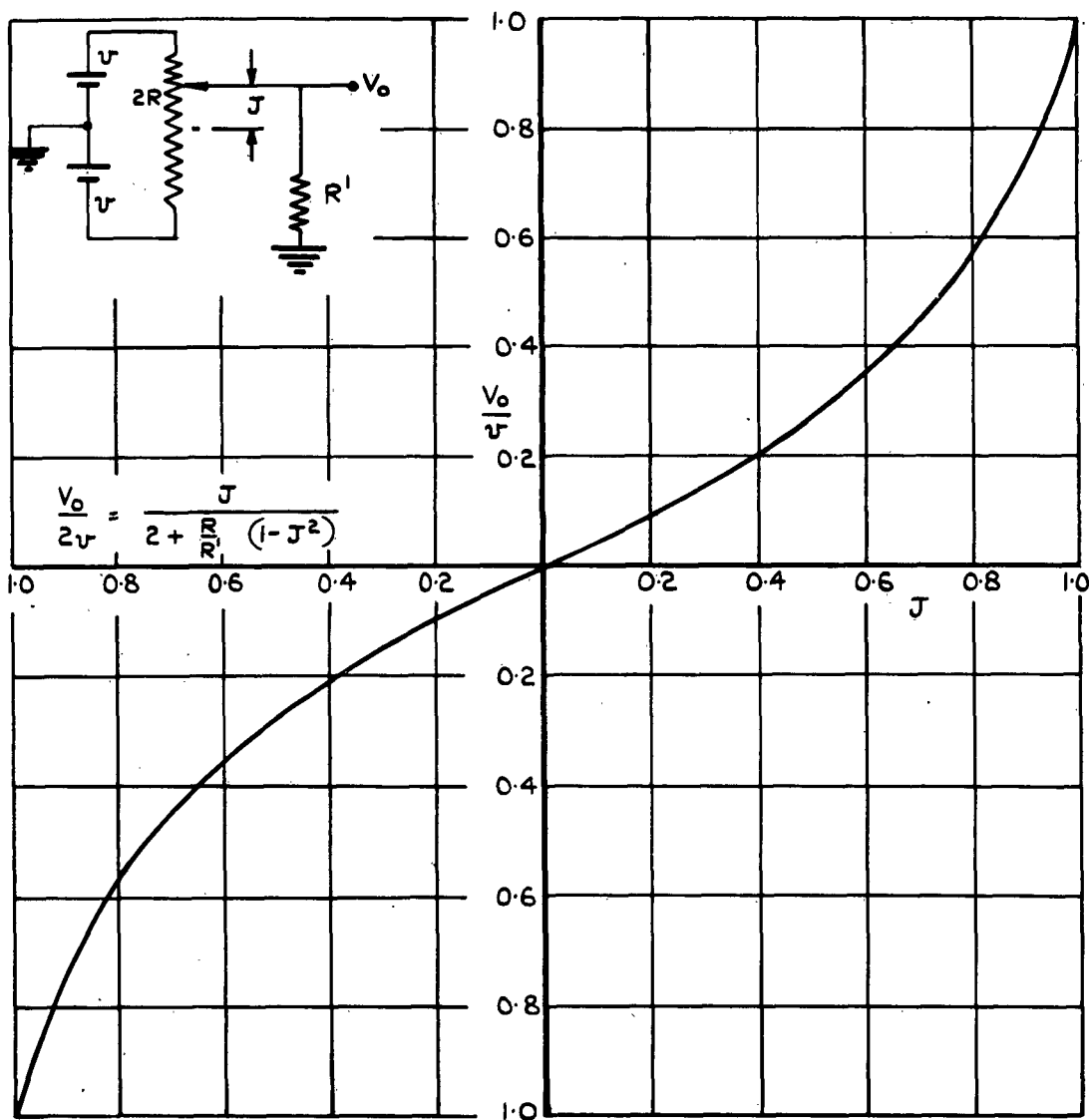


FIG. 26. CURVE OF JOYSTICK DISPLACEMENT  $J$  AGAINST ITS NORMALIZED OUTPUT  $\frac{V_o}{V}$  FOR  $R \approx 45 \text{ K}\Omega$  AND  $R' \approx 11 \text{ K}\Omega$



FIG.27. AIR LOOK-OUT SIGHT DESIGNED BY  
A.P.R.U. FOR TRACKING

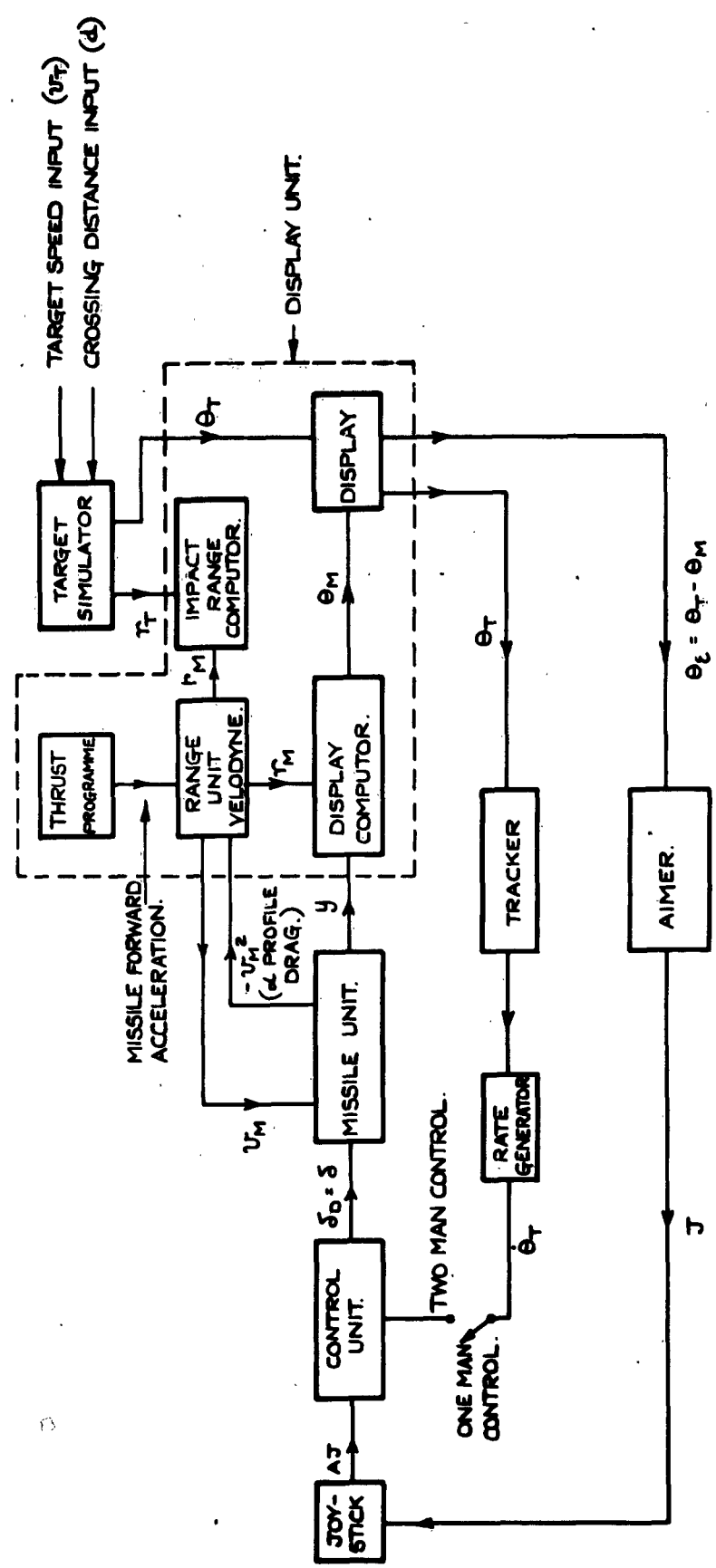


FIG. 28. BLOCK DIAGRAM OF LABORATORY SIMULATOR.

TARGET SIMULATOR

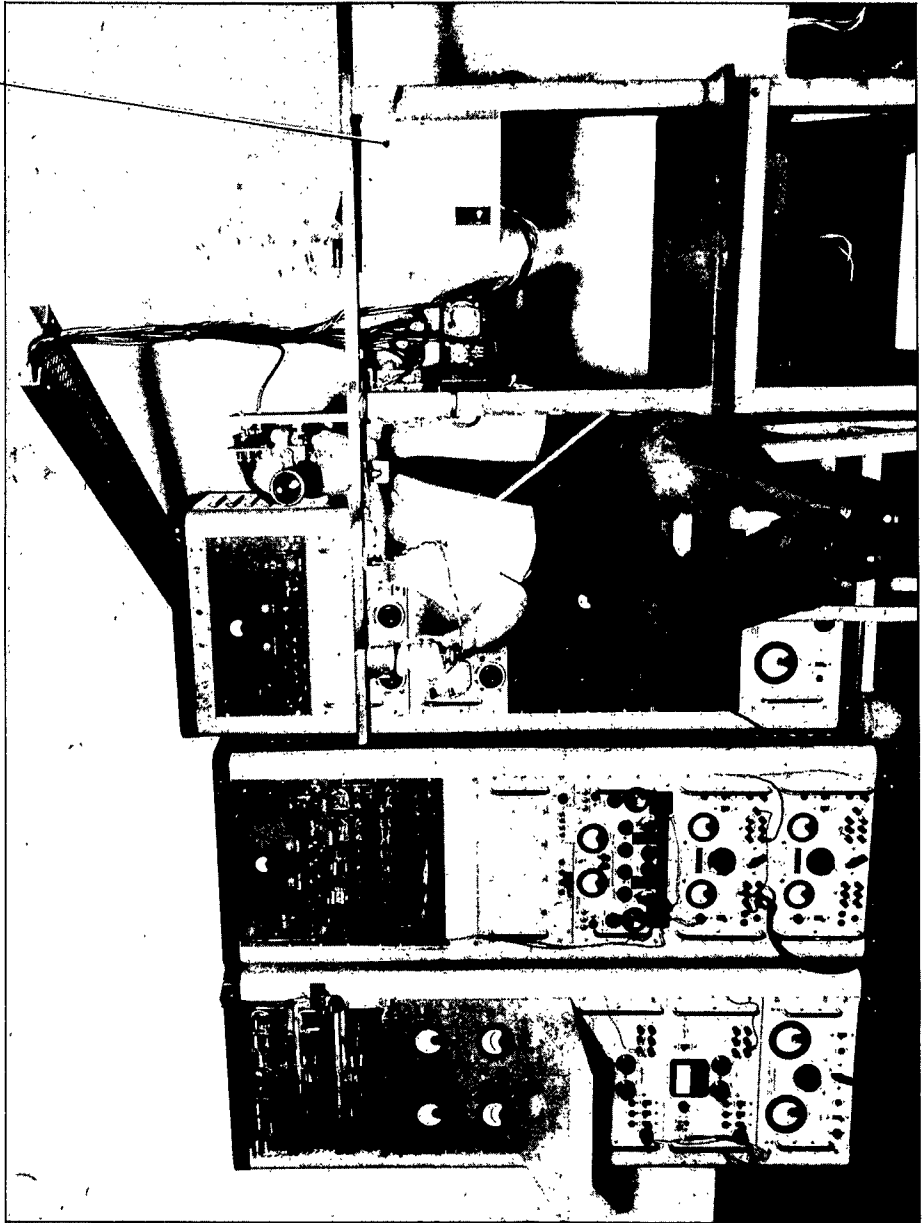


FIG.29. LABORATORY SIMULATOR SHOWING COMPUTING GEAR  
AND AIMING STAND. THE OPERATOR'S RIGHT HAND  
IS ON THE JOYSTICK GRIP



FIG. 31.

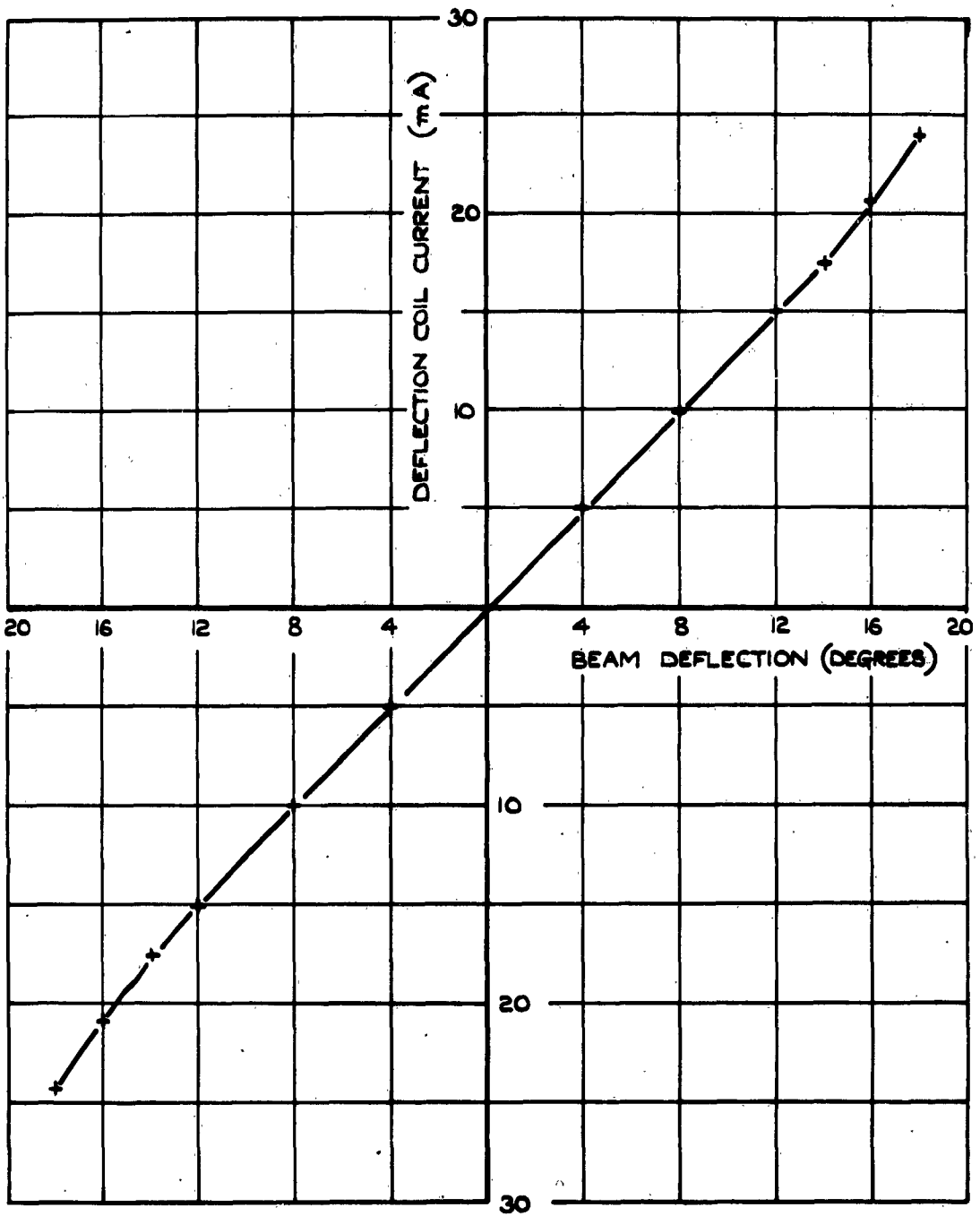
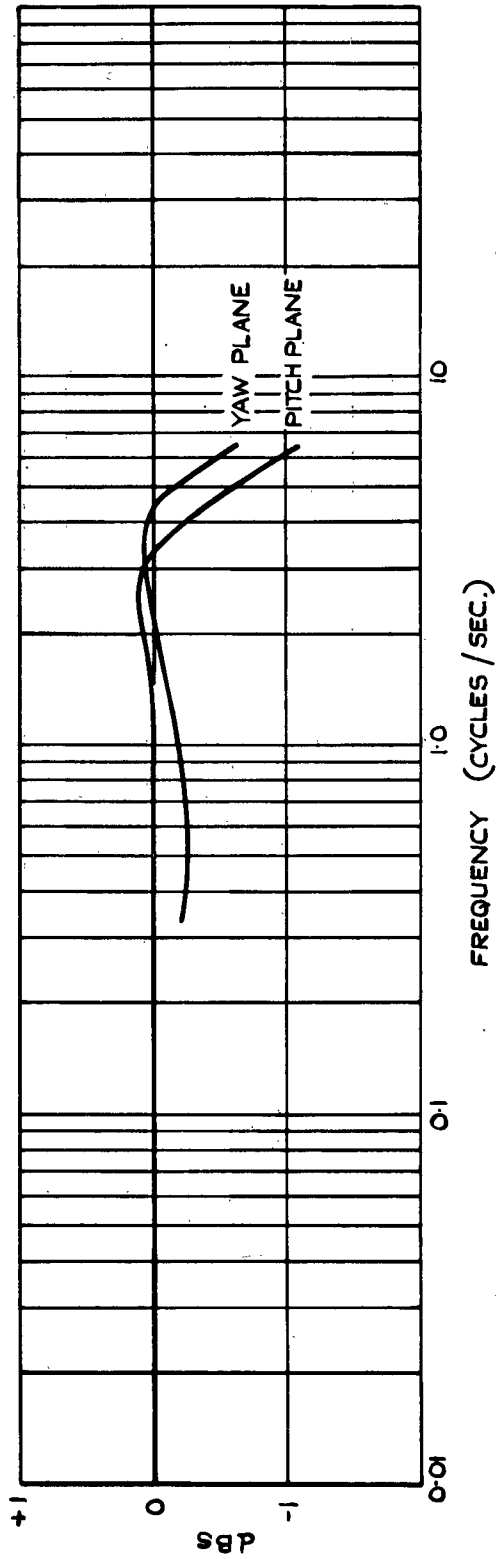


FIG. 31. GRAPH ILLUSTRATING GYRO GUNSIGHT MIRROR LINEARITY.



OUTPUT/INPUT RATIO FOR AN  
INPUT SIGNAL  $\pm 5^\circ$  (e)

**FIG. 32. FREQUENCY RESPONSE OF G.G.S. MIRROR IN  
BOTH PLANES OF MOTION.**

FIG.33

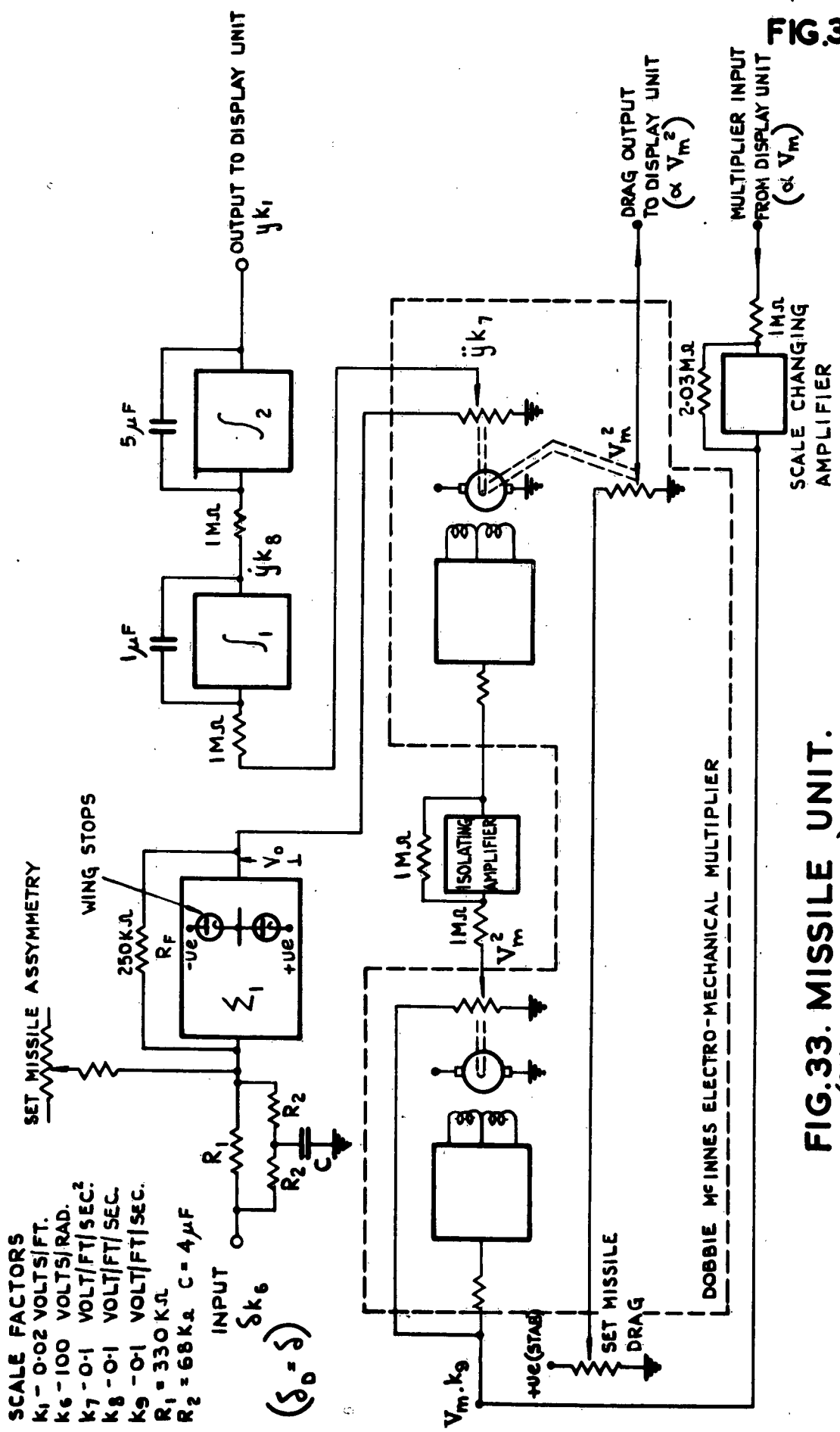


FIG.33. MISSILE UNIT.  
(ONE PLANE ONLY)



FIG. 35.

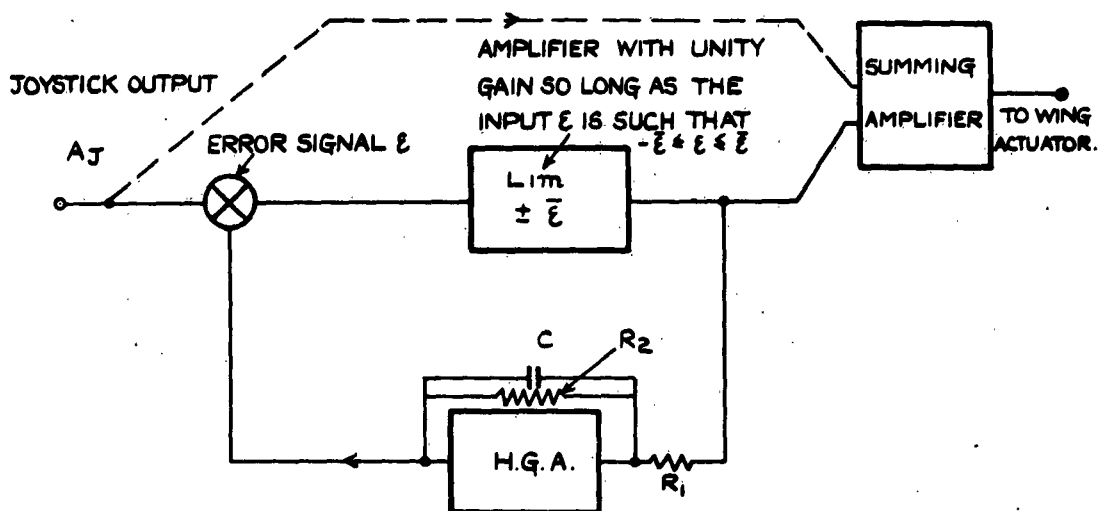
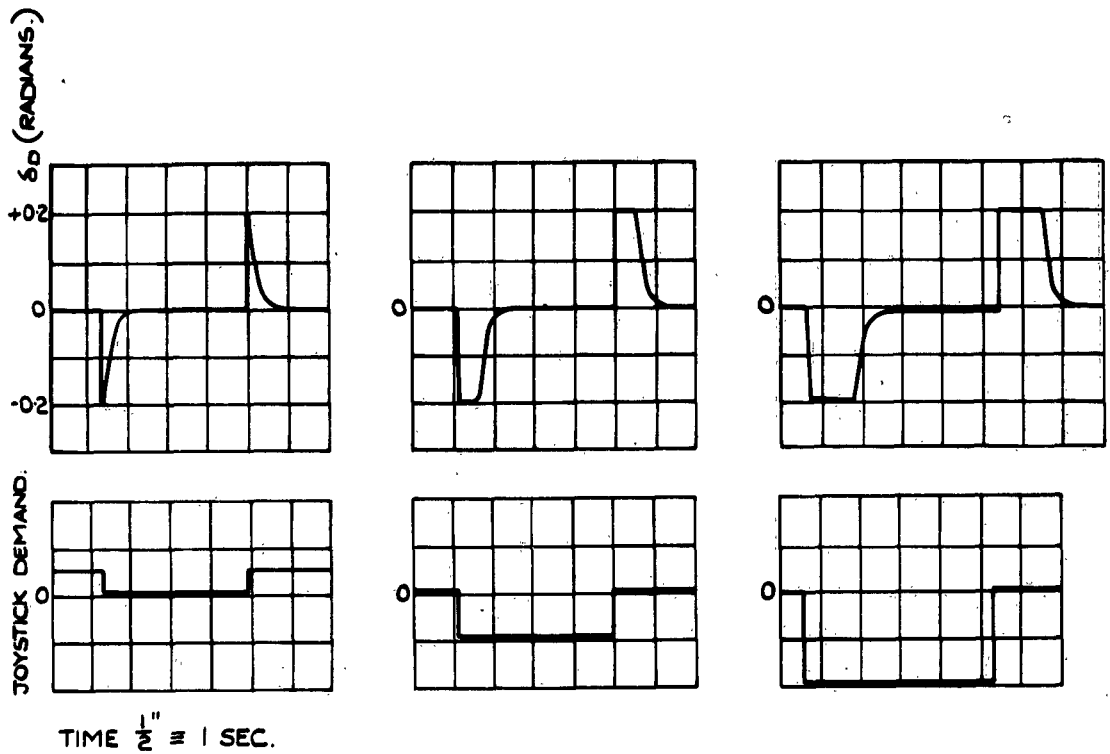
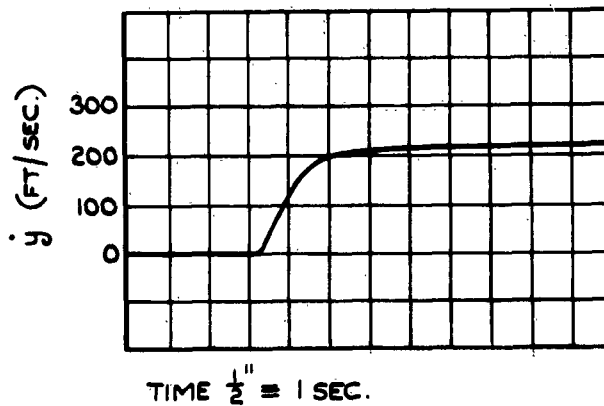


FIG. 35. 'DEMAND STORAGE' CIRCUIT  
FOR PHASE-ADVANCED ACCELERATION  
DEMAND.



**FIG.36. CONTROL UNIT RESPONSE (LATERAL VELOCITY DEMANDS ONLY) TO INCREASING STEP JOYSTICK DEMANDS.**



**FIG.37. TYPICAL MISSILE LATERAL VELOCITY RESPONSE TO A STEP JOYSTICK DEMAND FOR A LATERAL VELOCITY OF 200 FT/SEC.**

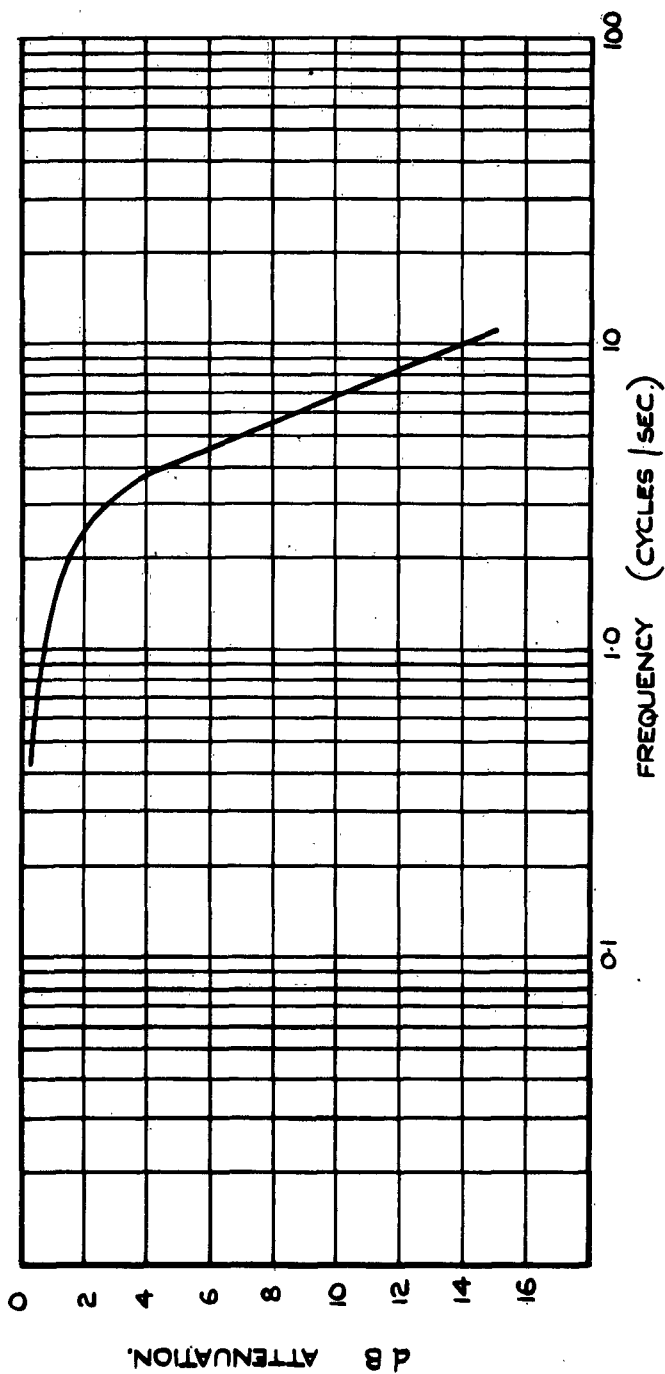
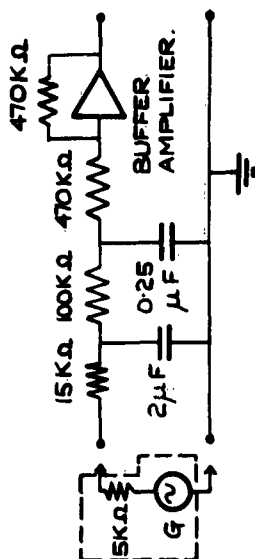


FIG. 38. FREQUENCY RESPONSE OF TRACKING GENERATOR NOISE FILTER.

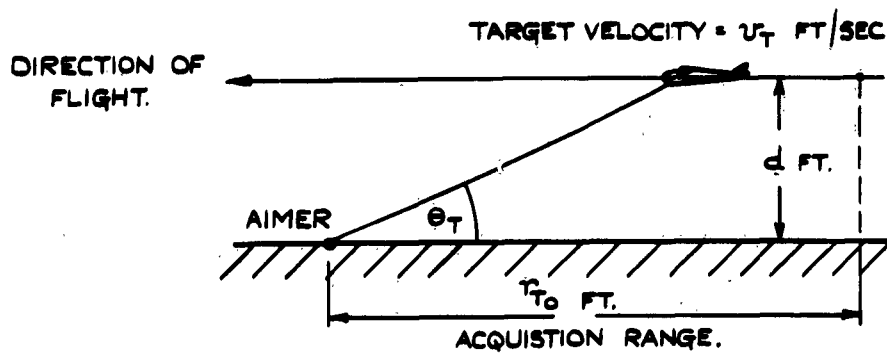


FIG. 39. TARGET GEOMETRY.

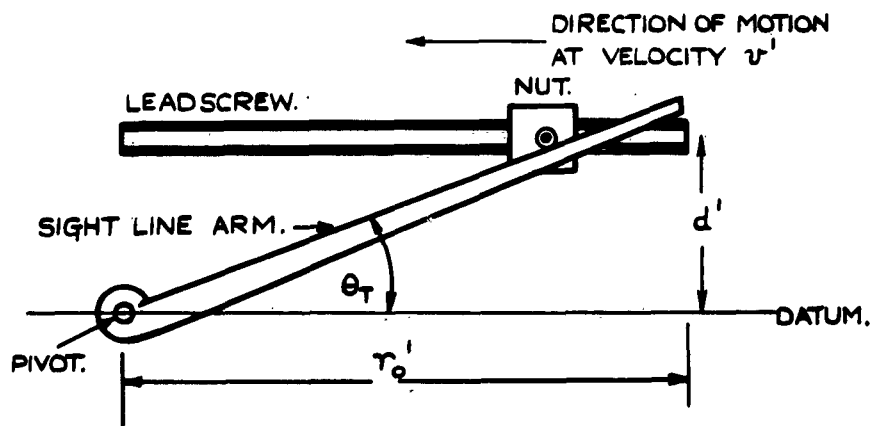


FIG. 40. BASIC TARGET SIMULATOR CONSTRUCTION.

FIG. 41 &amp; 42.

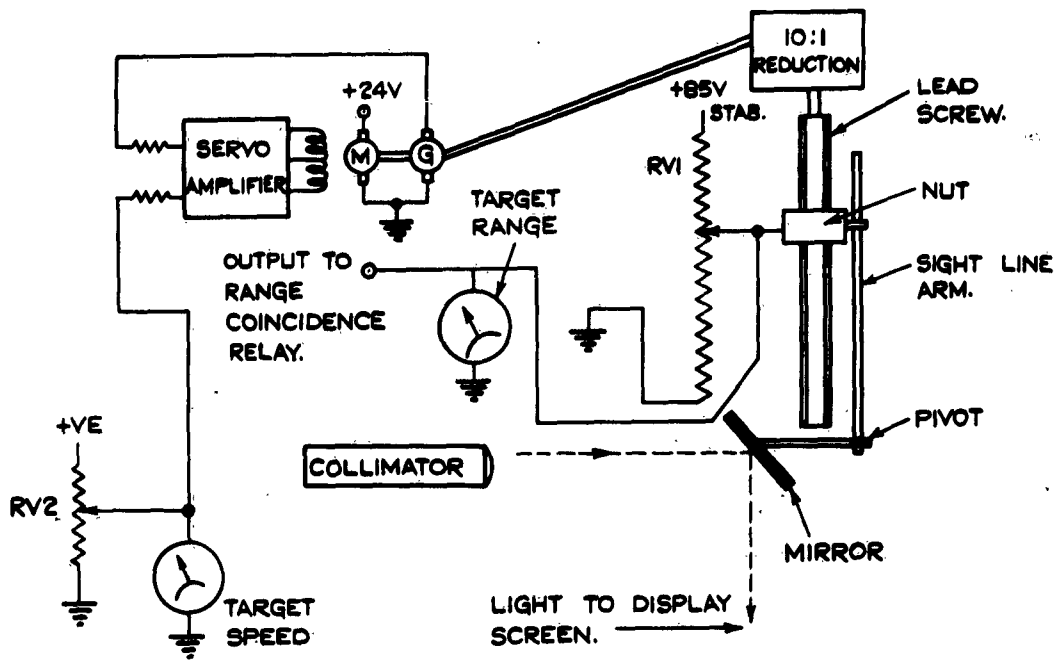


FIG. 41. SCHEMATIC DIAGRAM OF TARGET SIMULATOR

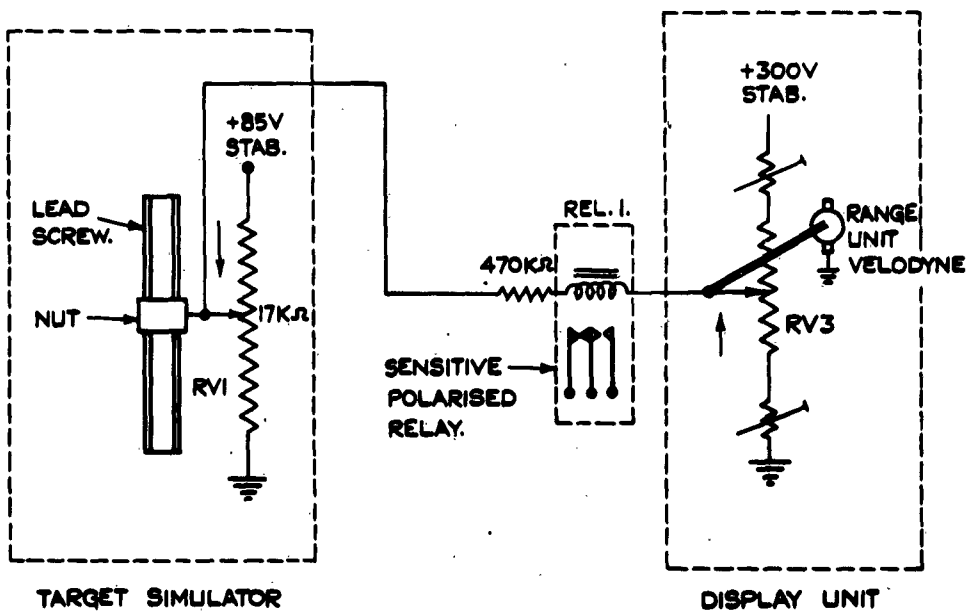


FIG. 42. SCHEMATIC DIAGRAM SHOWING METHOD OF DETERMINING IMPACT RANGE.

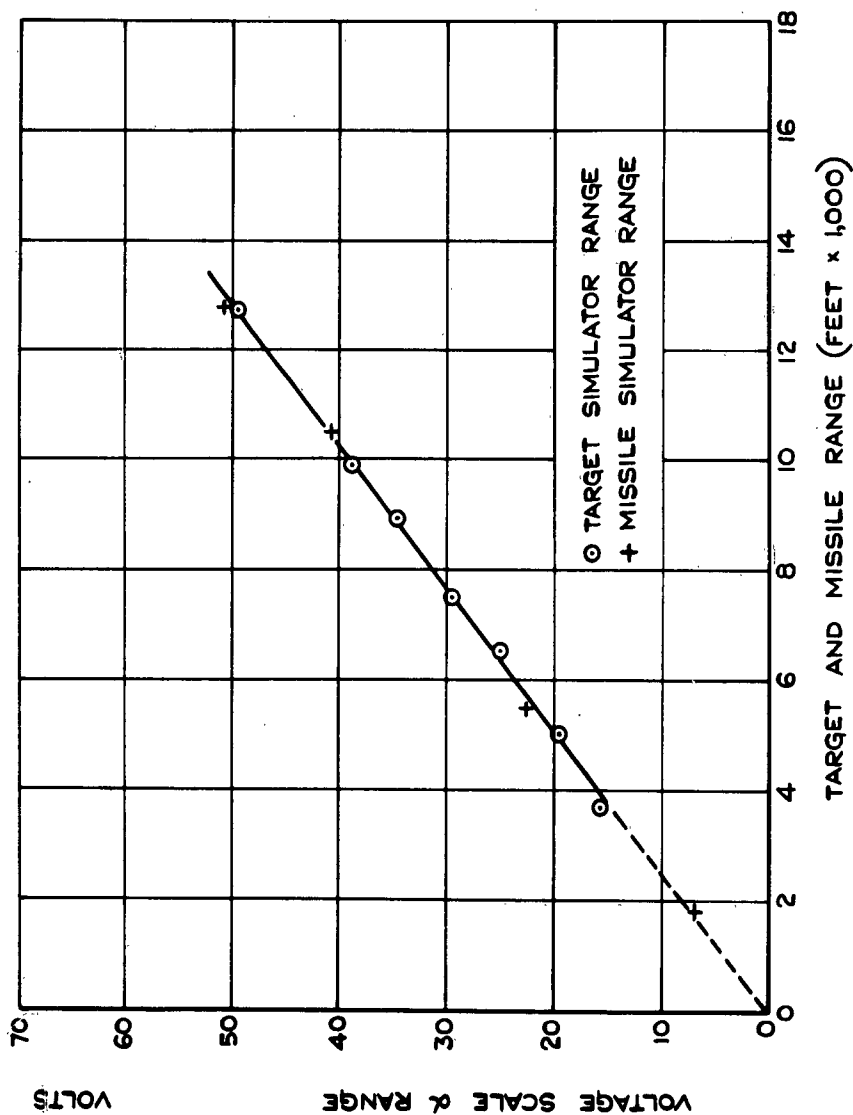


FIG. 43. MISSILE RANGE ERRORS IN COMPUTING  
TARGET / MISSILE IMPACT RANGE.



FIG.44. TRAINABLE AIMING STAND MOUNTED  
IN TRAILER. (FIELD SIMULATOR)

FIG. 45

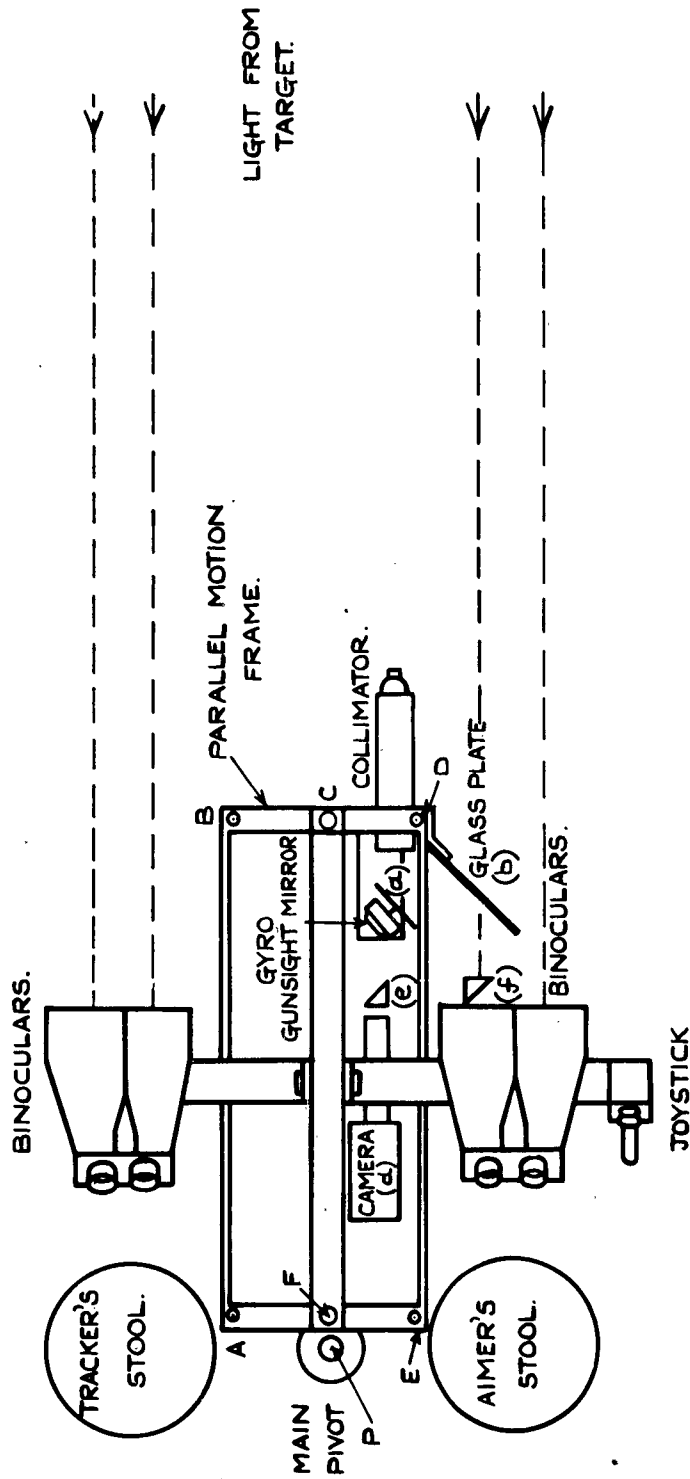
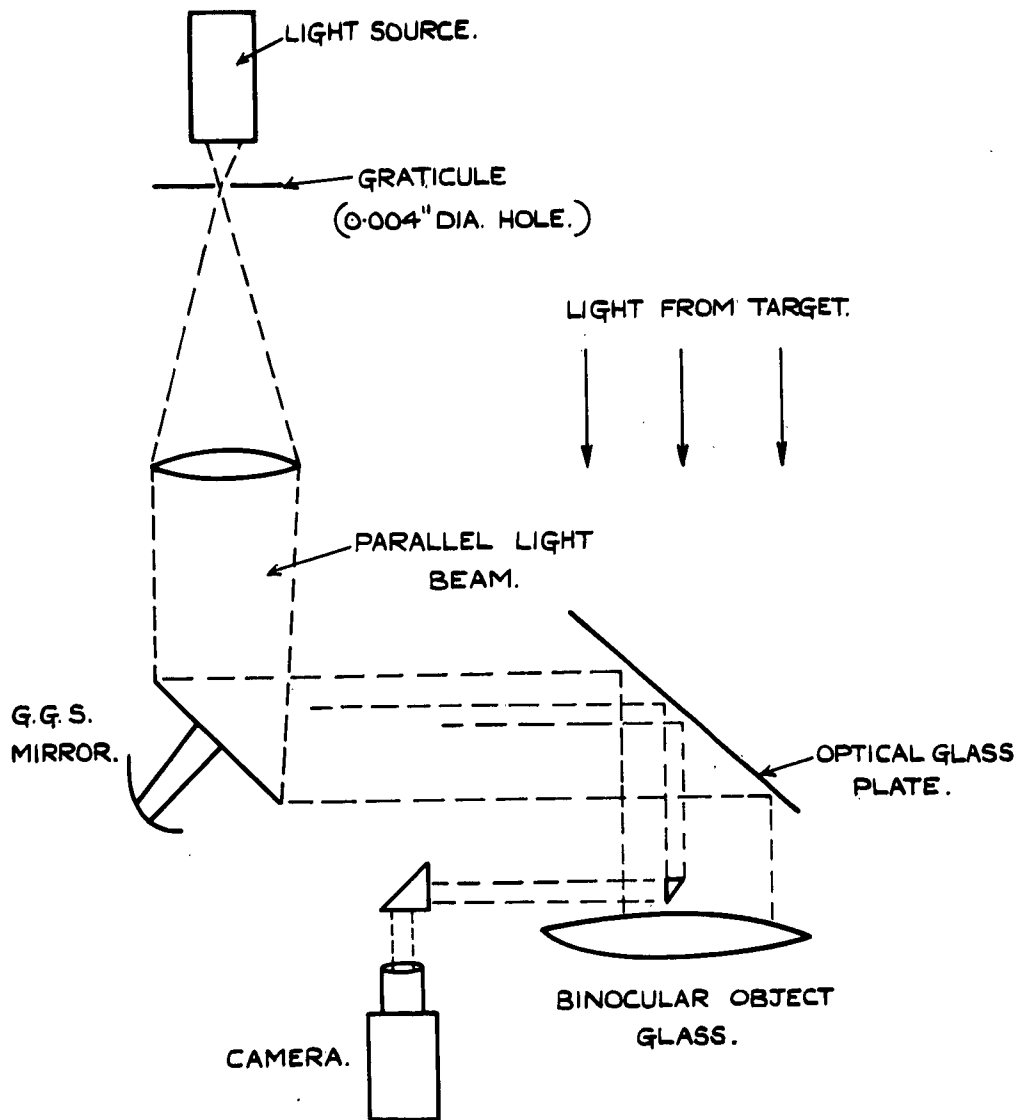


FIG. 45. DIAGRAM OF AIMING STAND FOR FIELD SIMULATOR.



**FIG. 46. OPTICAL ARRANGEMENTS OF THE FIELD SIMULATOR.**

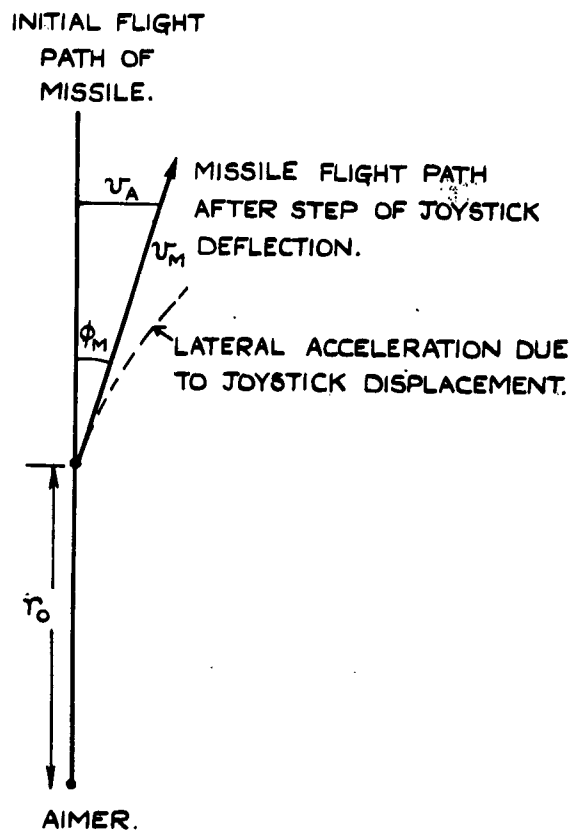


FIG. 47. IDEALIZED EFFECT OF JOYSTICK DISPLACEMENT.

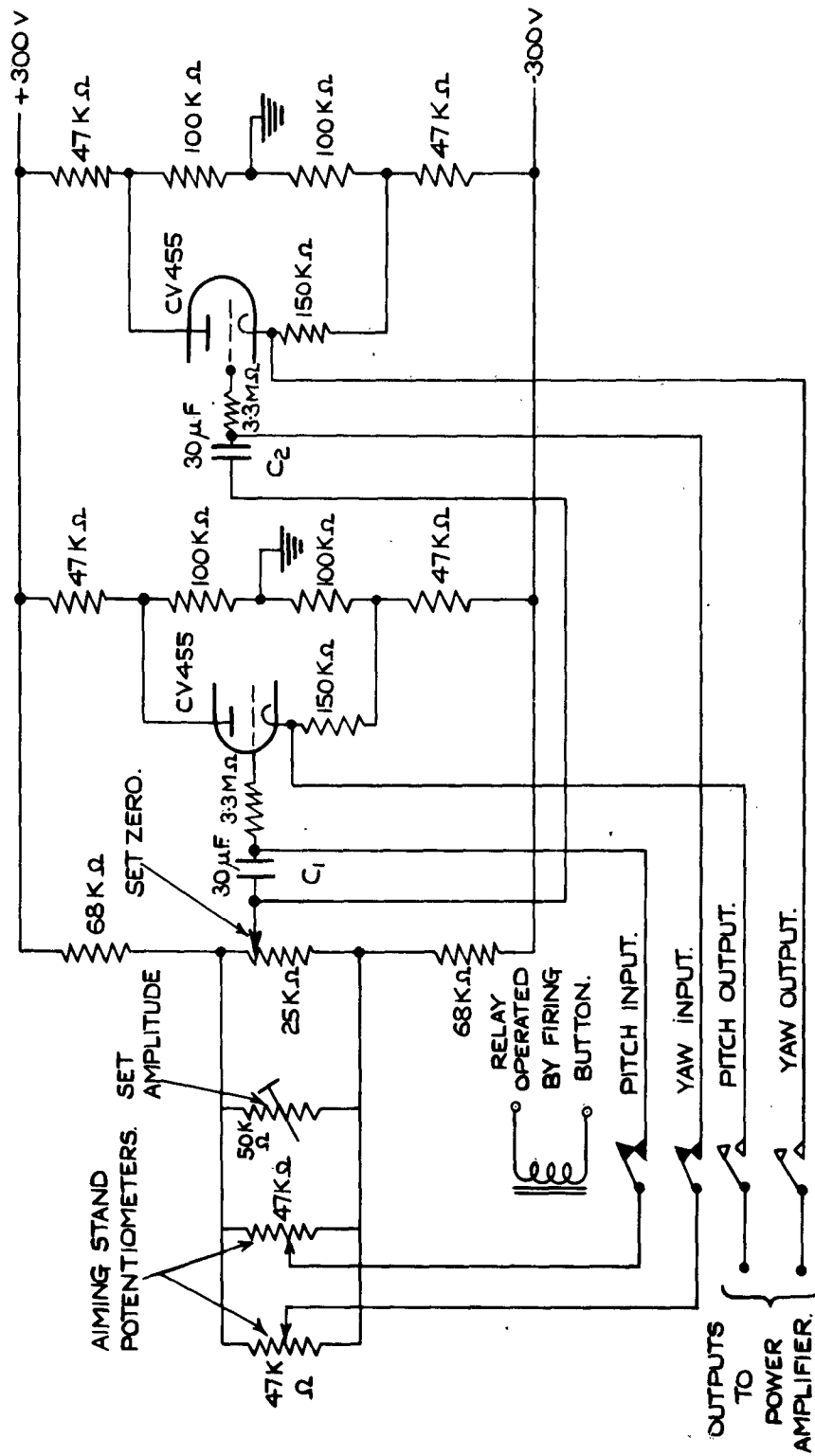


FIG.48. LAUNCHER ANGLE STORAGE UNIT.

# DETACHABLE ABSTRACT CARDS

These abstract cards are inserted in Reports and Technical Notes for the convenience of Librarians and others who need to maintain an Information Index.

Detached cards are subject to the same Security Regulations as the parent document, and a record of their location should be made on the inside of the back cover of the parent document.

<p><b>SECRET</b></p> <p>Royal Aircraft Est. Tech Note G.W.402 1956.3 Squires, M., Brown, G., Allen, D.W.</p> <p>VISUAL COMMAND GUIDANCE SYSTEMS FOR G.W. DEFENCE AGAINST LOW-FLYING AIRCRAFT</p> <p>The use of visual command guidance to control the flight of a missile from sea-level so as to intercept approaching, low-flying aircraft is examined. It is found that a human operator can perform this task by means of a thumb-operated joystick if (i) a suitable relation between joystick deflection and output signal is chosen, and (ii) an anatomically correct form of target tracking mechanism is provided so as to minimize effort and concentration.</p> <p><b>SECRET</b></p> <p>P.T.O.</p>	<p><b>SECRET</b></p> <p>Royal Aircraft Est. Tech Note G.W.402 1956.3 Squires, M., Brown, G., Allen, D.W.</p> <p>VISUAL COMMAND GUIDANCE SYSTEMS FOR G.W. DEFENCE AGAINST LOW-FLYING AIRCRAFT</p> <p>The use of visual command guidance to control the flight of a missile from sea-level so as to intercept approaching, low-flying aircraft is examined. It is found that a human operator can perform this task by means of a thumb-operated joystick if (i) a suitable relation between joystick deflection and output signal is chosen, and (ii) an anatomically correct form of target tracking mechanism is provided so as to minimize effort and concentration.</p> <p><b>SECRET</b></p> <p>P.T.O.</p>
<p><b>SECRET</b></p> <p>Royal Aircraft Est. Tech Note G.W.402 1956.3 Squires, M., Brown, G., Allen, D.W.</p> <p>VISUAL COMMAND GUIDANCE SYSTEMS FOR G.W. DEFENCE AGAINST LOW-FLYING AIRCRAFT</p> <p>The use of visual command guidance to control the flight of a missile from sea-level so as to intercept approaching, low-flying aircraft is examined. It is found that a human operator can perform this task by means of a thumb-operated joystick if (i) a suitable relation between joystick deflection and output signal is chosen, and (ii) an anatomically correct form of target tracking mechanism is provided so as to minimize effort and concentration.</p> <p><b>SECRET</b></p> <p>P.T.O.</p>	<p><b>SECRET</b></p> <p>Royal Aircraft Est. Tech Note G.W.402 1956.3 Squires, M., Brown, G., Allen, D.W.</p> <p>VISUAL COMMAND GUIDANCE SYSTEMS FOR G.W. DEFENCE AGAINST LOW-FLYING AIRCRAFT</p> <p>The use of visual command guidance to control the flight of a missile from sea-level so as to intercept approaching, low-flying aircraft is examined. It is found that a human operator can perform this task by means of a thumb-operated joystick if (i) a suitable relation between joystick deflection and output signal is chosen, and (ii) an anatomically correct form of target tracking mechanism is provided so as to minimize effort and concentration.</p> <p><b>SECRET</b></p> <p>P.T.O.</p>

SECRET

An effective two-man system, which has the advantage that the aimer's task is virtually the relatively simple one of hitting a fixed target, has also been found. Only preliminary studies have been undertaken, using experimental apparatus. Miss distances of up to 15 feet are to be expected at the present stage of development, although skilled experimenters can halve this figure under laboratory conditions.

SECRET

SECRET

An effective two-man system, which has the advantage that the aimer's task is virtually the relatively simple one of hitting a fixed target, has also been found. Only preliminary studies have been undertaken, using experimental apparatus. Miss distances of up to 15 feet are to be expected at the present stage of development, although skilled experimenters can halve this figure under laboratory conditions.

SECRET

SECRET

An effective two-man system, which has the advantage that the aimer's task is virtually the relatively simple one of hitting a fixed target, has also been found. Only preliminary studies have been undertaken, using experimental apparatus. Miss distances of up to 15 feet are to be expected at the present stage of development, although skilled experimenters can halve this figure under laboratory conditions.

SECRET

SECRET

An effective two-man system, which has the advantage that the aimer's task is virtually the relatively simple one of hitting a fixed target, has also been found. Only preliminary studies have been undertaken, using experimental apparatus. Miss distances of up to 15 feet are to be expected at the present stage of development, although skilled experimenters can halve this figure under laboratory conditions.

SECRET



*Information Centre  
Knowledge Services*  
**[dstl]** *Partnership  
with the  
USAF  
and the  
UK MoD  
to provide  
the best  
information  
available*

Defense Technical Information Center (DTIC)  
8725 John J. Kingman Road, Suit 0944  
Fort Belvoir, VA 22060-6218  
U.S.A.

AD#: AD93327  
Date of Search: 22 Oct 2009

Record Summary: AVIA 6/17315  
Title: Visual command guidance systems for GW defence against low flying aircraft.  
Held by The National Archives, Kew

This document is now available at the National Archives, Kew, Surrey, United Kingdom.

DTIC has checked the National Archives Catalogue website (<http://www.nationalarchives.gov.uk>) and found the document is available and releasable to the public.

Access to UK public records is governed by statute, namely the Public Records Act, 1958, and the Public Records Act, 1967.  
The document has been released under the 30 year rule.  
(The vast majority of records selected for permanent preservation are made available to the public when they are 30 years old. This is commonly referred to as the 30 year rule and was established by the Public Records Act of 1967).

**This document may be treated as UNLIMITED.**